PREDICTING URBAN SPRAWL PATTERNS AROUND ELDORET TOWN USING REMOTE SENSING AND GIS TECHNIQUES

BY

SAMSON ODHIAMBO

A THESIS SUBMITTED IN PARTIAL FULFILMENT OF THE REQUIREMENTS FOR THE DEGREE OF MASTER OF SCIENCE IN ENVIRONMENTAL PLANNING AND MANAGEMENT, UNIVERSITY OF ELDORET, KENYA

JULY, 2022

DECLARATION

Declaration by Candidate

This thesis is my original work except for the citations and quotations which have been duly acknowledged and has not been submitted for any academic award in any institution; and shall not be reproduced in part or full, or in any format without prior written permission from the author and/ or University of Eldoret.

Signature.. Date..

Odhiambo Samson

SENV/EPM/M/004/16

Declaration by Supervisors

This thesis has been submitted for examination with our approval as University Supervisors.

Signature.. Date..

Dr. Benjamin N. Mwasi

University of Eldoret, Eldoret, Kenya.

Signature..Date..

Dr. Job K. Ngetich

University of Eldoret, Eldoret, Kenya.

DEDICATION

I dedicate this thesis to my parents for educating me to be who I am, my spouse and children for understanding me when I was occupied doing the study.

ABSTRACT

One of the most rapidly growing urban phenomena in the 21st Century is emergence of sprawling settlements. Such settlements provide essential services but also cause some strain on these centers. Controlling and managing the growth of such settlements is necessary in order to maximize the services they provide and mitigate against the stresses they cause. This requires an understanding of both spatial and temporal sprawling patterns and factors that control them with a view to enabling planners to predict, guide and minimize patterns of urban sprawls. Satellite data plays a vital role in studying urban growth and sprawl patterns. However, despite most sensors delivering medium and high resolution satellite imageries and development in computer technology, a great percentage uses pixel based classification techniques. These techniques overlook variations in soft classifiers, sub-pixel classifiers and spectra un-mixing. This study therefore used classifiers that combine spectral and structural characteristics, involving rule-based object classification, to determine urban sprawl patterns around Eldoret Town and isolate factors that governs or controls the patterns in order to use them in predicting possible future sprawl patterns around Eldoret town in 2029. The findings revealed that different sprawl areas have different patterns for example Kapseret, Maili nne, Jua Kali showed linear patterns while Soy, Kuinet, Kipkorgot showed leapfrog pattern and attracted by economic factors during 2000-2020. Five of the selected factors, that is, distances to roads, powerline, waterline, employment centers and population density were the most significant factors contributing by 84.12% to sprawling patterns while three of the factors, that is, distance to restricted areas with 6.02%, elevation and slope tying with 4.94% each contributing least to sprawling patterns. The CA-Markov chain and AHP models predicted that sprawl areas would take different sprawl patterns of linear and leapfrog, increasing from 138.91 km^2 to 154 km^2 during 2020 to 2029, respectively. The study recommends that Uasin Gishu County government should direct areas destined for development by supplying roads, energy and water and control these services in areas that are not in order to control urban sprawl.

TABLE OF CONTENTS

LIST OF TABLES

LIST OF FIGURES

LIST OF ABBREVIATIONS, ACRONYMS AND SYMBOLS

ABM-Agent Based Modelling

AC-Accbestals

AHP-Analytical Hierarchy Process

ANN-Artificial Neural Network

BCI-Biophysical Composition Index

BRBA-Band Ratio Built-up Area

CA-Cellular Automata

CBD-Central Business District

CBI-Combination Built-up Area

CI-Consistency Index

CR- Consistency Ratio

DEM-Digital Elevation Model

DN-Digital Number

EA-East Africa

ELDOWAS-Eldoret Water and Sanitation

ETM+-Enhanced Thematic Mapper Plus

FDB-Facility Database

Fo- Orthic Ferralsol

GI-Galvanized Iron

GIS-Geographic Information System

GPS-Global Positioning System

HDPE-High Density Polyethylene

Hn-Humic Nitosols

IEBC-Independent Electro and Boundaries Commission

IRS-Indiana Remote Sensing

JPG-Joint Photogrammetric Group

KDF-Kenya Defense Force

KFS-Kenya Forest Service

KML-Keyhole Markup Language

KMZ-Keyhole Markup language Zipped

KNBS-Kenya National Bureau of Statistics

KPLC-Kenya Power & Lighting Company

LR-Logistic Regression

LULC-Land Use Land Cover

MC-Markov Chain

MCE-Multi Criteria Evaluation

MR-Multi Resolution

MSI-Multi Spectral Instrument

MSS-Multi Spectral Scanner

NASA-National Administration Space Agency

NBAI-Normalized Built-up Area Index

NDBI-Normalized Difference Built-up Index

NDVI-Normalized Difference Vegetative Index

NDWI-Normalized Difference Water Index

NIR-Near Infrared

NN-Near Neighbourhood

OBIA-Object-Based Image Analysis

PVC-Polyvinyl Chloride

RADAR-Radio Detection and Ranging

RI-Random Index

RMS-Root Mean Square

SAR-Synthetic Aperture Radar

SAVI-Soil Adjusted Vegetation Index

SDS-Spectral Difference Segmentation

SLEUTH-Slope, Land use, Exclusion, Urbanization, Transportation and Hill-shade

SPOT-System Pour l' Observation de la Terre

SRTM-Shuttle Radar Topography Mission

SWIR-Shortwave Infrared

TM-Thematic Mapper

TPM-Transition Probability Matrix

UN-United Nations

UNEP-United Nations Environmental Program

UTM-Universal Transverse Mercator

USGS-United States Geological Survey

VHR-Very High Resolution

WGS-World Geodetic System

WRS-Worldwide Reference System

OPERATIONAL DEFINITION OF TERMS

Ground truthing- Actual visiting the places to ascertain the facts as recorded by the sensor on-board satellite.

Land cover- refers to the aspects of land's surface which can be natural, semi-natural or man-made. Remote sensors can observe them in real time.

Land-use- refers to land-based activities or land classification based on how it is used which a remote sensor may not always detect.

Mixed pixel- is one in which the digital number (DN) indicates the average energy reflected or radiated by multiple different types of surfaces within the area it represents on the ground. Also called mixels.

Object-based image analysis- it is a technique that involves grouping pixels into image objects based on their spectral and structural similarity.

Rule-based object based classification- refers to the process of taking a portioned image and grouping similar objects into groups using indices.

Soft classifier- refers to pixel having several degrees of membership several classes other than one class.

Spectral unmixing- refers to the process of decomposing measured spectrum of a mixel into a collection of constituent spectra present in the pixel.

Sub-pixel classification- refers to detecting and extracting land cover form a mixed pixel in a multi spectral image.

Urban area- refers to cities and towns.

Urban growth- is a demographic and spatial process that refers to the growing importance of cities and towns as a concentration of population within a particular economy and society.

Urban sprawl- refers to growth of towns outside municipality boundary into rural lands characterized by low density developments in mostly unplanned areas.

ACKNOWLEDGEMENT

CHAPTER ONE

INTRODUCTION

1.1 Overview

In this chapter, explanation of problem, general and specific objectives, research question, justification, rationale for the study and organizational structure of the work is explained.

1.2 Background to the study

Urbanization is the transformation of natural environments into built-up areas *(Xie et al., 2005).* The world is experiencing rapid rates of urbanization, especially in the developing countries. The ratio of total population to total built-up area is used to categorize urban sprawl in terms of sprawl patterns in an area *(Sudhira et al., 2004).*

According to the United Nation Urbanization Prospects report 2021, 225.3 million (30%) of the global persons were city inhabitants in 1950, and is anticipated to rise to 6.68 billion (68%) by 2050, from 4.46 billion (56.61%) in 2021. Between 2021 and 2050, Asia and Africa are expected to account for 90% of global urban population growth. North America, Latin America, the Caribbean, Europe, and Oceania are the most urbanized regions with 82.75%, 81.5%, 75% and 68% respectively. Although the degree of urbanization in Asia is about 52%, Africa is mostly rural and 44% of its population is urban. Africa has the fastest urban population growth rate of 3.56% in 2021 followed by

Asia with 1.98% and Europe tailing at 0.32% as shown in Table 1.1 of the World's urban

population   by   region.

Table 1.1: World's Urbanization by Region

Region	Population 1950		Population 2021		Population 2050		Urban (%)		
	urban	rural	urban	rural	urban	rural	1950	2021	2050
Asia	246,192,916	1,157,868,674	2,408,318,385	2,252,719,984	3,479,058,559	1,777,868,940	17.53	51.67	66.16
Africa	32,658,962	196,011,057	608,654,401	777,000,214	1,488,920,045	1,038,636,716	14.28	43.93	58.91
Europe	284,085,263	265,289,756	558,453,858	185,042,265	598,857,027	116,863,987	51.71	75.11	83.67
Latin America and the Caribbean	69,759,111	99,158,582	545,983,737	124,527,251	685,070,437	94,770,764	41.30	81.43	87.85
North America	110,300,439	62,302,185	307,697,259	64,133,908	386,689,862	47,964,961	63.90	82.75	-
Oceania	7,906,247	4,741,529	29,309,513	13,623,859	41,160,232	15,961,223	62.51	68.27	-

Source: UN World Urbanization Prospects 2021.

Urbanization occurs around a compact city or along highways. According to *Padmanaban et al. (2017),* the global urban people are projected to grow by 72%, but urban areas in cities with more than 100,000 inhabitants could grow by 175% between 2000 and 2030. The rapid population growth calls for provision of more housing, schools, transportation network and utilities resulting in rapid but skewed urbanization driving conversion of Land Use/Cover (LULC). Increase in impervious surfaces is resulting in more water runoff and hence water pollution and flooding (*Shuster et al., 2005*). Fertile agricultural land, natural resources are also irreversibly depleted as a result of the urbanization process (*Joshi et al., 2017*). Uncontrolled increase in concrete land cover that have been officially farmland lands, forests, water features and wetlands coupled with population increase leads to food shortage among other environmental challenges (*Maktav et al., 2005).*

Barnum et al. (2017), demonstrates that impervious surfaces are environmental indicators and urbanization is the environmental conditions that it manifests.

In the United States, urban sprawl began in 1950s where residents preferred to settle outside the Central Business District (CBD) to avoid traffic, noise, crime among others and to have residence with more square footage and yard space. Seven million acres of agricultural land, seven million acres of sensitive natural ecosystem and five million acres of other lands will be lost to built-up lands during the year 2000-2025 (*Burchell et al., 2005*).

India being one of the developing countries is experiencing rapid urbanization (*Udeaja et al., 2020*). It is reported by *Bhat et al. (2017)* that India's uncontrolled growth in

population, combined with development activities which are not planned, has led to urban sprawl. UN's report (*1993*), indicate towns in India up scaled from 1827-5161 between 1901- 2001 respectively. The total population up scaled to 102.7 million in 2001 from 23.84 million in 1901, with urban inhabitants increasing from 258 million in 1901 to 2.85 billion in 2001.

Similarly, the urban East Africa population also increased from 11.2-77.2 million in 1970- 2010, and the city's share increased from 10% to 24% over the same period with built-up areas growing to 460, 000 ha (43.5%) (UN HABITAT and UNEP, 2010).

Kenya's total population soared from 10.9-38.6 million in 1969- 2009 respectively, with a compounded growth rate of 2.9%- 3.4%, it increased to 47.6 million in 2019 (KNBS, 2019). Urban population from the total population is projected to increase from 8.8% in 1960 to 1970 to 20.9% from 2000 to 2010 and exceed 36% by 2030 to 2040. 32.3% of 38.6 million people in 2009 census (12,487,375) lived in urban areas and 67.7% (26,122,722) lived in rural areas (KNBS, 2009). Kenya's urban population increased to 14, 744, 474 (KNBS, 2019). Table 1.2 shows population distribution of some ten main urban centres in Kenya.

Table 1.2: Distribution of Population of Urban Centres by Sex and County in Kenya

Urban Center	County	Total population 2009	Male 2009	Female 2009	Total population 2019	Male 2019	Female 2019
Kenya	**Kenya**	**12,487,375**	**-**	**-**	**14,744,474**	**7,309,839**	**7,433,955**
Nairobi	Nairobi	3,133,518	1,602,104	1,531,414	4,397,073	2,192,452	2,204,376
Mombasa	Mombasa	915,101	473,433	441,668	1,208,333	610,257	598,046
Nakuru	Nakuru	286,411	145,038	141,373	570,674	280,701	289,941
Ruiru	Kiambu	236,961	118,143	118,818	490,120	239,013	251,075
Eldoret	Uasin Gishu	252,061	127,808	124,253	475,716	237,223	238,477
Kisumu	Kisumu	259,258	131,062	128,196	397,947	195,432	202,515
Kikuyu	Kiambu	-	-	-	323,881	157,008	166,855
Thika	Kiambu	136,576	68,254	68,322	251,407	123,308	128,081
Naivasha	Nakuru	91,993	45,253	46,740	198,444	99,109	99,313
Karuri	Kiambu	99,739	49,692	50,047	194,342	94,707	99,623

Source: KNBS, (2009 and 2019)

More than 80 % of Kenya's economy depends on farming, but only 20 % of the country's land mass can support rain-fed farming. Of this, 20 % of the land is covered by houses for sheltering three-quarters of Kenya's population.

Eldoret town is the fifth most populated urban Centre in Kenya after Nairobi, Mombasa, Nakuru and Ruiru (2019, KNBS). The total population of Eldoret town has been increasing in the recent past such that by 2019 it was home to over 475,716 inhabitants (KNBS, 2019) from 289,380 in 2009 (KNBS, 2009) and from 193,830 in 1999 (KNBS, 1999). At a compounded growth rate of 5.096% total inhabitants will increase to 782,036 by 2029, an increase of 306,320 occupying a municipal land area of 147.9km^2 (Uasin Gishu county physical planning department).

Urbanization is always associated with urban sprawl, that is, the development of urban-like settlements outside the city since urban growth is further pushing cities further and further out. The ratio of total population to total built-up area is used to categorize urban sprawl in terms of sprawl patterns in an area (*Sudhira et al., 2004*). These sprawl areas resulting from urbanization can take place in different spatial patterns including; linear, leapfrog, clustered (*Wilson et al., 2003*). Sprawl occurs in towns and cities around the globe because of unplanned growth although we can identify some factors which supports or repel sprawl.

Eldoret Town is currently experiencing rapid urban growth in all directions exerting great pressure on biophysical and socio-economic environments. Urban-like developments are occurring in all areas surrounding Eldoret Town at different rates and spatial extents. What is not clear is the factors that support the development of these sprawl areas. This knowledge would be useful for better planning and management of urban growth as policy makers could control the growth of these factors and hence direct the patterns of urban sprawl.

As these developments are physically recognized in high resolution satellite imagery, it is possible to link the development of urban sprawls with bio-physical and socio-economic factors. Further, with the determination of the contribution of specific environmental factors, it is possible to model different growth patterns based on different factor scenarios.

This study therefore, uses analysis of high resolution satellite images to identify sprawl areas and their bio-physical characteristics in combination with socio-economic factors to

identify significant factors responsible for sprawl developments. Using these factors and different change trends future sprawl patterns are also predicted.

1.3 Problem Statement

Eldoret town experiences a number of urban management challenges including traffic snarl-ups, solid waste management, proliferation of slums and informal settlement as well as uncontrolled urbanization as manifested by urban sprawl around its scheduled areas. These sprawl areas lead to fertile agricultural land being converted into patches of built-up areas which could lead to a decline in food production in a region that has been for a long time known as the grain basket of Kenya. Proliferation of urban sprawls affect urban service delivery as well as environmental quality, thus ability to manage sprawl development is key to urban planning and management. This study uses Geographic Information System (GIS) and remote sensing techniques to analyze the urban sprawl development process with a view to determine the significant bio-physical and socio-economic factors that support sprawling. The study also predicts future sprawl growths under different scenarios. The resultant information can inform planning urban growth by either enhancing or suffocating specific growth factors as a mechanism of controlling sprawl patterns.

The study therefore sought to determine urban sprawl patterns, determine the contribution of selected factors that support urban sprawl patterns and using the factors to predict possible future sprawl patterns around Eldoret Town. The study used high resolution Sentinel-2 imageries of 2016 and 2020 and pan-sharpened Landsat 7 Enhanced Thematic Mapper Plus (ETM+) of 2000.

1.4 General Objective

The overall objective of the study is to investigate and analyze future urban sprawl patterns and land conversion around Eldoret town during the last 20 years (2000-2016-2020) with a view to add or limit factors supporting sprawl.

1.4.1 Specific Objectives

1. To determine urban sprawl patterns around Eldoret town

2. To determine the contribution of selected factors supporting urban sprawl patterns around Eldoret town

3. To predict possible future sprawl patterns around Eldoret town in 2029 using Cellular Automata (CA)-Markov model

1.4.2 Research questions

1. How is the nature of urban sprawl patterns around Eldoret town?

2. How do the identified factors contribute to urban sprawl patterns around Eldoret town?

3. Which areas are likely to become new urban sprawl spread areas in the future?

4. What can be done to contain urban sprawl in Eldoret?

1.5 Justification of the study area

Agricultural land and natural resources are irreparably depleted due to urbanization (*Mittal et al., 2015*) because of rapid increase in population, leading to food shortages, informal settlements, pollution and destruction of ecological structures, unemployment, and so on (*Maktav et al., 2005*).

Eldoret town is the largest in Uasin Gishu County and an agricultural town that has been for a long time the bread basket of the country. The town is followed by other medium satellite towns namely; Burnt forest, Turbo, Kesses, Ziwa, Moiben, Soy and Moi's Bridge. It is also the fifth most populated urban Centre in Kenya (KNBS census, 2019). Thus timely understanding of the nature of urban sprawl and adhering to physical planning and zoning of the urban environment, will help to control and manage services provision. In addition, it will help solve regional and local planning problems by contributing to National government planning policy and also the Uasin Gishu County government to be able to persuade people to settle only on non-fertile areas and thereby leave back fertile land for agricultural activities.

1.6 Significance of the Study

Urban sprawl and proliferation of informal settlement is a topic of global concern leading to advocating for compact development designed to cover less footprints, protect and conserve nature thus providing a healthier and more sustainable quality of life. Results from this study will reveal the main variables contributing to urban sprawl patterns around Eldoret town thus contributing to ongoing body of research into the topic of urban sprawl.

1.7 Limitation of the Study

Lack of high resolution open source satellite image for year 2000 resulted in use of low resolution pan-sharpened Landsat 7 ETM+ satellite image at 15m spatial resolution. Also only eight supporting urban sprawl factors were analyzed because of time limitation.

1.8 Thesis Organizational Structure

The study report is presented in six sections with each section beginning with an introduction of what the chapter contains. Chapter one contains background information of the study whereby global trends in urban growth and sprawl are discussed then narrowing down to study objectives, problem statement and motivation. Chapter two highlights review of literature that are related to urban growth and sprawl in order to determine the knowledge gap. Chapter three is a methodological chapter containing a description of study area, data collection and analytical methods presented according to study objectives. Chapter four presents results and findings per objective and chapter five is a core chapter discussess the results. Chapter six concludes and recommends policies which would be applicable in shaping future urban areas. At the end of last chapter, appendices are attached.

CHAPTER TWO

LITERATURE REVIEW

2.1 Introduction

This chapter reviews literature on urban sprawl both at global and regional level, its causes, impacts and strategies to counter and finally identification of the knowledge gap.

2.2 Understanding the concept of Urban Sprawl

Earl Draper of the Tennessee River Basin Corporation, at the National Planners' Meeting in 1937, was the pioneer of using the term "sprawl" (*Maier, 2006*). Urban sprawl was described as an aesthetic rather uneconomical form of habitats. The term "urban sprawl" was applied the first time in 1958 introducing paragraph of an article by Fortune magazine sociologist William Whyte (*Maier, 2006*). Since then, planners have used this term to classify urban developments that have unforeseen negative social impacts. In the 1990s, sprawl element was taken up by other scholars and other citizens in the United States. During this period, a counter-sprawl initiative began, and the initial counter sprawl initiative was implemented. General Citizens and policy makers regularly use the term as a medical term. Spread of urban areas is considered an illness that can be recognized by its unwanted symptoms. Although there seems to be a lack of exact factors causing it and ways to counter it, there are many treatments available for this 'illness'.

The term "urban sprawl" is widely used in many disciplines dealing with related and town development and urban morphology. In addition, it is also used as a buzzword in urban politics and public debates surrounding the growth and shape of cities. The term

"sprawl" is often misleading and confusing because of its use in different professions and has different definitions. Michigan Land Use Leadership Council (2005): "In the field of land use and planning, no other word spurs more controversy and confusion than sprawl". Different authors define sprawl in different ways. For example, *Hasse* and *Lathrop (2003)* define sprawl as a particular form of urban development with low density, decentralization, self-sufficiency, environmental and social characteristics. Urban growth and decentralization itself have not been negatively evaluated.

Sprawl is defined by *Travisi* and *Camagni (2010)* as "the uncontrolled spreading out of a given city and its suburbs over more and more semirural land at the periphery of an urban area." They further say; the vast expansion process is chaotic and not planned, often resulting in effective and inapplicable town growth patterns. It is notable that the definitions of the term sprawl according to most authors; the sprawl phenomenon is a multidimensional phenomenon and for this study, the definition of urban sprawl by *Travisi* and *Camagni (2005)* is agreed as the correct definition since in this context sprawl has spilled over to the fertile agricultural land in the suburb areas.

2.3 Manifestations of Urban Sprawl

According to *Johnson et al. (2001)* sprawl is categorized into two: first, low-density sparse development. Second, non-residential sparse commercial and industrial constructions. Scattered construction may be mostly related to sprawl. The advances portrays ten focuses that characterise urban sprawl specifically; low-density sparse development, boundless outward expansion of modern development, spatial isolation of different types of land uses through zoning regulations, leapfrog (irregular) development,

no centralized ownership of land or planning owned motor vehicles, all transportation dominated by privately owned engine vehicles, great variance in the fiscal capacity of local government because the revenue-raising capabilities of each are strongly tied to the property values and economic activities occurring within their own borders, widespread commercial strip development along major roadways and major reliance upon the filtering or trickle-down process to provide housing for the low-income households.

The categorization brings a lot of points into dialog. Inside this list, the limits between symptoms and effects of spread of towns are equivocal and a direct refinement between these categories isn't totally conceivable (*Galster et al., 2001*). *Galster* suggests that sprawl is characterized by eight measurements to be specific;

a. Density: could be a broadly utilized marker spread of towns where distinctiveness sorts of thickness can be explained.

b. Continuity: is the degree to which the unused arrive has been built thickly in an unbroken design. Sprawl can be nonstop or irregular in other places.

c. Concentration: depicts the degree to which improvement is found excessively instead of spread evenly.

d. Clustering: sprawl is as often as possible clustered what implies that it as it were possesses a little parcel of the respective arrive area.

e. Centrality: the misfortune of centrality is one of the foremost genuine concerns almost sprawl.

f. Nuclearity: depicts the degree to which an urban zone is characterized by a mononuclear design of development.

g. Mixed employments: sprawl is seen as a prepare that isolates the distinctive sorts of arrive employments including division of homes, working environments, comforts, wage isolation along private communities.

h. Proximity: Land use is close to each other in terms of housing, work and shopping. The lack of accessibility contributes too much of the externalities that result from urban sprawl.

2.4 Causes of Urban Sprawl

Causes and impacts according to *Galsters (2001)* are regularly befuddled, due to a semantic wilderness of the term sprawl and observational shortages. He contends that: "a thing cannot at the same time be what it is and what it causes". *Torrens et al. (2000)* demonstrates that it is difficult to discover arrangements to sprawl in the event that we don't completely get it its causes. It is because of this that it is essential to measure fundamental variables of sprawl before measuring their impacts. A few causes of urban sprawl that shows at worldwide, territorial and neighborhood levels are worth noting.

2.4.1 Population growth

Characteristic population increment and movement to urban zones are the two population development variables. Common population development comes about from increase in births over death. *Couch et al. (2005)* reports that, more youthful families advance sprawl and designs by looking out for reasonable housing at the urban fringe.

2.4.2 Economic Growth

The expansion of the economic base (e.g., increased per capita income, increased labor force) brings market for housing (*Friedman et al., 2017*). Developers are also encouraged to build many new homes quickly, creating a large number of discontinuous and uncorrelated developments.

2.4.3 Industrialization

The establishment of new industries in the countryside will lead to a rapid increase in the concreate areas since industry needs to provide workers with a wide range of housing. The process of transition from agriculture to industry requires more urban housing hence leading to sprawl.

Infrastructure drives the growth of the city by providing an essential framework for housing development. As new developments take place, residents are calling for improvements in infrastructure that further facilitate suburban development. Wider access enabled by improved transportation infrastructure and availability of relatively cheap gas prices allows developers to use cheap land outside the city center (*Gillham, 2002*).

2.4.4 Cogitation

Reflecting about future growth, government policies, transportation and other utilities can lead to premature growth without proper planning. Multiple political foundations can also encourage people to speculate on the direction and scale of future growth, thereby confining land and leading to discontinuous development (*Cotula et al., 2009*).

2.4.5 Expectations of Land Prices Increase

The desire to raise land prices around cities means that landowners withhold land from the market (*Bhatt B, 2010*). It varies from one property owner to another resulting in a discontinuous development. Concurring to *Schoer (2006)*, the cost of rural migration is very lower than plot consequently draws in businesses in agrarian migration hence a major calculate causing urban sprawl.

2.4.6 Land Hunger Attitude

Majority of institutions and individuals want land ownership. In many cases, these parcels are vacant in the city center and the infill policy fails (*Bhatt B, 2010*).

2.4.7 Court Battle Problem

Court battles such as ownership, land subdivision, taxes, and tenant issues often result in vacant or one-story downtown buildings. This also leads to outward growth, leaving vacant lots and one-story buildings in the city *(Bhatt B, 2010)*.

2.4.8 Physical Geography

Urban sprawl can be caused by inadequate suitable landform, such as slope, valleys, natural resources, often leading to the expansion of leapfrog development (*Barnes et al., 2001*). In many instances this problem can't be overcome and therefore should be overlooked since it's a natural phenomenon.

2.4.9 Lack of Affordable Residential

Developers build houses in the countryside because there are no affordable homes in the city. *Carruthers et al. (2002)*, say that residents prefers to settle where housing options are more affordable generally located in the suburbs of metropolitan areas.

2.4.10 Demand of more Living Space

Growing nations lacks enough residing area, for CBD citizens. This leads to construction in the suburb area since one can purchase extra residing area outside the CBD at a lower cost. The increase in living space leads to population density and sprawl. Cities in growing nations are 3 times denser than those in advanced nations (*Bhatt B, 2010*). Demand for extra residing area forces fast low-density improvement which is a demonstration of sprawl.

2.4.11 Road network

Roads link places ensuring the development of straight branches. Expressways and highway construction cause both congestion and outward growth of a town. Transportation networks are an important catalyst for urban sprawl and are often included in the modeling and prediction of sprawl (*Christiansen et al., 2011).* It is important to recognize that transportation is essential for the city and its surroundings. According to *Schoer (2006),* new transportation linkages enables development of economic fields, human habitats areas also encourages construction of related economic fields. Thus the interactions between sectors cause increase of sprawl. An investment in transportation infrastructure also promotes outward urban expansion due to decreasing commuting cost (*Bruecker, 2000*).

2.4.12 Single Detached Dwelling

In many cases, individuals built single detached dwelling instead of apartments. This also wastes considerable vertical space, lead to increase in the size of the city greatly *(Bhatt B, 2010)*.

2.4.13 Inconsistent Planning Policies

Exclusive zoning policies leads to separation of residential, commercial, industrial, institutional, and other land uses hence sprawl. A mixed policy is recommended to combat urban sprawl *(Bhatt B, 2010)*.

2.4.14 Road Width

The government does not allow the construction of skyscrapers if the site is not easily accessible. Narrow streets in urban areas limit the construction of skyscrapers, resulting in squandered upward space. This squander of vertical space has turned into even development. This is often a common issue in exceptionally ancient cities in numerous creating nations, where past organizers did not visualize future needs and did not arrange more extensive roads. Later street multiplication measures taken in numerous creating nations have fizzled due to their financial suggestions, as they require huge amounts of money to meet roadside homeowners and political constraints (*Bhatt B, 2010*).

2.4.15 Land Ownership

Large plot size is another reason for urban sprawl. Private landowners who own vast amounts of land may not want to sell their land. This also leads to outward growth, with undeveloped land remaining in the city (*Bhatt B, 2010).*

2.5 Impacts of Urban Sprawl

Urban sprawl has both advantages and disadvantages. However, the disadvantages are generally emphasized because this growth is often uncontrolled or unadjusted, and therefore the disadvantages outweigh the advantages (*Zhao P, 2013*).

2.5.1 Loss of Fertile Farmland

General urbanization and especially urban sprawl have contributed to the conversion of farmland and unbuilt space (*Zhang et al., 2008*). For USA alone, between 2000 and 2025, urban growth is projected to cover seven and five million acres of agricultural, environmentally sensitive, other lands respectively (*Burchell et al., 2005*).

2.5.2 Pollution

Zohoori et al. (2017) identifies population as the main problem of cities in developed countries. Sewage, industrial effluent, urban run-off and agricultural run-off are the sources of this problem. According to *Chen et al., (2019*) increased run-off due to urban development can have negative impacts on the downstream watershed hence the surrounding ecosystems.

2.5.3 Inadequate Urban Services

A significant number of urban populations live in slums around the city in poor state and unclean environments. Slum towns have dense settlements and are always with unclean air due to lack of utilities such as water, sewerage, garbage collection, electricity and paved roads, though cities are more economical than rural areas since they provide opportunities to people (*Bhatta B, 2010*).

2.5.4 Impact on Wildlife and Environment

In places where spreads are not managed, urban population and factory environments can transform environment (*Grimm et al., 2000*). Urban sprawl doesn't only reduce but also sustains forest cover, farmland, forests, and open spaces (*Pares-Ramos 2008*).

2.5.5 Increase in Heat

The positive relationship between surface temperature and closed surface clearly shows a temperature rise within the concrete regions. On warmer days, urban zones are 3.5-4.5 ° C (6-8 ° F) hotter than the surrounding zone. This is often an impact known as the urban heat island. This warm island effect is due to two factors. To begin with, dull surfaces such as roads and rooftops effectively absorb heat during daylight and re-radiate back as infrared radiation. Earth materials can reach temperatures of 50-70 ° F (28-39 ° C). Moment, town zones are generally short of biodiversity, particularly trees. As the city grows outwards, the warm island impact extends in both in geographic extent and in intensity (*Armson, 2012*).

2.5.6 Effect on Public and Social Health

Connection with nature is one of the special inspirations for relocation to the rural areas. Individuals ordinarily select to remain with trees, winged creatures, and blossoms; and those are more prominently helpful within the rural areas than in denser city regions. Moreover, contact with nature may offer benefits beyond the purely aesthetic; it may benefit both mental and physical health (*Czamanski et al., 2008*). The involvement of getting away from the turmoil of city ways of life to the rural areas, the sensation of non-violent asylum can be soothing and helpful to some individuals leading to urban sprawl.

2.5.7 Impact on Water Quality and Quantity

Urban sprawl contains a genuine effect on water quality and quality. Miles of roads, parking lots, and houses paved over the countryside, rainwater and snowmelt cannot enter the ground and recharge the aquifer. Urban development and urban sprawl lead to expanded fixing, which in turn leads to higher add up to runoff. In this manner, urban zones in flood-prone regions are at expanded chance of flooding, such as immersion and disintegration. As new development continues in the periphery of the existing urban landscape, the public, the government, planners and insurance companies are more and more concerned by flooding disasters and increasing damages (*Jacquin et al., 2008*).

2.5.8 Poor Air Quality

Urban sprawl is cited as a contributor of contamination since the car-dependent way of life forced by urban sprawl leads to expanded fossil fuel utilization and emissions of greenhouse gases. The chaotic spread of the city reduces the quality of the air by promoting the use of automobiles, thereby reducing gases in the atmosphere and microscopic particles (*Bhatta B, 2010*).

2.5.9 Energy Inefficiency

Crowding is an impact of higher densities. In spite of vehicles consuming more fuel in crowded areas, fuel use per capita is still absolutely less in those zones because few individuals drive. Urban sprawl brings more commuting from the suburbs to the city core and hence more fuel utilization. In addition, it also leads to traffic snarl-up caused by more cars driving greater distances leading to increase in fuel consumption. Consequently, detached houses accounts for 80 % of energy consumptions while multi-dwelling houses accounts for just 15 % because most energy used in households goes towards heating's. The heating appliances in multi-dwelling buildings are mostly smaller and share walls requiring minimal heating and cooling than in detached houses (*Nechyba et al., 2004*).

2.6 Methods of Detecting Urban Sprawl

Sprawled areas can be identified through visual interpretation of aerial photographs, and satellite remote sensing. Urban sustainability can be achieved by examining and minimizing the present and future patterns of urban areas. Mapping of urban expansion can show complex and simplified changes in urban areas (*Al-Sharif et al., 2017*).

2.6.1 Visual Interpretation

Objects are the basic elements that make up a scene, photograph, or image. For example, when you look at a photograph, you break it down into different objects and analyze it by understanding the scene using properties such as shape, texture, color, and context. The human brain has the unique ability to interpret the wealth of information content available in the scene and intuitively identify objects such as cars, homes, golf courses,

and other features that exist in the scene. In addition, our cognitive ability can instantly acquire the knowledge already stored in the brain and turn it into an expert rule base for interpreting images. Visual image interpretation has the limitation of displaying ranges and growth patterns.

2.6.2 Aerial Photography

Aerial photography has a very long archive record. The benefit of this method is that you can view a large area in a bird's eye view. This allows you to see the features of the Earth's surface in a spatial context. The photographs are able to show the extent of sprawl but not the patterns (*Paine et al., 2012*).

2.6.3 Satellite Remote Sensing

Remote sensing involves the interaction between the incident radiation and the target of interest. It also involves the sensing of emitted energy and the use of non-imaging sensors.

The use of satellite images to map cityscapes has been successful to varying degrees since the launch of first Landsat satellite producing imageries of 30m spatial resolution (*Gao, 2012*). With this low resolution images, the extent of sprawl can be shown but not the sprawl patterns. The larger the floor, the more mixed pixels instead of uniform pixels, so the image is not enough to show the non-uniformity in the city center.

The study by *Bhatta (2007)* demonstrates that LISS-IV images of 5.8m pixel size, though able to show the sprawl patterns, also suffers 15 to 20 percent overall accuracy when used for about the classification of cityscapes by pixels and mixed classes. Therefore, despite

the ease of interpretation by a human observer, very high spatial resolution is also undesirable. This is due to the increased variety of objects that can cause problems when automatic classification algorithms are applied to the data. Therefore the latest Sentinel-2 satellite data, with very high resolution of up to 10m, launched on July 2015 providing more fine remote sensing data for urban analysis (USGS, https://earthexplorer.usgs.gov/) was preferred for this research.

Object-based image analysis allows one to group pixels with similar spectral and spatial properties into identifiable objects. Therefore, applying the object-oriented paradigm to image analysis means analyzing the image in object space instead of pixel space, and objects can be used as image classification primitives instead of pixels. Image segmentation is the primary technique used to transform a scene or image into multiple objects. Compared to pixels, objects have many other attributes, such as shape, texture, and morphology, in addition to the spectral values that can be used in image analysis. The advantage of such an approach is that you can hide objects that you are not interested in on a large scale and focus on extracting the features that the end users are interested in. One can also leverage parent-child relationships to enhance the application's feature extraction process, such as change detection, by creating objects at different levels. OBIA uses all aspects of remote sensing, including spectral, spatial, contextual, structural, and temporal properties for feature extraction (*Blaschke et al., 2010*).

a) Nearest-Neighbor (NN) Supervised Classification

NN feature extraction algorithm uses samples of different classes to assign membership values. The procedure consists of two main steps. Train the system by giving the system a specific image object as a pattern and classifying the image objects in the domain based on the adjacency of the closest pattern. Image objects are classified by NN in a particular functional space using specific examples of classes of interest (eCognition Developer User Guide). If the closest pattern of an image object belongs to class A, the object is assigned to class A. The eCognition class assignment is determined by the assignment value in the range 0 (no allocation) to 1 (full allocation). If the image object is identical to the pattern, the unique membership value is 1.

When image object is differs from the sample, the feature space sample depends on the ambiguity of the feature space distance to the nearest sample of a class (*Boiman et al., 2008*). Figure 2.1 shows membership function created by NN. *2008*). Figure 2.1 shows

membership function created by NN.
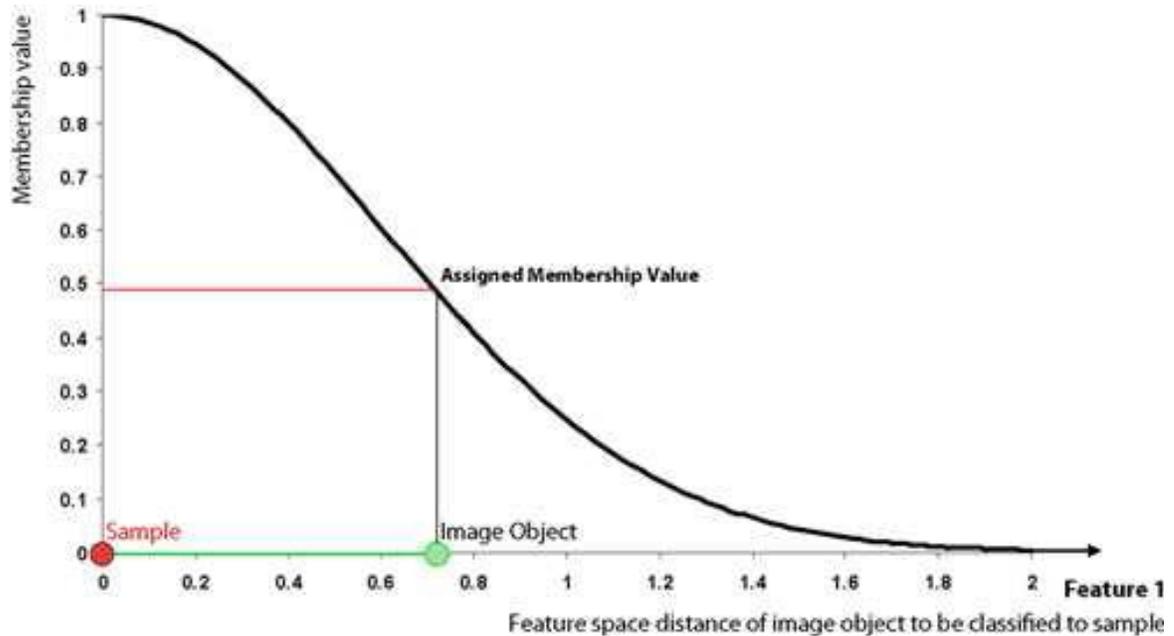
Figure 2.1: Membership Function created by NN classifier (e Cognition developer guide)

b) Rule-Based Supervised Classification

These are further rule-set defined in order to refine the objects. This can be done using customized feature which are either arithmetic or relational (relational features depend on other features). All customized features are based on the features that come with eCognition Developer. Arithmetic functions consist of existing functions, variables, and constants. These are combined using arithmetic operations and can be configured with several features. Relational features are used to compare a particular feature of an object to that of a related object of a particular class within a particular distance (*Jabari et al., 2013*). Related objects are neighbors, sub-objects of the parent object, or surrounding objects such as the entire image object layer. Relational are composed of only a single feature but refer to a group of related objects (*e Cognition developer guide, 2014*).

Modern space borne Synthetic Aperture Radar (SAR) sensors like TerraSAR-X and Cosmo-SkyMed provide georeferencing accuracy of one meter. PAMIR airborne sensor and SETHI airborne sensor achieve even accuracy (*Thiele et al., 2010*). In data of such kind, manmade structures like buildings, bridges and roads in urban areas become visible in detail independently from daylight or cloud coverage. *Wegner (2009)* notes that due to side-looking scene illumination by the SAR sensor, it complicates interpretability. Radar signal transit, shortening, shadowing, total internal reflection, and multi-bounce scattering make manual and automated analysis difficult, especially in densely populated urban areas with skyscrapers. These shortcomings can be partially overcome by using additional information such as topographic maps, optical images, or SAR acquisition from several aspects.

From the review of the methods, it is noted that radar images are preferred but since cannot be obtained easily due to cost implication, therefore use of the Sentinel-2 images for urban sprawl analysis was be employed for this study.

2.7 Techniques for Image Segmentation

Image segmentation refers to fragmenting satellite image to meaningful objects as per the criteria of homogeneity and heterogeneity. Satellite image objects are group of connected pixels in a scene. The segmented features should look a lot like a real ground object. The need for image segmentation is especially important for high frequency images of urban and suburban environments where the scene is very complex and has detailed structures. Different techniques are available for segmentation (Hands on exercise using *eCognition developer, 2014*).

2.7.1 Chess Board Segmentation Technique

Chess board segmentation divides the image into equal sized squares. In chess board, the problem is that, it divides the image into equal size and does not divide the picture on similarity basis so various objects are mixed and can't be differentiated. They have no well-defined boundaries in segments. It would be better if we would have regular sized and properly shaped parcels in an image of a planned settlement. Figure 2.2 show segmented image by chess board technique.
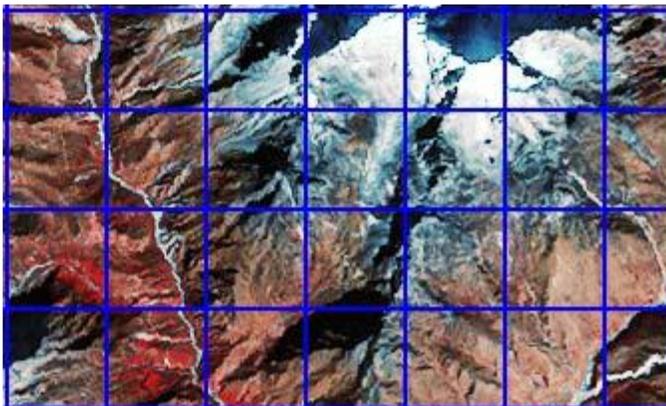
Figure 2.2: Image Segmentation by Chess Board Technique

(Source: Hands on exercise using eCognition developer, 2014).

2.7.2 Quad Tree Segmentation Technique

Quad tree segmentation divides an image into different sized square objects. It segments the image on the basis of similarity of spectral response. The region in the image segment will be formed and in the region of dissimilarity segments are small in size. Figure 2.3 show segmented image by Quad Tree Technique.
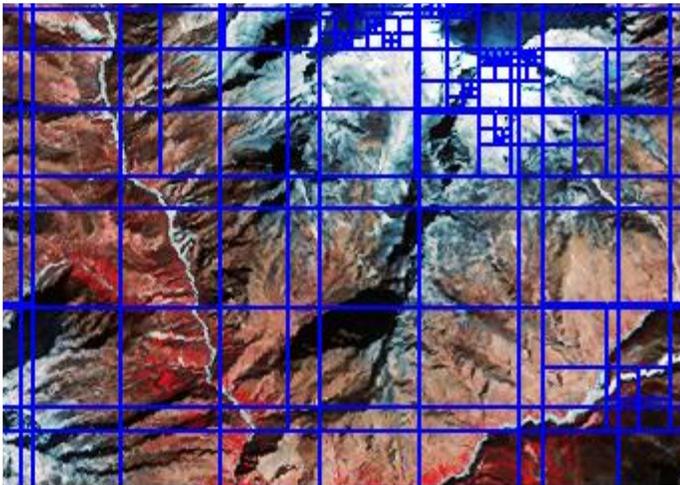
Figure 2.3: Image Segmentation by Quad Tree Technique

 (Source: Hands on exercise using eCognition developer, 2014).

2.7.3 Multiresolution Segmentation Technique

The Multi-Resolution (MR) segmentation algorithm is a technique for merging regions from bottom to top, and the next step in merging small image objects into large image objects is to merge single pixel objects into many objects. It starts with optimization technique that minimizes the average non-uniformity and maximizes the uniformity of each for a specific number of image objects. For this research MR segmentation method was used. Figure 2.4 shows image segmentation by multiresolution segmentation

techniques. Scale parameter was set to 35, shape to 0.3 and compactness to 0.6 in Idrisi Selva.
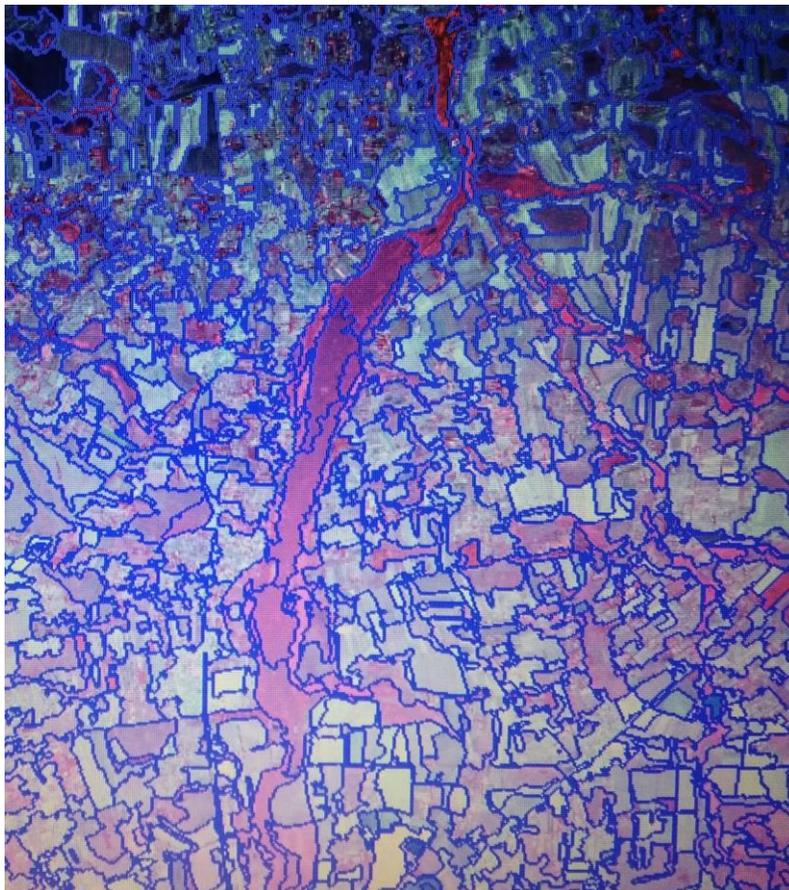
Figure 2.4: Image Segmentation by Multiresolution Technique
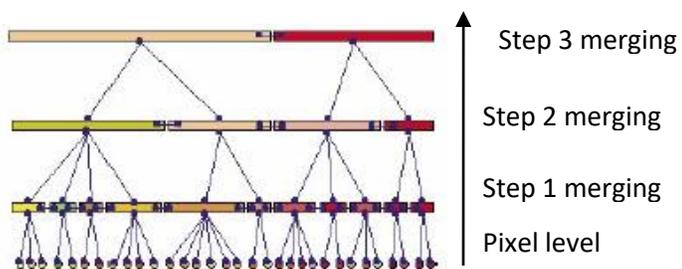
Figure 2.5: Image Object Hierarchy (eCognition guide, 2014)

2.7.4 Spectral Difference (SDS) or Contrast Split Segmentation Technique

SDS is the merging algorithm that merges adjacent features with a spectral value below a specified threshold that contains the maximum spectral difference to produce the final object. It divides the scene into light and dark objects based on the threshold that maximizes the contrast between the scenes. You already need a segmentation (level) to use this segmentation algorithm. Clear segments are formed between houses and their shadows, vegetation, roads. Houses and shadows area clearly segmented using this method.

2.8 Methods of Modelling Urban Sprawl

In 1960's spatial interaction models were developed (Lowry Pittsburgh model). These models were static and operated at aggregate level. *Joy Forrester, (1996*) proposed his model of urban growth dynamics. The model was non-spatial in nature and most of the model parameters were defined without any proof (*Williams, 2019*).

Till mid 1980's regional models which were based on regions described by several stocks as in population and job became the mainstream. The basic drawbacks of these regional models were that, they were hyper comprehensive i.e. they try to explain a lot of phenomenon about urban areas, they were data hungry, they were complicated and operated at a very gross level for example at city level and not at micro level.

Pooyandeh et al. (2007) analyzed the spatiotemporal model into two classes', that is, a) complex model and b) GIS time based model. Complexity models are further grouped into cellular automata, agent, neural network, and fractal-based modeling.

2.8.1 Cellular Automata Model

Towards 1980's Cellular Automata (CA) was developed as an alternative after development of computer technology. The advantages of CA were; spatial in nature, capability of linking macros to the micro-approach and integrating GIS and remote sensing techniques was inherently very dynamic, easy to understand and visualize (*Torrens et al., 2000*).

A CA is an entity that changes state based on its former state and the state immediately next to it, according to certain rules;

$\{S_{t+1}\} = f(\{S_t\}, \{I^h_t\}, \{V\})$

Where; $\{S_{t+1}\}$ is the state of the cell at time (t+1)

$\{S_t\}$ is the state of the cell at time (t)

$\{I^h_t\}$ refers to the neighborhood

$\{V\}$ refers to suitability of a cell for urban growth

f is the transition rule

h is the neighborhood size

Some of the problems faced in CA are; how to define transition rules and what should be the size and shape of the neighbor, that is, could it be 3×3, 5×5, rectangular or circular. A cellular automaton (CA) was developed by Ulam in 1940 for use in modeling land use change (*Mishra et al. (2016)*; *Parsa et al. (2016)*). Later, Tobler (2014) applied CA in

location modeling (*Arsanjani et al., 2013*). CA is mostly used in spatial models (*Halmy et al., 2015*) to predict later land use urban sprawl.

The basic principle of CA is that changes in land use at any site (cell) can be explained by changes in the current state and adjacent cells (*Koomen and Borsboomvan Beurden, 2011*). Figure 2.6 shows components of cellular automata. A study by *Garcia et al. (2012)* comparing CA model for simulating LULC of small urban centers in Galizia, NW Spain shows that models that uses diversity of land use captures good land use changes.
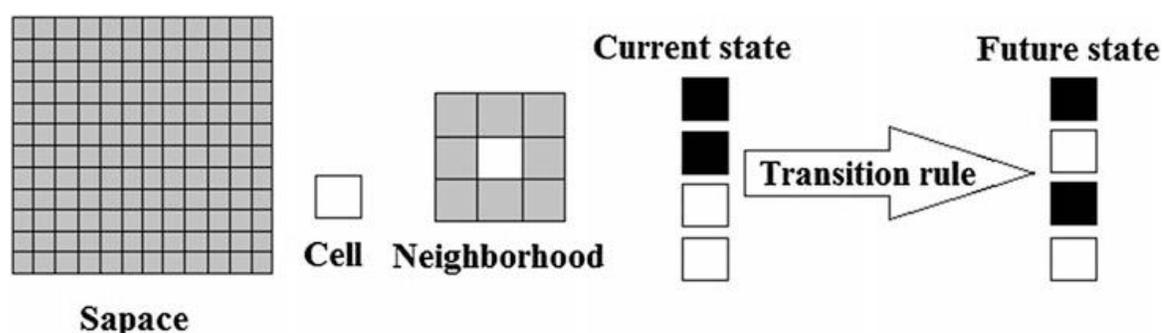
Figure 2.6: Components of Cellular Automata (Biswajeet Pradhan, 2017)

2.8.2 Markov Chain Model

Markov chain model is commonly used to simulate changes, trends, and dimensions of urban growth though the models cannot simulate changes in spatial trends (*Guan et al., 2011*). Markov chains are powerful models that can simulate changes in land use and coverage. Andrei A. Markov, a Russian mathematician was the first to present Markov chain (MC) model in 1970. Few years later, Burnham used MC in 1973 for land use modelling as reported by *Mishra et al. (2016)*; *Parsa et al. (2016). de et al. (2003)* notes that it's a stochastic method for predicting one land cover being modified to another. According to *Lopez et al. (2001),*

Yan et al. (2005) and *Sang et al. (2011*) the method is regularly implemented in modelling and simulation, especially the changes, dimensions and dispositions of city land use.

Koomen et al. (2011) consequently proposes that integration with different spatial-primarily based totally strategies is required.

2.8.3 CA-Markov Chain Model

The CA and Markov chain models integrated together can adequately integrate this type of GIS with remote sensing models and data, providing an effective method for estimating quantities and modeling spatiotemporal dynamic. (*Al-Sharif and Prahan, 2013*).

CA dynamic simulation integrated with Markov chains statistical and empirical models has overcome the lack of a single model. Each of those difficulty or statistical simulations is ultimately addressed and instead complements each other (*Aburas et al., 2017*).

According to *Mishra et al. (2016)*, a combined model of cellular automata and Markov chains, has advantage of modeling land-use changes. There is no specification for the spatial dispersion of each event within the land use category, as there's no spatial premise for the results when Markov chains are used and they are potentially categorically accurate (*Arsanjani et al., 2013*). Adding cellular automata to a Markov model results in spatial transitions that can occur in specific regions over specific periods. In other words, the change set from the Markov chain model is geographically referenced and spatially created by the cellular automaton (*Mishra and Rai, 2016*).

Therefore, the CA-Markov model is considered to be a robust approach for modeling LULC dynamics and spatial and temporal dynamics (*Arsanjani et al., 2013; Mishra and Rai, 2016*; *Subedi et al., 2013*). To better understand the changing patterns of urban growth, urban growth drivers such as physical, environmental, socio-economic and practical forces need to be applied to the CA Markov chain model forecasting process. To further improve the performance, CA-Markov chain model needs to be integrated with other models such as analytic hierarchy process (AHP), frequency ratio (FR), and logistic regression model (LR) (*Al-Sharif and Pradhan, 2013*). *Koko et al. (2020)* used CA-Markov model in monitoring and forecasting LULC change in Zaria city, Nigeria and revealed that barren land will be lost to built-up and vegetation for the next 30 years by 65.88% and 29.95% respectively during 2035 and 2050.

2.8.4 Agent Based Model (ABM)

ABM is an approach based on the science of manufactured insights and object-oriented innovation for modeling the intelligent of person substances within the framework (*Macal et al., 2006*). ABM comprises of assorted and interconnected operators. The experts are decision-making components recognized by a set of conditions permitting operators to gather data, handle input, and impact changes within the outside environment (*Zhai et al., 2020*). ABM employs computer program substances or operators that have goal-oriented behavior (objectives) and can associated with and alter the environment whereas seeking after the objective. ABM has been used for simulating occurrences of residential crime at personal level giving promising results of use of this model (*Malleson et al., 2010*).

2.8.5 Artificial Neural Network (ANN) Based Model

Artificial neural network models attempt to mimic the structure of the human brain through mathematics. The ANN model tries to show a scientific or computational aspect of a biological neural network. This can be an interconnected bunch of counterfeit neurons that handle data employing a connectionist approach to computation (*Zhang et al., 2020*). *Afram et al. (2017)* used ANN model predictive control and optimization of systems in residential house in Ontario found that ANN would save 6-73% operating cost compared to fixed set point.

2.9 Land Use and Urban Growth Modelling Theories

2.9.1 Growth Pole

Growth pole model refers to congregating of activities and the concentration of growth in poles, from where the diffusion of growth is expected to occur to the peri-urban area (*Ke et al., 2010).* The growth pole strategy has ruled the field of policy practice at an international level during the last two decades and most specifically after World War Two. In the late nineteen sixties and early nineteen seventies, industrialized and growing nations alike implemented the growth pole idea of their urban, regional, and country wide improvement planning. The model is applied depending on a particular characteristic and the stage of development of a county.

2.9.2 Johann Heinrich Von Thunen Theory

Developed by *Johann Heinrich von Thunen*, this theory clarifies how market forms impact and control the spatial dissemination of land-use changes and urban development *(Al-Sharif, 2017)*.

2.9.3 Concentric Zone Theory

Proposed by *Burgess in 1926*, it describes the town as a several circular land zones centered on the city core (*King, 2020*).

2.9.4 Central Place Theory

It was formulated by *Walter Christaller in 1933* which clarifies the size, number, spatial dissemination, and progressive course of action of cities (*King, 2020*). It is additionally concerned with the conveyance of retail and discount regulatory arrive employments and community offices.

2.9.5 Sector Theory

Functional land-use extending from the CBD into wedge-shaped zones that radiate outward is based sector theory (*Torrens, 2000*).

2.9.6 Multiple Nuclei Theory

Hubs that acts as centers of cohesive growth not just CBD (*Torrens, 2000*) is based on multi nuclei theory.

2.9.7 Bid-Rent Theory

Transportation among other urban factors is based on Alonso's theory. Rents usually try to fall proportionally as distance from the market increase, transportation costs also increase with. Figure 2.7 shows a past urban growth model.
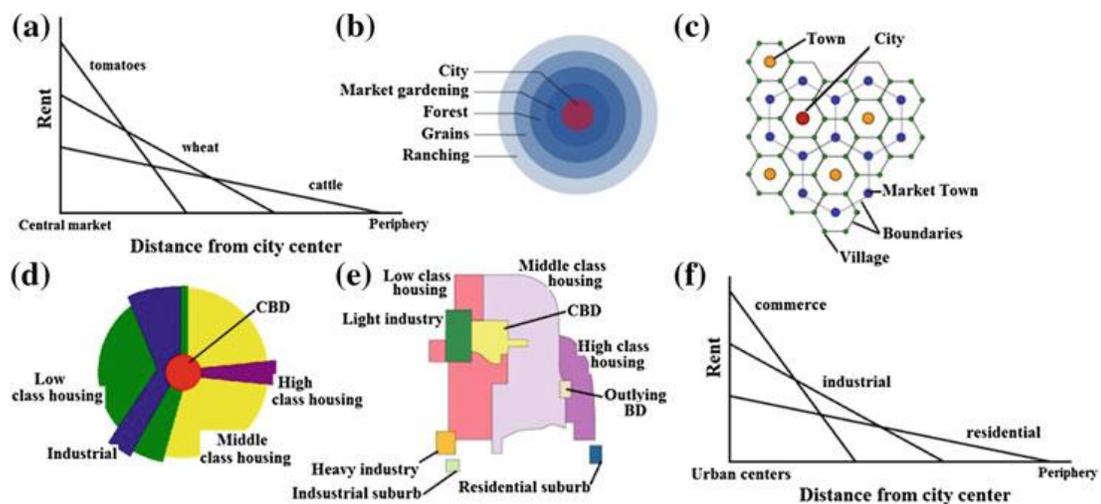
Figure 2.7: Historical Urban Growth Modelling: a) Johann Heinrich Von Thunen Theory, b) Concentric Zone Theory, c) Central Place Theory, d) Sector Theory, e) Multiple Nuclei Theory and f) Bid-Rent Theory (*Abdullahi et al., 2017*)

2.10 Principles of Land Use Change Prediction Model

Four key principles underpin all land cover prediction models (*Koomen and Borsboomvan Beurden, 2011*). These are historical bases, suitability bases, neighborhood bases and actor base.

2.10.1 Historical Bases

Loonen et al. (2007) demonstrate that background information helps predict future changes in land use. The past being the key to the future is the concept behind the historical foundation.

2.10.2 Suitability Bases

It consists of multiple factors of a property (physical, social, environmental, among others) to evaluate an assignment to a particular reason. For example, site suitability assessment for specific applications for example hospitals, schools (*Abdullahi et al., 2014*). Therefore, the main thing is to increase profits and reduce adverse impacts.

2.10.3 Neighborhood Bases

It addresses the neighborhood interactions of each pixel that affect the change from one land use to another. *Kocabas and Dragicevic (2007); Zhang et al. (2008)* agreed that most of researches are based cellular concept implemented through the cellular automata approach.

2.10.4 Actor Bases

Multiple actors or agents are assumed to be result of interactions in land use/cover changes. The study applied both neighborhood and actors' bases to generate models predicting future urban sprawl around Eldoret town.

2.11 Empirical Studies on Urban Growth and Modelling

This sub topic highlights some of the urban growth and modelling studies related to the topic of study.

2.11.1 Studies of Urban Sprawl

Bhatta et al. (2010a) explains how to use compounded information obtained from satellite data to calculate the future growth from the current urban growth. The findings shows that level of urban sprawl, level of freedom and quality of urban sprawl can be calculated. All of these controls were applied in three different areas, patterns, processes, and as a whole. Degrees of freedom indicate deviation from the observed expected growth of the city. The higher the degree of freedom in the zone, the more unstable the development within the zone over time, and the higher the degree of freedom from the period thus higher the variability between the zones in the growth of the city. *Bhatta*

(2009a) shows how to analyze and model urban growth using accumulated data obtained from remote sensing images. Population and urban growth rate; household proportion and urban proportion. Urban growth, existing development, arable land, changes in the number of employees.

Addison et al. (2013) used land data on housing conversion to study how externalities of land use affect the speed of development, manage urban growth, and change policy designs to maintain open spaces. Several smart growth strategies have been found to have a significant impact on land transformation, including clustering development strategies that focus development and create conserved open spaces.

Wilson et al. (2003) uses LULC information obtained in satellite images to find geographic extents and patterns. The model isolates three classes of vacant lots and prefabricated lots on both dates based on neighborhood information. These two images are used to create a more detailed change map than traditional change analysis by using undeveloped land classes and incorporating contextual information. The map serves as an input to the urban growth analysis and identifies five categories of growth. Fill, expand, isolate, linear branch, and grouped branches.

Sutton (2003) measured the urban area using satellite images taken at night by comparing nighttime satellite images to population density. As a result of this comparison, both the area and population of all urban areas were measured.

2.11.2 Studies on Urban Growth Modelling

Liu et al. (2019) uses the SLEUTH (Slope, Land Use, Constraints, City, Roads, Hill Shade) model, to simulate the growth of the city in various scenarios of eastern China Hefei from 2015 to 2040. Historical growth scenarios, city planning growth scenarios, and land suitability growth scenarios were considered and he concluded that by 2040, urban areas will increase to 1434 km2 in historical growth scenarios, 1190 km2 in urban planning growth scenarios, and 1217 km2 in land-adapted growth scenarios, according to forecasts.

Samat (2009) evaluated urban spatial expansion using a GIS and a CA-Markov model. The findings indicate that this model might be used in conjunction with current planning documents to assess the influence of a proposed planning strategy on the existing urban landscape.

Using remote sensing and GIS techniques in monitoring and modeling urban sprawl in Ajmer, India, *Jat et al. (2008*) used Landsat MSS, TM, ETM+, and IRS LISS-III to extract information related to sprawl, area of impervious surfaces, and their geographic and temporal variability. In order to measure the urban form or impervious area, they used Shannon's entropy and landscape metrics to compute patchiness and map density in terms of spatial phenomena. The association between urban sprawl and its causative elements has also been established using multivariate statistical approaches. Over a 25-year period, Shannon's entropy and landscape metrics indicated the city's spatial dispersion (1977-2002).

2.12 Strategies to Counter Urban Sprawl

Some of the policies to control urban sprawl and address its impacts are worth discussing.

2.12.1 Promoting levels of urban density and fragmentation that are socially desirable

High density and proximity are crucial features of sustainable urban development; however there are some cautions to be aware of.

2.12.2 Reform Urban Containment Policies

The most direct form of governmental intervention to control urban expansion is urban containment policies. They essentially impose bounds to urban expansion, with the goal of protecting neighboring forestland and farmland, lowering public service costs, and encouraging infill development on vacant land inside the restricted region.

2.12.3 Relax the restrictions on maximum density

Building height restrictions, or limits on building Floor-to-Area Ratios, are the most common examples of legislation that impede densification (*Bertaud and Brueckner, 2005; Brueckner and Sridhar, 2012*). Despite their utility in certain situations, like as near airports, historic buildings, or other cultural assets, strict maximum density limits are frequently unjustified.

2.12.4 Reform assets taxation to higher mirror the social fee of positive city improvement Patterns

Property taxes are the most typically used instrument applied to land use. A property tax is a recurrent advert valorem tax on immovable assets, normally levied with the aid of using the nearby authority of the jurisdiction wherein the assets is located. In practice, the

number one goal of property taxation has been to elevate public sales for the financing of nearby services (*Brandt, 2014*), in preference to deal with the bad externalities of city improvement. For example, in Italy, assets taxes accounted for approximately 48% of overall Municipal sales in 2010 (*Ermini and Santolini, 2017*). In most countries, assets taxes are levied on each land and land improvements, that is, homes and different structures (*Bird and Slack, 2004).*

2.12.5 Using of split property tax

A more targeted financial tool to promote high density is split or two split property tax, which is the value of land rather than the value of buildings and other land improvements. The higher land value in the city center discourages living space (or undeveloped) land there, thus reducing pressure on development in the suburbs of provincial (*Slack, 2002*).

2.12.6 Develop incentive-primarily based total mechanisms to save on conversion of farmland and forestland

In many cities, the evaluation of assets values or the assets tax charge varies in step with land use. For example, preferential, or use cost, tax evaluation is a generally used tool within United States (*Bengston et al., 2004*). It gives tax incentives to proprietors of farmland; forestland and different kinds of undeveloped land to hold it in its contemporary use, in place of promote it for city development. This is carried out via way of means of taxing land at a lower cost when used for, for example, agriculture or forestry compared to when it is allocated to residential or industrial uses (*Bengston et al., 2004*).

2.12.7 Developing policies based on development rights

 Strategies Development rights-based strategies are based on the idea that ownership of land is equivalent to owning a set of separable rights such as property (*Musole, 2009*). Obtaining building rights is a frequently used means of securing open space. The landowner sells the development rights to the government (or a private nonprofit) and the land is permanently reserved for conservation purposes. In areas where development pressure is low, government purchases of development rights can be much cheaper than public land purchases (*Bengston et al., 2004*).

2.12.8 Development taxes, which provide developers with an incentive to provide public infrastructure for new development

Are fees charged by the developer to cover the cost of capital for providing public infrastructure for new development (*Bengston et al., 2004; Roberts, 2013, p.319*). Although primarily it is used to fund the development of public infrastructure, development taxes can serve as a powerful tool for directing urban expansion to areas close to existing infrastructure (*Bengston. et al., 2004*). Due to the low cost of building new infrastructure in these areas, developers are indirectly encouraged to build on adjacent land**.**

2.13 Knowledge Gap and Conceptual Framework

From the above review, most of the researches done are about the extent of urban sprawl only without looking at the factors supporting the sprawl in Kenya specifically around Eldoret Town. Therefore, this study attempts to fill the knowledge gap.

Satellite data

- Landsat 7 ETM+ image of 2000
- Sentinel-2 images of 2016 &

Ancillary data

- Road network (2000-2020)
- Elevation
- Slope
- Employment centers (2020)
- Population (2000-2020)
- Powerline network (2000-2020)
- Water network (2000-2020)
- Sub-locations shapefile (2019)
- Restricted areas (2020)

Image Pre-processing

- Layer stacking
- Pan sharpening,
- Mosaicking
- Sub setting
- Geometric correction

Image Segmentation

- Multiresolution Segmentation
- Spectral Difference Segmentation

Land cover classification scheme

Rule- based classification

Accuracy assessment

Thematic raster/factors maps

- Road (2000-2020)
- Population density (2000-2020)
- Slope
- Elevation
- Restricted area (2020)
- Powerline (2000-2020)
- Water network (2000-2020)
- Employment centers (2020)

LULC change detection analysis (2000-2016, 2016-2020, 2000-2020)

- Analytical Hierarchy Process

CA-Markov model

Results

- Urban Sprawl Prediction map for 2029

Figure 2.8: Methodological Flowchart Diagram for the Study

CHAPTER THREE

MATERIALS AND METHODS

3.1 Introduction

The section describes study area, datasets, research design, how the data was collected and analyzed in order to address the project objectives that involved (determination of urban sprawl patterns, factors that support their growth and prediction of potential sprawl patterns) in Eldoret Town.

3.2 Study Area

The study area are areas around a gazetted Eldoret Municipality boundary in Uasin Gishu County, Kenya, bounded by Latitudes 00°52' 00"N and 00°18'00"N and Longitudes 34°51'00"E and 35°31'00"E covering approximately 1973km^2 (Figure 3.1).
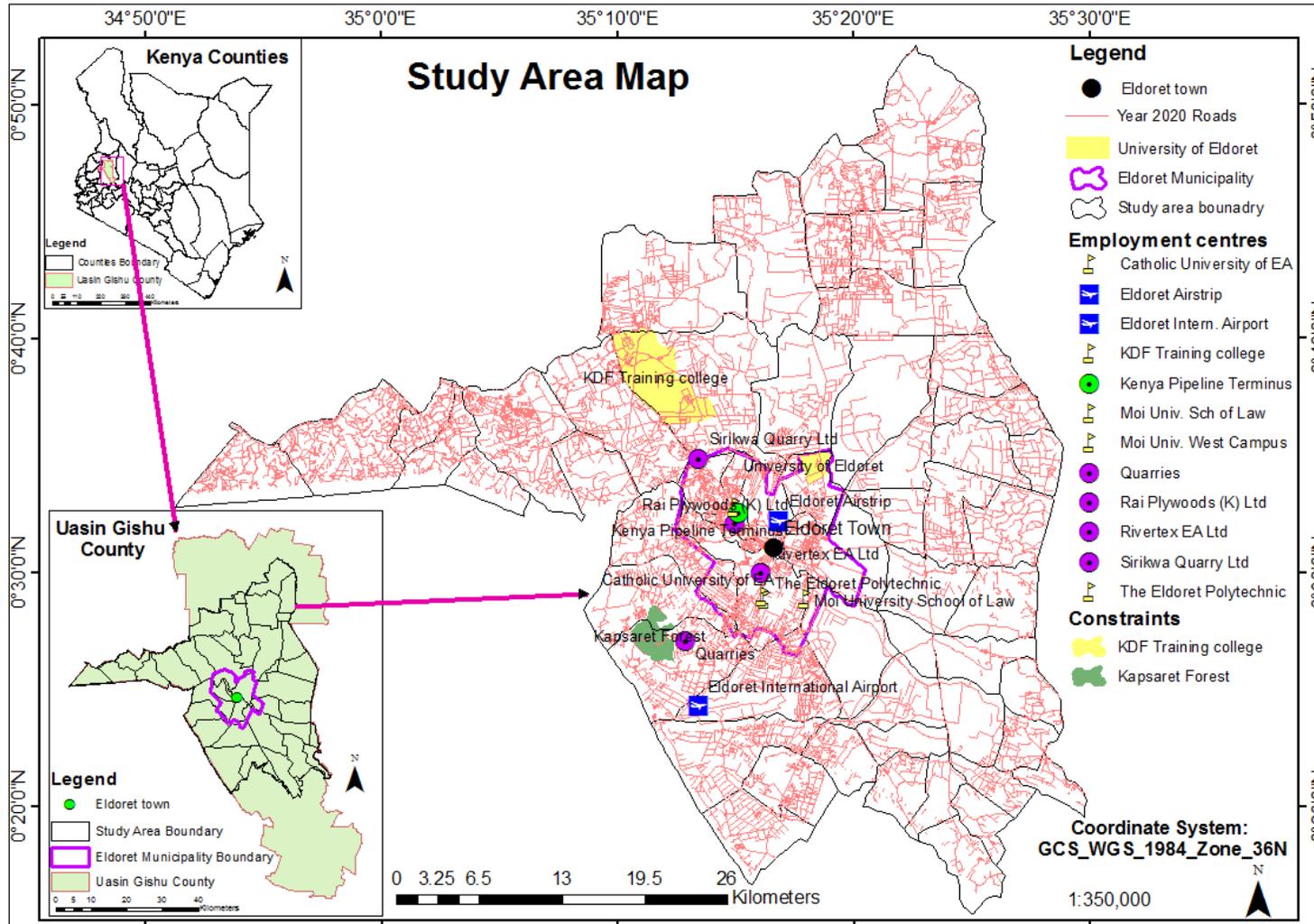
Figure 3.1: Location of the Study Area

3.3 Biophysical Characteristics

Biophysical characteristics of the study area comprise of its geology, geomorphologic features, drainage, soils, vegetation and climate (*Benjamin, 2004*).

3.3.1 Geology

The Uasin Gishu Plateau is the most extensive single physiographical unit in the area and is solely determined by the present limits of the Uasin Gishu phonolite lava. The edge of the lava outcrops are deeply incised by the main rivers and their tributaries, so that prominent escarpments overlook the Nzoia valley in the North, and the Sosiani valley in the West.

In the vicinity of Eldoret, the plateau is approximately 2089m above sea level; it rises progressively towards the rift valley at Elgeyo escarpment some twenty kilometers to the East of Eldoret, where at Kamorin it reaches an elevation of about 2390m. The present surface of the gradient is directed towards the North-West, so that elevations at the North-Western limits of the plateau, for instance near Hoey's Bridge, are roughly 298m less than those near Eldoret. The comparatively flat profile of the plateau is interrupted at Sergoit (2349m) and Karuna (2296m), where inliers of Basement System gneisses and quartzites protrudes through the lava flows and stand above the level of the surrounding county. Geology affects settlement since people settle where there are natural resources

to build their homes, land that can provide farmland and water and to places that are easily accessible to them (*Jackson et al., 2005*).

The Uasin Gishu phonoloite rocks forms into soil through the process of weathering encouraging plant growth and improving land productivity. These attract settlement patterns in areas that were initially inhabitable hence urban sprawl. Figure 3.2 shows the geological features of the area.
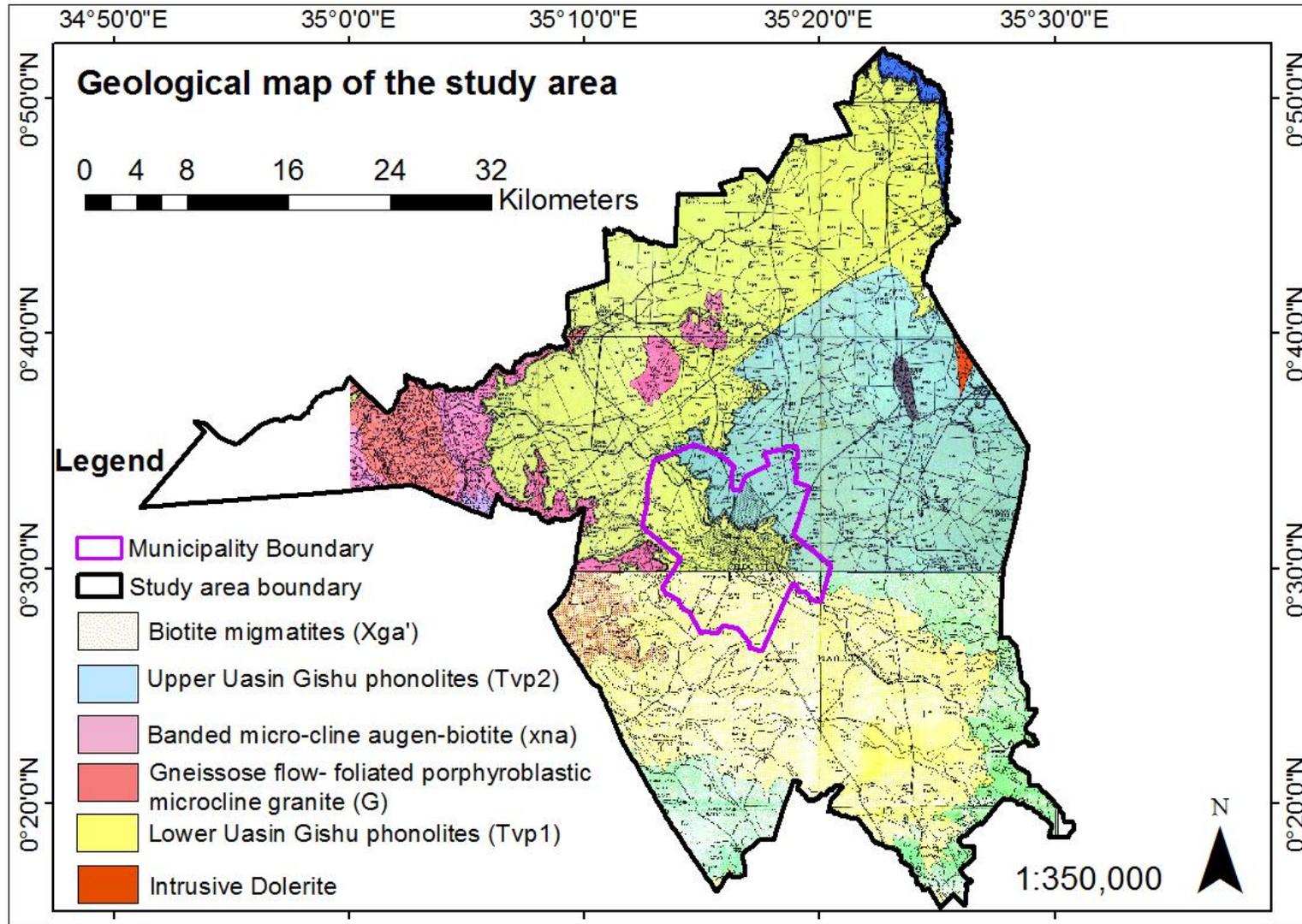
Figure 3.2: Geological Map of the study Area

3.3.2 Drainage

The Southern part is drained by Kerita, Naru and Nureri tributary rivers coming from Tingwa Forest in Keiyo Escarpment which confluence forming River Kipkaren which later confluences with River Sosiani at Kiboloss market and eventually joins River Nzoia after Lugari market. The South-Western part of the area is drained by Endoroto, Kipsinandi and Ellegirini tributary rivers coming from Kaptagat Forest in Elgeyo Escarpment. They confluence at two river dam forming River Sosiani which flows westward through Eldoret town to Selby Falls where it plunges from the edge of the Uasin Gishu phonolite onto metamorphic rocks and then flows along the foot of the lava escarpment to Turbo bridge where it confluences with River Sergoit. It then flows up to Kibollos market where it confluences again with River Kipkaren. The North-Western part is drained by River Chepkoilel which flows into Marura swamp which extends up to Kaprobu Bridge. After the bridge, the name changes to River Sergoit which flows through Soy Bridge to Turbo Bridge where it confluences with River Sosiani. The map was made from DEM image of the study area using ArcMap's hydrology tool. Figure 3.3 shows drainage system of the study area.
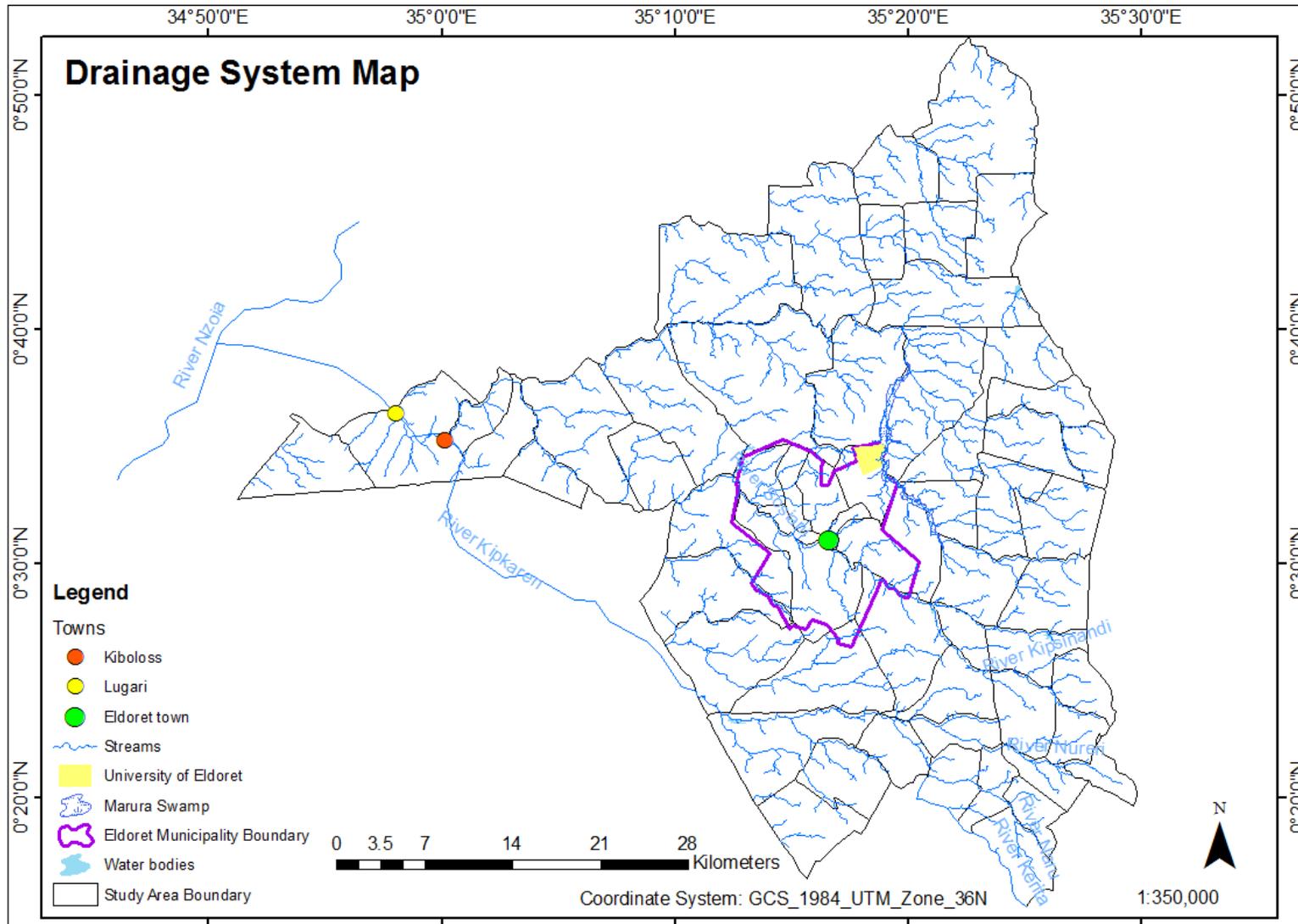
Figure 3.3: Drainage Systems Map of the Study Area

3.3.3 Climate

Most location of the study area, that is, western part (Turbo area), eastern part (Ainabkoi and moiben area), northern part (Ziwa area) and southern (Kapseret and Cheptiret area) receives an average rainfall of between 625 mm to 1,560 mm, with two distinct peaks between March and June, August and September. The drying period occurs between November and February. Temperatures are between 7°C and 29°C.   In general, the study area is a potential area for agriculture and these climatic conditions are suitable for livestock, crops and fish farming. The main cereal crops grown in these locations of the study area are maize and wheat (*Kibii et al., 2021*).

3.3.4 Vegetation

The above climatic environment support the natural growth of savannah trees over much of the region, but with agricultural development the bushes have been progressively cleared and land placed under the plough, so the original character of the country can only be seen outside the arable areas.

3.3.5 Soils

The soils in the area are thin because of the presence of underlying Uasin Gishu phonolite rock. The dominant soil types are Orthic Ferralsol (Fo) and Humic Nitosols (Hn). The map was made from scanned copy of Kenya soils map obtained from Kenya Soil Survey Office by clipping it using the shapefile of the study area then digitizing the dominant soil types. Figure 3.4 shows soil map of the study area.
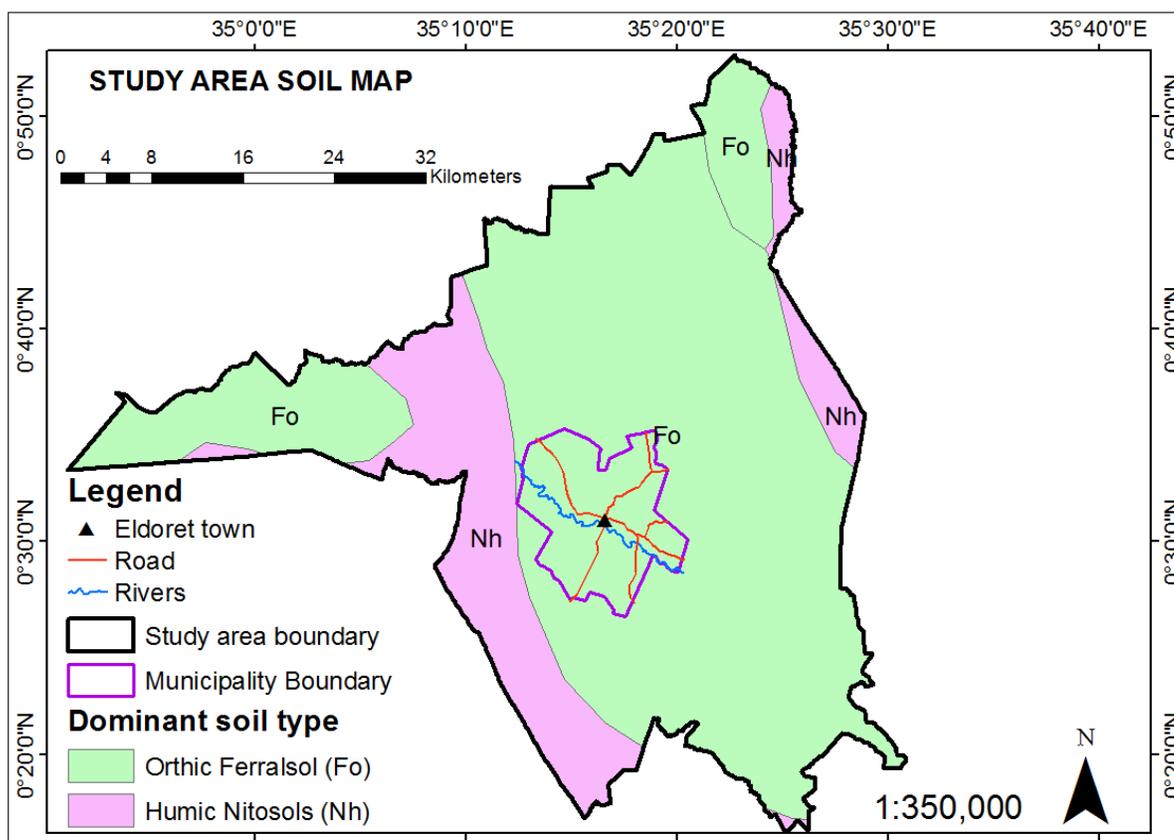
Figure 3.4: Soil Map of the Study Area

3.4 Socio-economic Characteristics

The socio-economic environment is characterized by variations in both demographic and land use activities. These are described below.

3.4.1 Population

The interpolated total population of the 58 sub-location covering the study area was 870,269 in 2020, compared to 774,200 in 2016. If the census population growth rate is about 2.977% per year, the total population of the survey area is projected to increase to approximately 1,132,281 by 2029. Population growth was assumed to be exponential,

and annual growth was calculated using 2019 data using the following equation (Angel et al. 2005).

''$P_{t+10}=P_t (1+g)^{10}$.................................equation 3.1''

Where;

P_t= the population of census year t,

P_{t+10}= the population of census year t+10, and

g = annual population growth rate between census years t and t+10 divided by 100

Interpolation of 2029 (P_{2029}) population was done using the formula:

$P_{2029}= P_{2019} (1+g)^{2029-2019} \approx 1,132,281$

g= $\{(P_2 \div P_1)^{1/t}-1 \times 100\}$

Where t is the number of years of census period (2009(P_1) to 2019(P_2) =10), P_2 is the population at the end of census period (2019=845,188), P_1 is the population at start of census period (2009=630,888).

The growth rate (g) between 2019 and 2009 was calculated as follows:

$\{(845,188 \div 630,888)^{0.1}-1\} \times 100 \approx 2.9674850941\%$ (growth rate between years 2009 to 2019).

3.4.2 Land Use Activities

Land use activities in the study area are heterogeneous comprising of commercial, residential, educational, industrial, recreational, public purpose, public utility and agriculture. However, the distributions and intensities of land use activities vary across space in the study area. In the CBD, there is a mixture of land use activities while along Uganda road (A104), that is, Maili nne- Annex stretch, along Kisumu road, along Iten road, along Ziwa road and along Eldama Ravine road, the land use activities changes gradually to agriculture as one move away from the Eldoret Town's CBD. Figure 3.6 shows diversity of land use features in Eldoret Town.

Texture was used to separate image curves that separate different textures. It gives information about the spatial arrangement of colors on an image. For example, on the image below, texture of forest is different from that of built-up areas, roads, farmlands. Pattern is used to separate repeated objects of similar tones and texture for example the built-up area in image below.   Figure 3.5 shows a variety of land use features in a section of Eldoret Town.
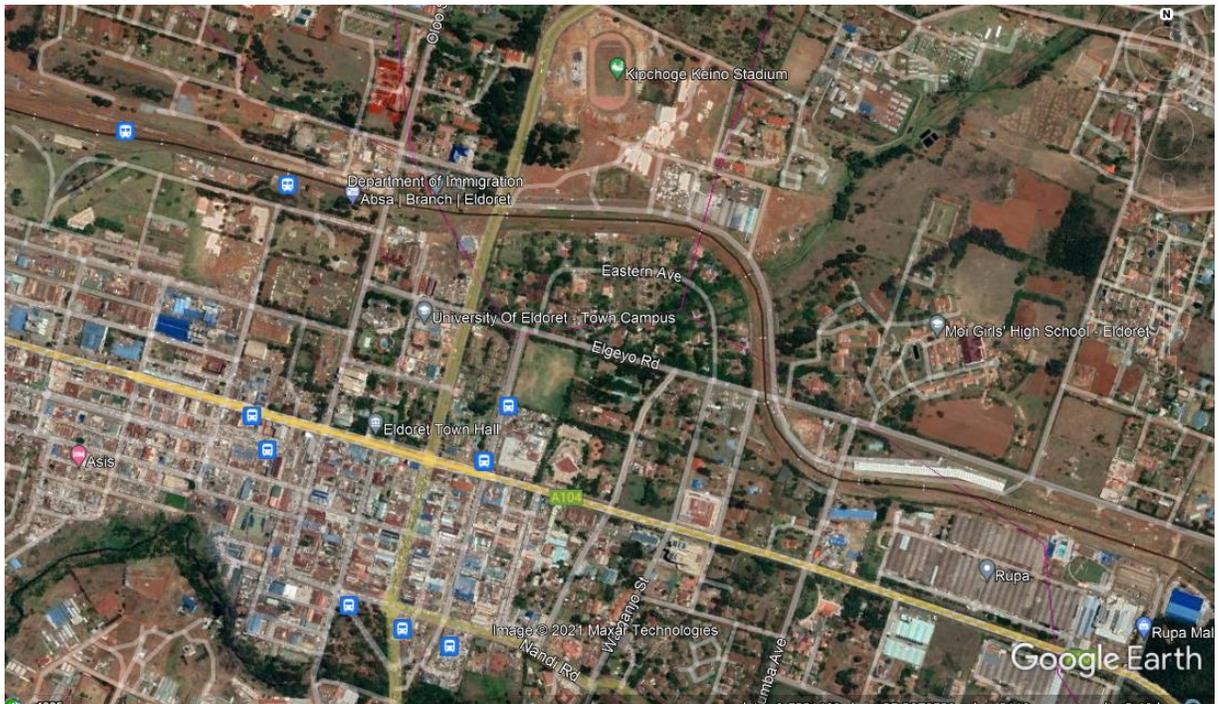
Figure 3.5: Google Earth Image of Land Use Activities in Eldoret town

3.5 Data and Data Processing

The data in this study are from both primary and secondary sources as shown in Table 3.1.

Table 3.1: Characteristics of Datasets Used

S/No.	Type of data used	Scale/Resolution	WRS_path/row, Granules/Tiles	Date of acquisition
1.	Landsat 7 ETM+ image	30m and 15m	169/060 and 170/060	27th Jan. 2000 and 6th March,2000
2.	Sentinel-2 image	10m	T36NYF-100×100km	13th Dec. 2016
3.	Sentinel-2 image	10m	T36NYF-100×100km	12th Dec. 2020
4.	Sub-locations shapefile			2019
5.	Roads network maps			2000, 2016 and 2020
6.	Census data	Decadal		1999, 2009 and 2019
7.	Powerline network map			2000, 2016 and 2020
8.	Water network maps			2000, 2016 and 2020
9.	Employment centers map			2000, 2016 and 2020
10.	Slope map and elevation map			2020
11.	Restricted areas map			2020

3.5.1 Primary Data

The data obtained from primary sources include; land use categories information which were obtained by classifying four sets of images i.e. two Landsat 7 ETM+ image for 27th January 2000 and 6th March 2000 and two Sentinel-2 images for 13th December 2016 and 12th December 2020 acquired from USGS website (USGS, https://earthexplorer.usgs.gov/). Five Landsat 7ETM+ bands layer stacked to form a composite image were bands 1,2,3,4 and 5 corresponding to blue, green, red, NIR and SWIR colours all at 30m spatial resolution. Pan-band 8 at 15m spatial resolution was used to pan-sharpen the composite image to 15m spatial resolution. For Sentinel-2 image, four bands at 10m spatial resolution layer stacked were bands 2,3,4,8 corresponding to blue, green, red, NIR colours and one band (band 12-SWIR) at 20m spatial resolution which was re-sampled to 10m spatial resolution as shown in Table 3.2. The study area straddles two Landsat 7 images which were mosaicked and clipped to cover study area. Sentinel-2 images for 2016 and 2020 were covering the whole study area hence there was no need of mosaicking. Geometric correction was done on the composite 2016 and 2020 Sentinel-2 Joint Photogrammetric Group (JPG) imageries in order to georeference them to match the Universal Transverse Mercator (UTM), World Geodetic System (WGS) 1984 map projection. For Landsat 7 ETM+ 2000 images, there was no need of georeferencing since they were downloaded auto georeferenced. All imageries and ancillary datasets were subset using shapefile of the study area in order to limit the study only to the desired extent. The specific bands used are shown in Table 3.2.

Table 3.2: Spectral and Spatial details of Sentinel 2 and Landsat 7 ETM+ imageries bands layer stacked in the study

Sentinel 2 Bands			
Band	**Description**	**Wavelength (µm)**	**Resolution (m)**
Band 2	Blue	0.490	10
Band 3	Green	0.560	10
Band 4	Red	0.665	10
Band 8	NIR (near infra-red)	0.842	10
Band 12	SWIR	2.190	20
Landsat 7 ETM+ Bands			
Band	**Description**	**Wavelength (micrometers)**	**Geometric Resolution**
Band 1	Blue	0.452-0.514	30
Band 2	Green	0.519-0.601	30
Band 3	Red	0.631-0.692	30
Band 4	NIR	0.772-0.898	30
Band 5	SWIR	1.547-1.748	30
Band 8	Panchromatic	0.515-0.896	15

Source: United State Geological Survey (USGS)

Road network data for the three study years (2000, 2016 and 2020) were digitized from their respective high resolution Google Earth images. Employment centers data were obtained through field data collection using Mobile Mapper 50 hand held GPS.

Water line supply and distribution network data was obtained from ELDOWAS GIS Department. In the attribute table, there was a field named Pipe Type with four record types namely; Accbestals (AC), Galvanised Iron (GI), Polyvinyl Chloride (PVC) and HDPE. From the information obtained from experts in the GIS Laboratory, AC and GI

pipe types were in use earlier than the year 2000, with PVC pipe type in use between year 2000 and 2019 and finally High Density Polyethylene (HDPE) pipe type used from year 2019 to date.

Powerline networks data were obtained from KPLC Eldoret office GIS facility database Department (FDB) and were transformed to WGS 1984 UTM Zone 36N in order to match the others since the three shapefiles were in Arc1960 UTM Zone 37S.

Slope and elevation data were derived from 30m Digital Elevation Model (DEM) from Shuttle Radar Topography Mission (SRTM) USGS website (USGS, https://earthexplorer.usgs.gov/). Data on areas not available for development, that is, restricted by physical, political and economic factors were collected from geographic locations using Mobile Mapper 50 hand held GPS.

3.5.2 Secondary Data

The secondary datasets used included; census and sub-locations datasets from Kenya National Bureau of Statistics (KNBS).

3.6 Research Design

Predictive research design was used in this study to determine the growth spots and predict the future planning urban growth pattern (*Creswell et al., 2003*). This research design involved;

  a) Determination of base conditions of growth patterns

  b) Determination of trends of these growth patterns

  c) Using the base and trends to predict future scenarios of growth patterns

3.7 Data Analysis

Data analysis was carried out in three steps as per each objective namely; 1) identification of the urban sprawl areas, 2) biophysical and socio-economic characterization of the sprawl areas to determine possible sprawl control factors using AHP and, 3) prediction of future sprawl patterns using CA-Markov model.

3.7.1 Identification of sprawl areas

Sprawl areas were identified in different images where they occured using object-based image analysis (OBIA). Eight steps were used including i) developing a land cover classification scheme, ii) image segmentation, iii) classification of 3 image sets, iv) exporting results from eCognition developer, v) post classification image processing in ArcMap, vi) accuracy assessment vii) change detection, and viii) LULC and Sprawl areas maps generation.

    i.   **Land Cover Classification Scheme**

Due to heterogeneous nature of land cover in the study area, a list of six LC classes were identified during reconnaissance survey considering their exhaustiveness to accommodate all surface features as shown in Table 3.3.

Table 3.3: Major Land Cover Classes in the Study Area

S/No.	Name	Description
1	Built-up area	Artificial structures, buildings, roads and other impermeable surfaces
2	Water	Rivers, ponds and other water bodies
3	Forest	Both planted and natural trees
4	Agricultural lands	Both cultivated and non-cultivated
5	Grassland/Shrubland	Both natural and planted
6	Swamps	Both permanent and seasonal

The six land cover classes were inserted into the image processing software under class hierarchy.

ii. Image segmentation

Image segmentation was done in two steps namely; multiresolution and spectral difference segmentation algorithm.

In the Multiresolution segmentation, the 'Scale parameter' was set to 35 since it's the restricting parameter that stops the object from getting too diversity or is the average size of the object. Since there is no rule for 'Scale Parameter', trial and error was used and value 35 was found to be the best value for 'Scale Parameter'. 'Shape' (geometric form of the object) was set to weight of 0.3 since it defines the shape criterion to be used when partitioning the image. The higher the value, the less the effect of color on the segmented process therefore care was taken not to put higher value to avoid distorting spectral

information. Finally 'Compactness', which defines the weight of the compactness criterion, was set to value 0.6. The higher its value, the more compact image object may be and the NIR value was set to 2.

Spectral Difference segmentation was performed next in order to merge already segmented image objects with same spectral values together. 'Maximum Spectral Difference' value was set to 15 and NIR band to 3.

iii. Classification of three image sets

Image classification was done using rule-based classification techniques and for comparison the same data was analyzed using supervised classification nearest neighbor algorithm and accuracy of classification compared to OBIA.

Rule-based classification was done using eCognition developer. Five indices were used, that is, Normalized Difference Vegetation Index (NDVI), Normalized Difference Water Index (NDWI), Normalized Difference Built-up Index (NDBI), Soil Adjusted Vegetation Index (SAVI) and Visible brightness (*Xu H. 2007)*. This was done by; clicking 'open project' on the main menu and adding the subset of Sentinel-2 2020 composite image, on the process tree 'Append New' was clicked and 'Rule-Based Classification' typed then 'Ok'. On the toolbar, 'Tools' was clicked and 'Feature View' selected, 'object feature', 'customized', and 'Arithmetic Feature' double-clicked to help create the NDVI. Under feature name, NDVI was typed then inserting the formula for NDVI which is (NIR-Red)/(NIR+Red) then 'calculate' and 'apply'. On the top toolbar, 'Image objects' was selected and 'image object information' right-clicked and 'feature to display' selected. From customized, 'NDVI' was chosen and from Layer value, 'mean' was selected then

'Ok'. NDVI was applied to help isolate dense vegetation (more than 30% cover). Vegetated areas possess positive NDVI values while non-vegetated have negative NDVI value. For all the six classes, the range for their lowest and highest NDVI values was noted by clicking various objects to define the range for the ruleset of the classes. The process was executed from the process tree, selecting 'Append New', in the Algorithm field, 'assign class' was selected then from the class filter 'unclassified' was checked. Then defining the Threshold values for the lowest and highest NDVI and selecting forest class under parameter. On the toolbar, 'View Classification' option was selected and .Transparent/Non-Transparent outlined objects..

SAVI (NIR-Red)(1+k)/(NIR+Red+k) was applied to extract vegetation less than 15% cover mostly within Eldoret town since it has high reflectance in NIR band. 'K' is the correction factor that ranges from 0-1 for very high vegetation density to very low density respectively. A correction factor of 0.6 was used (*Jensen, 2000*).

NDWI (Green-NIR)/(Green+NIR) was applied to extract open water features since reflectance of water in green light is more compared to NIR light which takes advantage of high reflectance in vegetation. Water features will have positive NDWI value while vegetated or soil surfaces will have zero or negative NDWI value though built-up areas also have high NDWI value (*McFeeters, 1996*).

NDBI (SWIR-NIR)/(SWIR+NIR) was used to isolate built-up areas since they have higher reflectance value of SWIR than NIR though drier vegetation also possess higher NDBI value (*Zha et al., 2003*).

To solve the mix-up of built-up areas misclassified under water in NDWI and drier vegetation misclassified under built-up in NDBI, a fifth index of visible brightness

(Red+Green+Blue)/3 was used since built-up areas have higher visible brightness value than water and dry vegetation hence will move the misclassified built-up area under NDWI to NDBI and the misclassified dry vegetation in NDBI to NDVI.Figure 3.6 shows steps in designing the indices in eCognition developer.
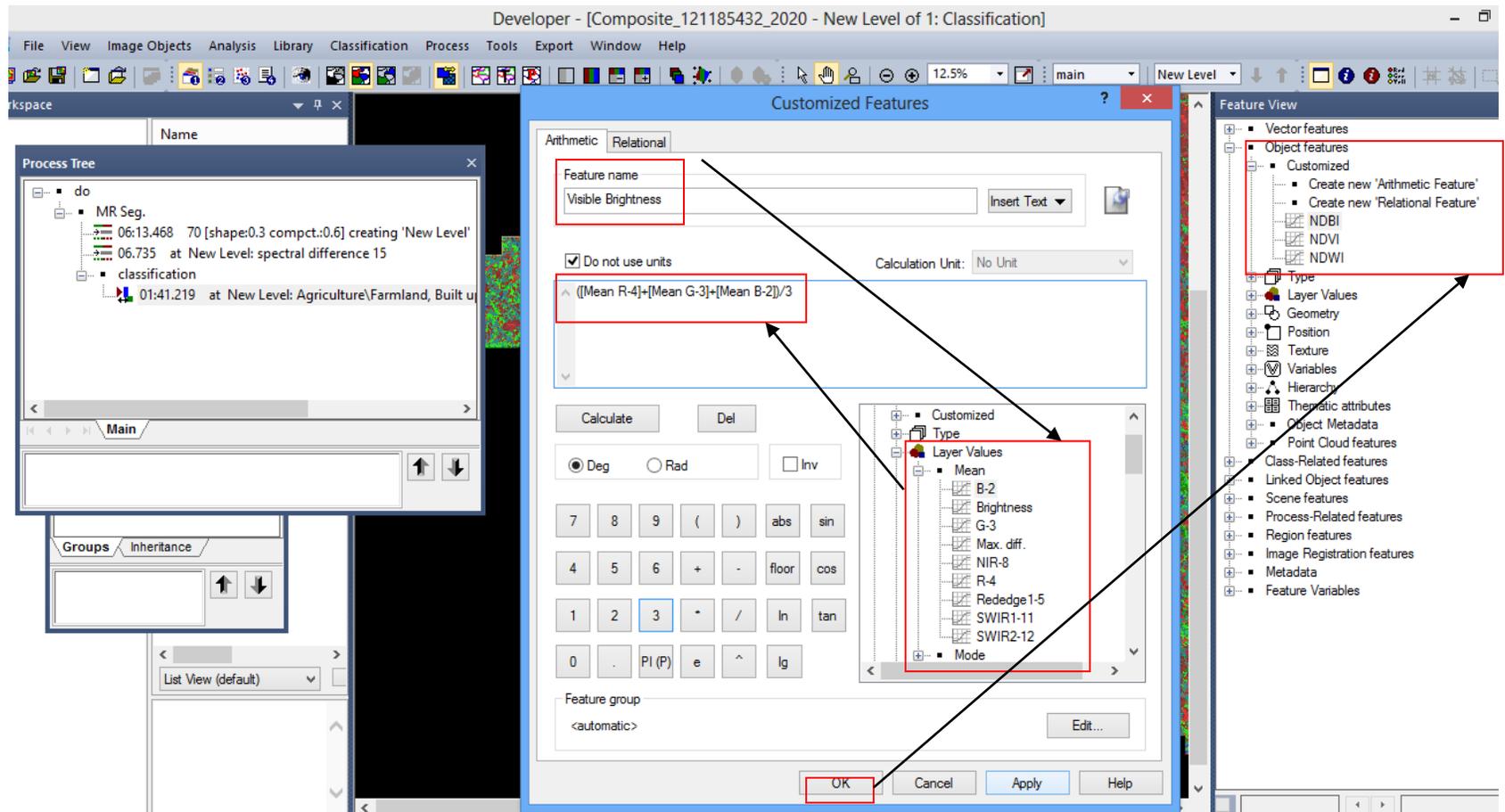
Figure 3.6: Defining the indices in eCogniton developer

Under Algorithm, 'assign class' is selected and 'Threshold condition' clicked and 'NDVI' indices double clicked and set to ≥ 0.028236 and ≤ 0.4713 and under parameter, built up areas is selected. This implies that the software will scan through the segmented image and look for objects which meet the above threshold condition and classify them under built up class. This process was repeated for all the other indices until all the features were classified. Figure 3.7 shows setting of threshold conditions in eCognition.
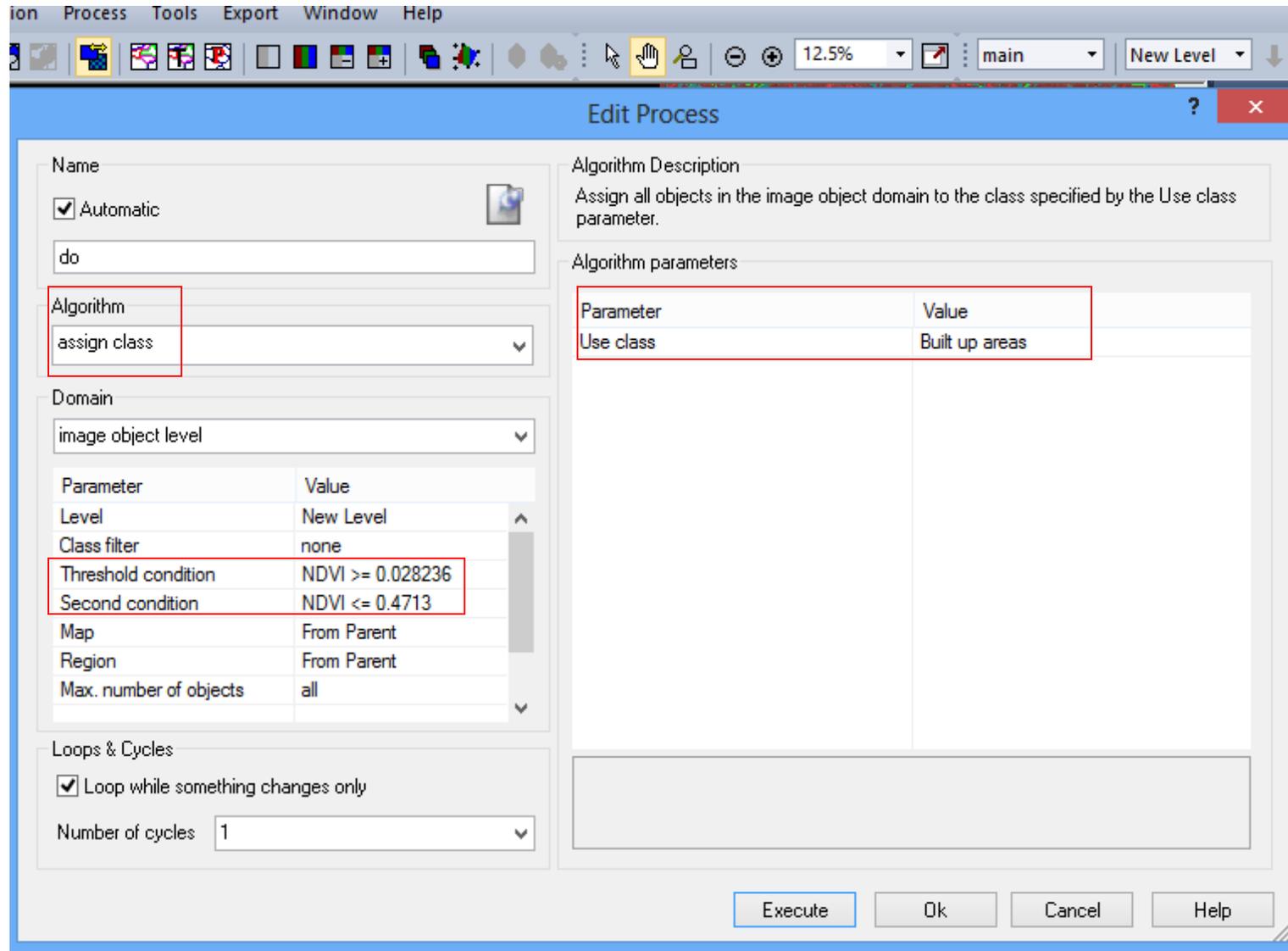
Figure 3.7: Setting of Threshold Condition using Indices in eCogniton developer

iv.   Exporting Results from eCognition Developer

After classification, the results were exported to be opened with ArcMap using the following process; under classification in the process tree, the classification rule set was right-clicked, 'Append New' selected and under Algorithm 'export vector layer' was selected, the six LULC classes checked under 'class filter'. On the right side of the 'Edit Process' dialog box, Export item name was given as Classification 2016, Attribute was clicked to open 'Select Multiple Features dialog box', then clicked was double clicked then Ok. For Shape type and Export type polygon and smoothed was selected, respectively then executed. The 'class name' will be the field that will appear in the attribute table.

v.   Post Classification in ArcMap

In ArcMap, the exported classified image i.e. Classification 2016 shapefile of polygon was added and its attribute table opened. Then its 'class name field' was highlighted and using Dissolve tool under Geoprocessing, the records were dissolved into six LULC classes. After dissolving classes, a field of Area in km^2 was created and areas auto generated using 'Calculate Geometry tool'.

vi.   Accuracy Assessment

Confusion matrix was created to assess accuracy of classification results. The process produces four metrics namely, the user's accuracy, the producer's accuracy, the overall accuracy and Kappa statistic (*Congalton, 1991a*). The producer's accuracy indicates the percentage of correctly classified ground truth sites for each class. The user's accuracy

indicates the proportion of correctly classified sites in the classified image for each class while the overall accuracy is a combination of the two accuracy measures. The Kappa statistic shows the probability that the values presented in the error matrix are significantly different than those from random sample of equal size (*Benjamin, 2004*). The sample points were randomly selected as reference data using 'create random point tool'. The accuracy assessment was performed with stratified random points and the original Sentinel-2 images and google earth as the reference data. A random point distribution was designed according to the heterogeneity potential and aerial coverage of the classes. Thirty test pixels for each class was considered to be the best sample for assessing the accuracy. The pre-classified images for the three years were used as reference images where the test pixels were selected. This was done using ArcMap involving; the pre-classified image for each of the three years was added independently into ArcMap and a shapefile created in form of Test pixel shapefile and two User's and Producer's field added in its attribute table. Thirty test pixels for each class was digitized considering even distribution across the image and unique from the training sites for classification then entering values that corresponds to each class in the Producer's field. For each reference image, a total of one eighty test pixels were digitized for the six LULC classes. The classified images were then opened individually and the Test pixel shapefile overlaid. Its attribute table was opened and each record 'clicked' to see if the pixel conforms to the one in the reference image. If it conforms, its User's field was labeled same as the Producer's field and if not, it was labeled with the value that corresponds to its class.

In the final step, the built-up class was extracted for each of the three years and overlaid on each other in order to identify and map the location of urban sprawl patterns. A shapefile of growth patterns was created, digitized and a total of twelve and eleven sprawl patterns for 2016 and for 2020 respectively were mapped.

vii. Land Use/Cover Change Detection Analysis

Land use/cover change detection analysis between three years (2000, 2016 and 2020) was done in ArcMap using intersect of geoprocessing tool. Classified image for the two consecutive years (2000- 2016, 2016-2020 and 2000-2020) were added into ArcMap and intersected to combine their attribute table. Two fields of 'change' and 'area_sqkm' were then added to the combined attribute table in order to calculate which class changed to what and at how much area. Using the field calculator, the change field was auto generated. The area field was also auto generated using calculate geometry. Then the attribute table was copied and pasted in excel and formatted to remain only with the 'change' and 'Area' fields. The two fields together with their records were used to generate the change graphs representing changes in land cover in square kilometer between 2000 to 2016, 2016 to 2020 and 2000 to 2020 as in Figures 4.6 - 4.8 respectively.

viii. Maps Generation in ArcMap

The LULC maps for the three years (2000, 2016 and 2020) and urban sprawl areas maps for 2016 and 2020 were designed into ArcMap and exported as Bitmap (BMP) format.

3.7.2 Contribution of Selected Factors Supporting Urban Sprawl Patterns

Literature on urban growth showed various factors that affect urban growth processes including physical factors of slope and elevation, social factors of population density and social services, political factors involving zoning policies and connection related factors, that is, distances from roads, powerline, waterlines, employment centers, and distance from constraints to development. Due to data availability, eight factors thought to strongly influence sprawl patterns in the study area shown in Table 3.4, were identified and ranked using analytical hierarchy process (AHP) model. The PCM ranking ranges from importance (value 1), equal to weak importance (value 2), weak importance (value 3), weak to strong importance (value 4), strong importance (value 5) and very strong importance (value 7) with their reciprocal importance to each other. This was done because all factors don't contribute equally to sprawling pattern (*Park et al., 2011; Al-Sharif et al., 2014; Shafizadeh et al., 2015; Arsanjani et al., 2013; Chowdhuryan et al., 2014; Zeng et al., 2015*).

Table 3.4: List of Factors included in the Analytical Hierarchy Process Model (AHP)

Variable	Description	Nature of variable
Dependent Growth patterns (Y) 2000-2020	0: no urban expansion; 1: urban expansion	Dichotomous
Independent		
X_1	Distance to nearest road	Continuous
X_2	Distance to nearest employment center	Continuous
X_3	Distance to water line	Continuous
X_4	Distance to power line	Continuous
X_5	Distance to constraints to development	Continuous
X_6	Population density	Continuous
X_7	Elevation	<1800m
		1800-2024m
		2025-2126m
		2127-2200m
		>2200m
X_8	Slope	0%-9% gradient
		10-18% gradient
		19-27% gradient
		28-36% gradient
		>36% gradient

i.   Computation of Factor Weights

The independent factors were used in Multi Criteria Decision model and assigned
weights using Analytical Hierarchy Process (AHP) approach. The first process in AHP
was to develop the hierarchical structure since the goal was to rank independent
variables/criteria to determine their order of importance in contributing to urban sprawl
patterns. The independent variables (X_1-X_8) which are the factors leading to growth
patterns are the criteria and kept in second level. The dependent variables/ growth
patterns areas (Y_1 to Y_n) are the alternatives and kept at level three of the model. Figure
3.8 shows AHP structure for weighting of independent variables.
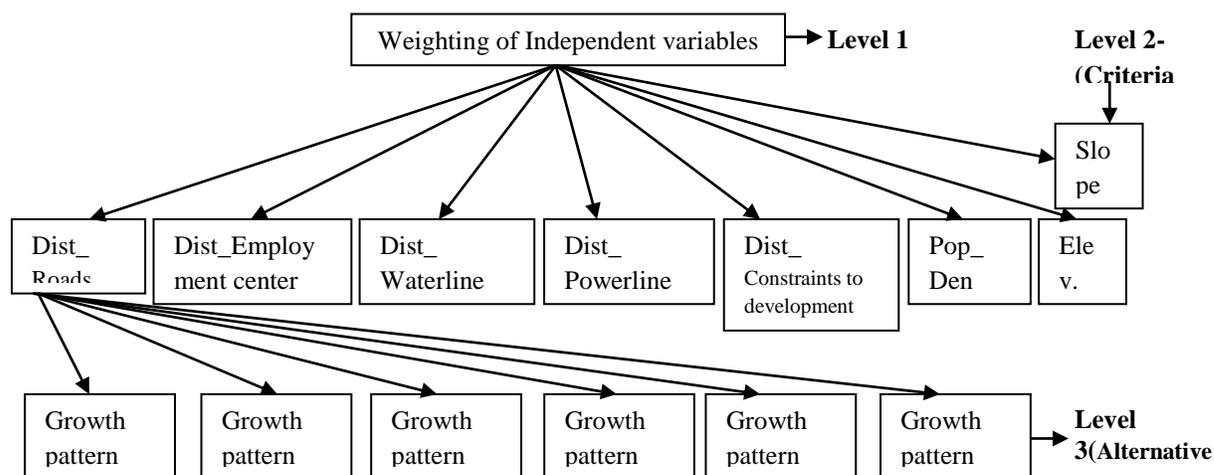


Figure 3.8: Analytical Hierarchy Process (AHP) Structure

In the second step, a pairwise comparison matrix was created to show the relative
importance of the independent variable to the goal. For example, how important is the
distance to the road when ranking variables. This pairwise comparison matrix was
created using the relative importance scale from Saaty's 9-point pairwise comparison

table as shown in Table 3.5 and its length corresponds to the number of independent variables used in the decision-making process.

Table 3.5: Saaty's 9 Point Pairwise Comparison Table

Intensity of importance	Definition	Explanation
1	Equal importance	Equal importance or indifference
3	Weak importance of one over another	Experience and judgement slightly favor one activity over another
5	Essential or strong importance	Experience and judgement strongly favor one activity over another
7	Very strong or demonstrated importance	An activity is favored very strongly over another; its dominance is demonstrated in practice
9	Absolute importance	The evidence favoring one activity over another is of highest possible order of affirmation
2,4,6	Intermediate values between adjacent scale values	-
1/3, 1/5, 1/7, 1/9	Values for inverse comparison	-

(Source: Saaty, 1980)

For this case it's an 8 by 8 matrix. The value in the pairwise matrix was based on the expert's/decision maker's judgment on urban sprawl causative factors. The diagonal elements were assigned a value of one (1) because each factor is of equal importance to itself, for example, distance to road (X_1) will be of equal importance to distance to road (X_1). The pairwise comparison matrix begins from second row of the first column. If distance to road is considered to be of 'weak to strong importance' than distance to employment centers, a value of four (4) is entered in row two of column one and its

fraction (1/4) is entered in row two of column one. Therefore if employment center is equivalent to n value, then distance to road will be 4n value. The row element (4n) was divided by column element (n), that is, 4n/n=4. Then dividing the column element by row element i.e. n/4n=1/4. The pairwise comparison process is continued until all possible criteria pairs are evaluated. The lower triangular half is the reciprocal of the upper triangular hence only one is filled to get the values for the other. Figure 3.9 shows values in pairwise comparison table entered into AHP model.

Figure 3.9: Analytical Hierarchy Process (AHP) Model

The pairwise comparison matrix values above were entered into the AHP model in order to normalize them resulting into a normalized pairwise comparison matrix produced by dividing all column elements by the summation of the column. The criteria weights were

calculated by averaging all elements in a row using IDRISI Weights command from the principal eigenvector (*Eastman et al., 1993*). Figure 3.10 shows eigenvectors of weight from the AHP model.
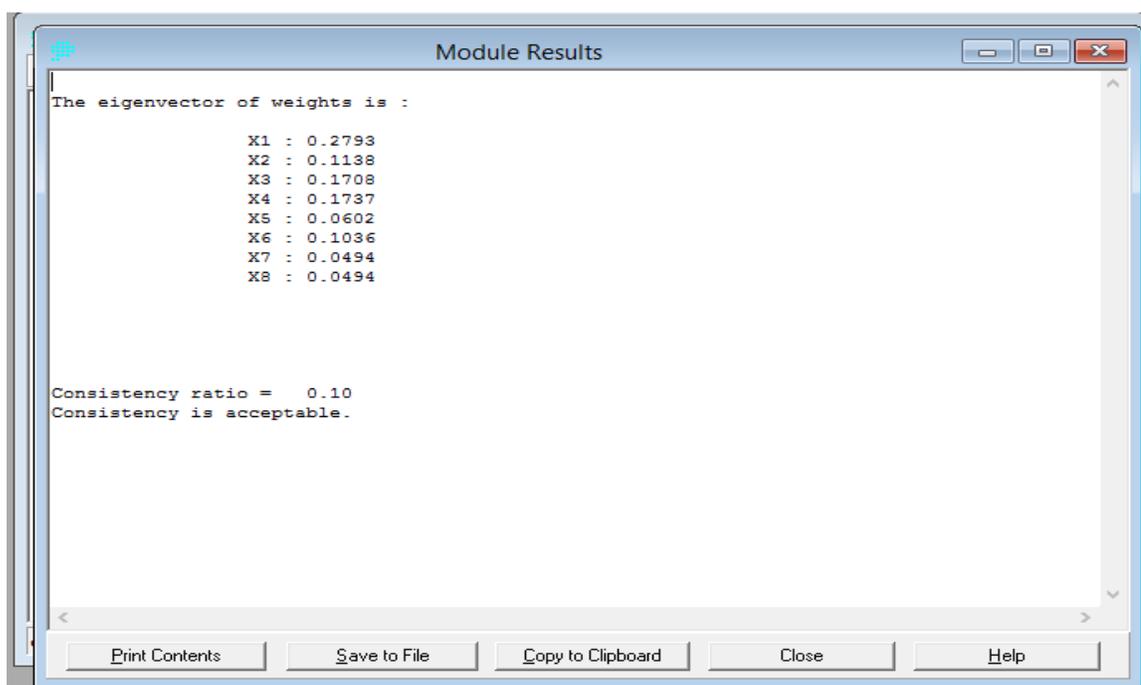
Figure 3.10: Eigenvectors of Weights

In order to check whether the calculated criteria weights are correct, consistency was calculated by multiplying the column values in the pairwise comparison matrix which is not normalized with the criteria values (*Saaty, 1980*). The row values were summed to get the weighted sum values. Each row weighted sum value was divided by each row criteria value and calculating the average summation the results to get the lambda. The consistency index (CI) was then calculated using the formula lambda minus n divided by n-1 where n=8 number of supporting factors.

Finally consistency ratio (CR) was calculated by dividing the CI with random index (RI) which is the consistency of index of randomly generated pairwise matrix. The calculated

consistency ratio value was 0.10. The standards for consistency ratio is that it should be less than 0.10 and since the calculated CR was 0.10, hence the suitability of the defined weighting scheme was confirmed (*Boroushaki et al., 2008*) and assumed that the matrix was reasonably consistent. If the calculated CR is higher than the standard CR, the matrix is re-evaluated (*Eastman et al., 1993*). The criteria weights calculated above was used to make a decision/ rank the criteria/independent variables in the order that they contribute most to urban sprawl growth patterns. The method is iterative since it allows those assigning weights a chance to revise their previous pairwise comparison table on the basis of criteria (*Eastman et al., 1993*). Higher weights factors are statistically more important. Finally, the factors were used to make raster maps for use in predicting future urban sprawl areas as follows;

The distance algorithm was used to create continuous surface images for five connectivity factors (distances to roads, employment centers, powerline, waterline and constraint to development) representing the Euclidean distances for all the growth patterns from these factors.

Maps showing population densities at a Sub- location unit for 2000, 2016, and 2020 was created (*Benjamin, 2004*).

Slope and elevation maps were derived from Digital Elevation Model (DEM) of the study area downloaded from USGS website ((USGS, https://earthexplorer.usgs.gov/).

3.7.3 Predicting Possible Future Sprawl Patterns

The last analysis process involved predicting and directing future sprawl patterns by introducing appropriate factors that attract or repel human settlements to see how they interact to project future (*Pontious et al., 2001*).

After classification, the land use maps for 2000, 2016 and 2020 were resampled to the same spatial resolution (10m×10m) to avoid decrease in spatial details of the images.

All the eight surface images representing biophysical, socio-economic and connectivity factors were used in the CA-Markov model, although biophysical factors are more or less unchangeable (*Benjamin, 2004*). The CA-Markov approach was used to produce the predicted land use/cover change future map of 2029.

CA-Markov approach has been used to find the link between urban development and factors that attract or repel human settlement. First, the consecutive LULC maps for 2000-2016 and 2016-2020 are inputted into Markov model to calculate the transition probability matrices (TPM) for the years showing the percentage that one land cover is likely to change to another.

Secondly, the 2000-2016 and 2016-2020 TPM, 2016 and 2020 LULC maps and 2016 and 2020 raster maps for factors are inputted each year at a time into CA model to generate the simulated 2016 and 2020 LULC maps.

Third, to assess the accuracy of the results from the model, kappa overall value obtained by simulating the 2020 LULC map was compared with the Jacob Cohen's Kappa Statistics (k), (1960) Table which is used to measure inter-rater reliability for qualitative items. It is generally thought to be more robust than simple percentage agreement calculation as (k) takes into account the possibility of occurring by chance. Table 3.6 shows Cohen's Kappa Statistics table. Its kappa values ranges from <0.00, 0.00-0.20, 0.21-0.39, 0.40-0.59, 0.60-0.79, 0.80-0.89 and 0.9-1.00 as shown in Table 3.6.

Finally, after validation the 2016-2020 TPM, 2020 simulated LULC map and 2020 raster maps for factors were inserted in the CA model to forecast 2029 LULC. Then the built-up area for simulated 2020 and predicted 2029 LULC maps were overlaid and 2029 sprawl areas identified and mapped. Figure 3.11 shows steps used in modelling the future urban sprawl pattern in the study area.
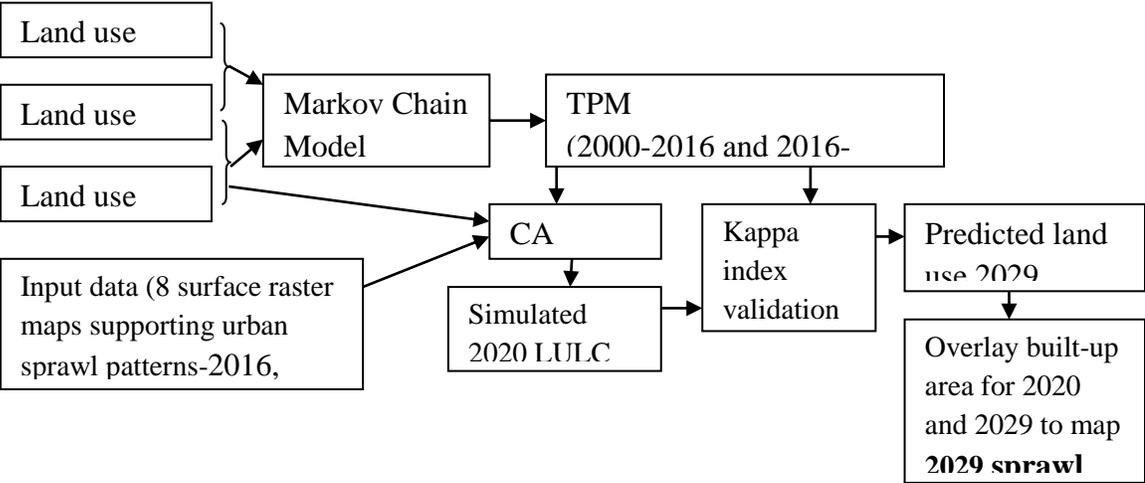

Figure 3.11: Methodological Flowchart used for Modelling Future Growth

Table 3.6: Jacob Cohen's Kappa Statistics Table

Cohen's Kappa Statistics (k)	Strength of agreement
<0.00	Poor
0.00-0.20	Slight
0.21-0.39	Fair
0.40-0.59	Moderate
0.60-0.79	Substantially
0.80-0.89	Strong
0.90-1.00	Almost perfect

Each cell has six different states representing land use activities in the study area. This is given by the equation 1 below.

$$^{t}LU_{ij} = \begin{cases} 1=\text{Agriculture} \\ 2=\text{Built-up} \\ 3=\text{Forest} \\ 4=\text{Grassland or shrubland} \\ 5=\text{Swamp} \\ 6=\text{Water} \end{cases} \tag{1}$$

Where $^{t}LU_{ij}$ = state of pixel i, j at time t

The study area is represented by the six land use categories. The evolution of cell from time t to t+1 is determined by the function of its state, its neighborhood space and the set of transition rule (*Narimah Samat., 2009*). This is given by the equation 2 below.

$$^{t+1}LU_{ij} = f\left((^{t}LU_{ij}) * (^{t}S_{ij}) * (^{t}P_{x,y,i,j}) * (^{t}N_{ij})\right) \tag{2}$$

Where;

$^{t+1}LU_{i\,j}=$ the potential of cell i, j to change at time $t+1$,

f $((^{t}LU_{ij})=$ state of cell i, j at time t,

$(^{t}S_{ij})=$ suitability index of cell i, j at time t,

$(^{t}P_{x,y,i,j})=$ probability of cell i, j to change from state x to state y at time t, and

$(^{t}N_{ij})=$ neighborhood index of cell i,j.

CHAPTER FOUR

RESULTS

4.1 Introduction

This chapter presents findings related to each of the three objective: 1) location of urban sprawl patterns around Eldoret town, 2) contribution of selected factors supporting urban sprawl patterns and 3) predicting possible future sprawl patterns around Eldoret town in 2029 using CA-Markov model.

4.2 Location of Urban Sprawl Areas around Eldoret Town from 2000 to 2020

Findings for the objective were presented in the following order;

4.2.1 LULC maps for 2000 to 2020

Classification techniques by Rule-Based discriminated the land cover classes well by use of their spectral values in order to separate features. Land use/cover changes in the study area showed that built-up areas (71.6-138.9), agriculture or farmlands (848.7-1524.8), and forest (56.1-106.8) km^2 has immensely increased with grasslands/shrubland (945.2-123.5), swamps (45.0-67.4) and water (6.3-11.4) km^2 varying from 2000 to 2020 as indicated in Table 4.1. In 2000, built-up areas were 71.60 (3.63%) km^2, 84.3 (4.28%) km^2 in 2016, 138.9 (7.04%) km^2 in 2020 and are predicted to be 154 (7.81%) km^2 by 2029. This indicates an increase of 82.4 (4.18%) km^2 for the year 2000-2029. Figure 4.1shows LULC map for the year 2000.
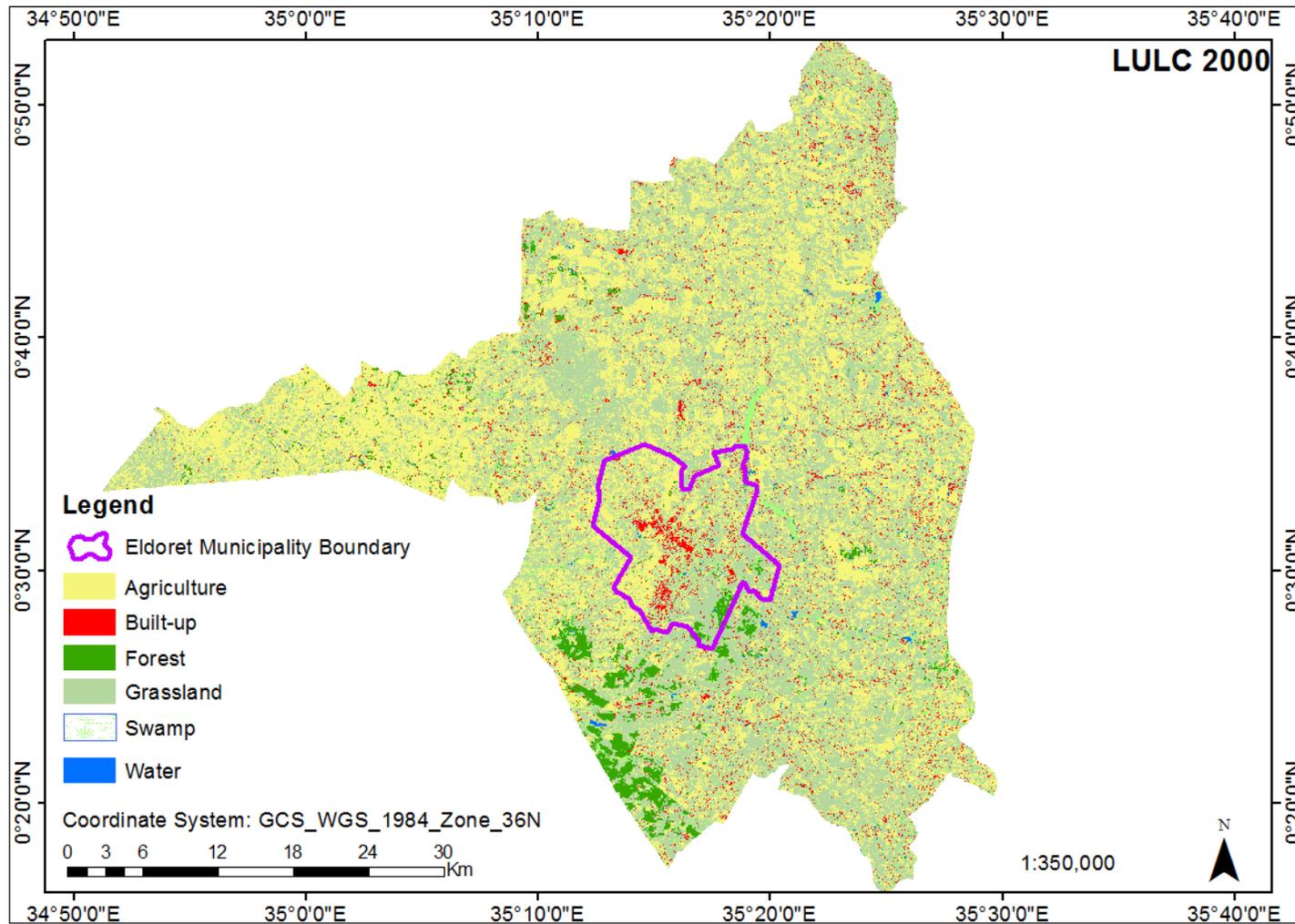
Figure 4.1: LULC Map of the study Area in Year 2000

Figures 4.2 shows LULC map for the year 2016.
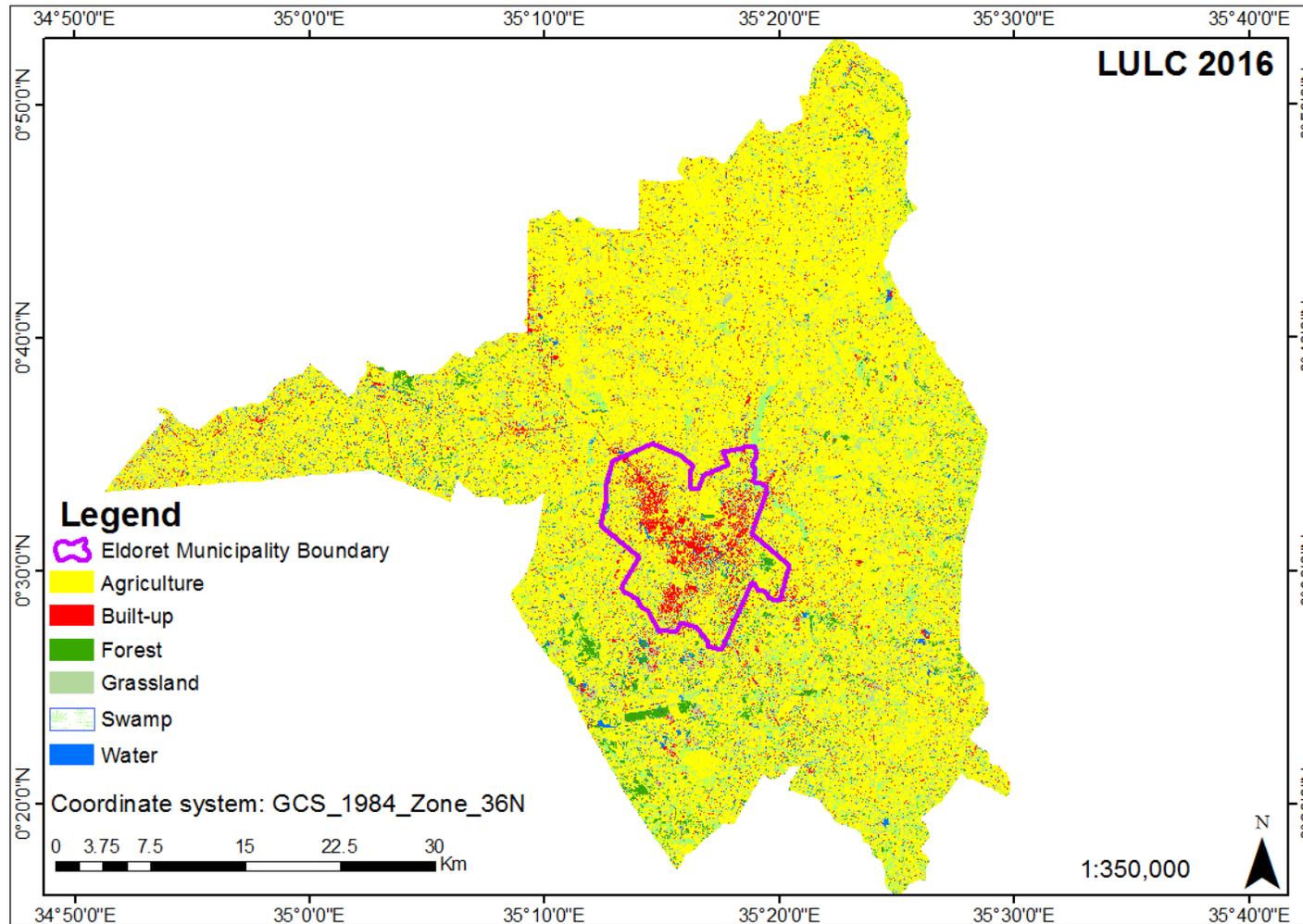
Figure 4.2: LULC Map of the study Area in Year 2016

Figures 4.3 shows LULC map for the year 2020.
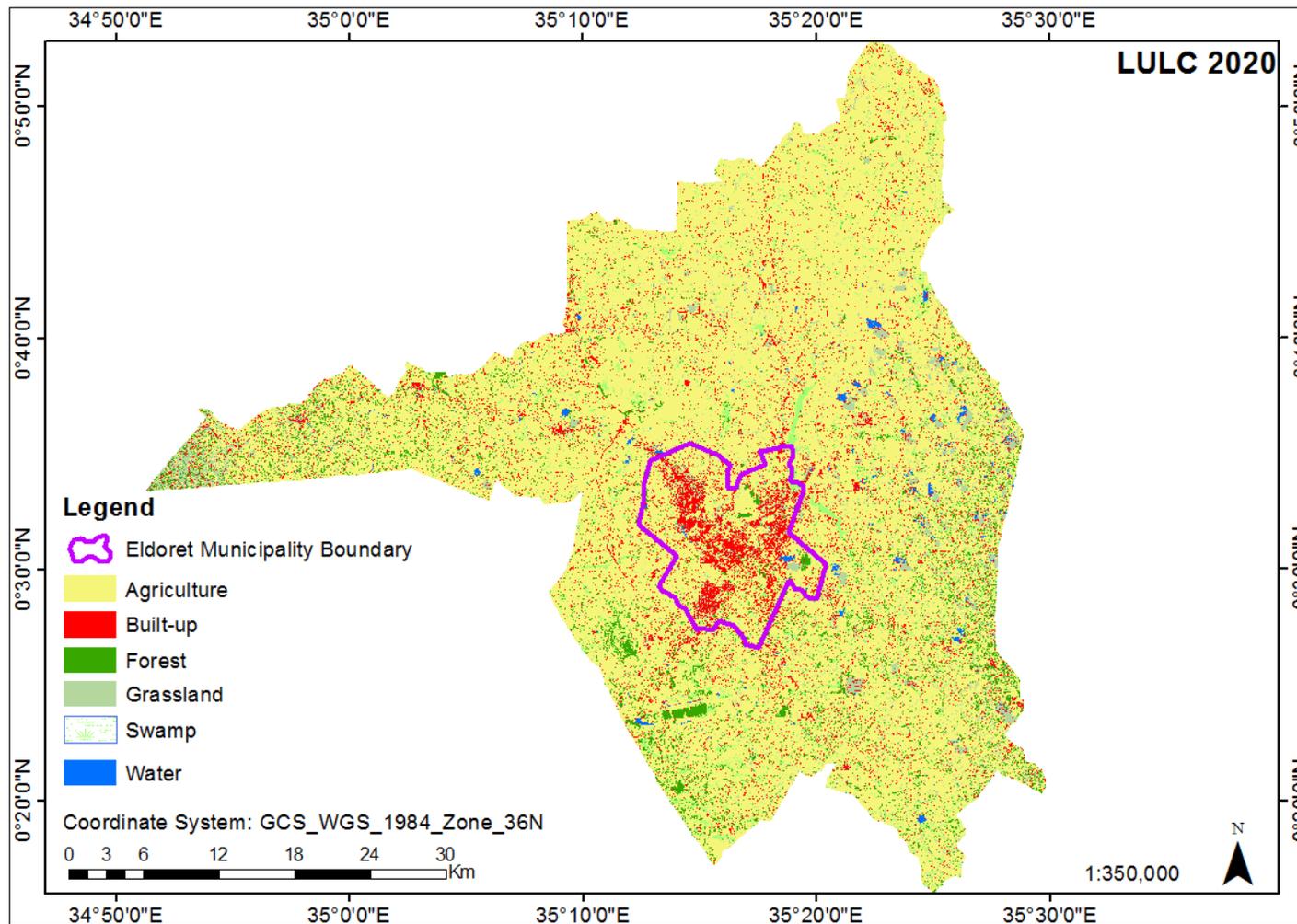
Figure 4.3: LULC Map of the study Area in Year 2020

Table 4.1 shows LULC statistics in square kilometers during 2000 to 2020.

Table 4.1: Summary of Land Use/Cover Classification Statistics Between 2000 to 2020 (area in km²)

LULC Type	Year 2000		Year 2016		Year 2020	
	Area in km²	(%)	Area in km²	(%)	Area in km²	(%)
Agriculture/Farmland	848.663	42.69	1444.72	72.23	1524.82	77.29
Built-up areas	71.5959	3.60	84.3366	4.28	138.912	7.04
Forest	56.0763	2.82	51.3249	2.60	106.757	5.41
Grassland/shrubland	945.1716	47.91	243.557	12.35	123.475	6.26
Swamp	45.0099	2.26	104.45	5.29	67.3586	3.41
Water	6.2523	0.31	44.3802	2.25	11.4492	0.58
Total	**1972.769**	**100**	**1972.769**	**100**	**1972.769**	**100**

4.2.2 Classification accuracies for 2000 to 2020

Figures 4.4-4.5 shows total of one hundred and eighty digitized test pixels for the six classes on a reference 2016 image and then overlaid on the classified 2016 image and records of the test pixels entered in the attribute table under User's and Producer's fields. The producer's and user's accuracies ranged from 65.63-100% and 66.67-96.67% respectively with overall accuracy and kappa coefficient ranging from 85-91.67% and 82-90% during 2000 to 2020.
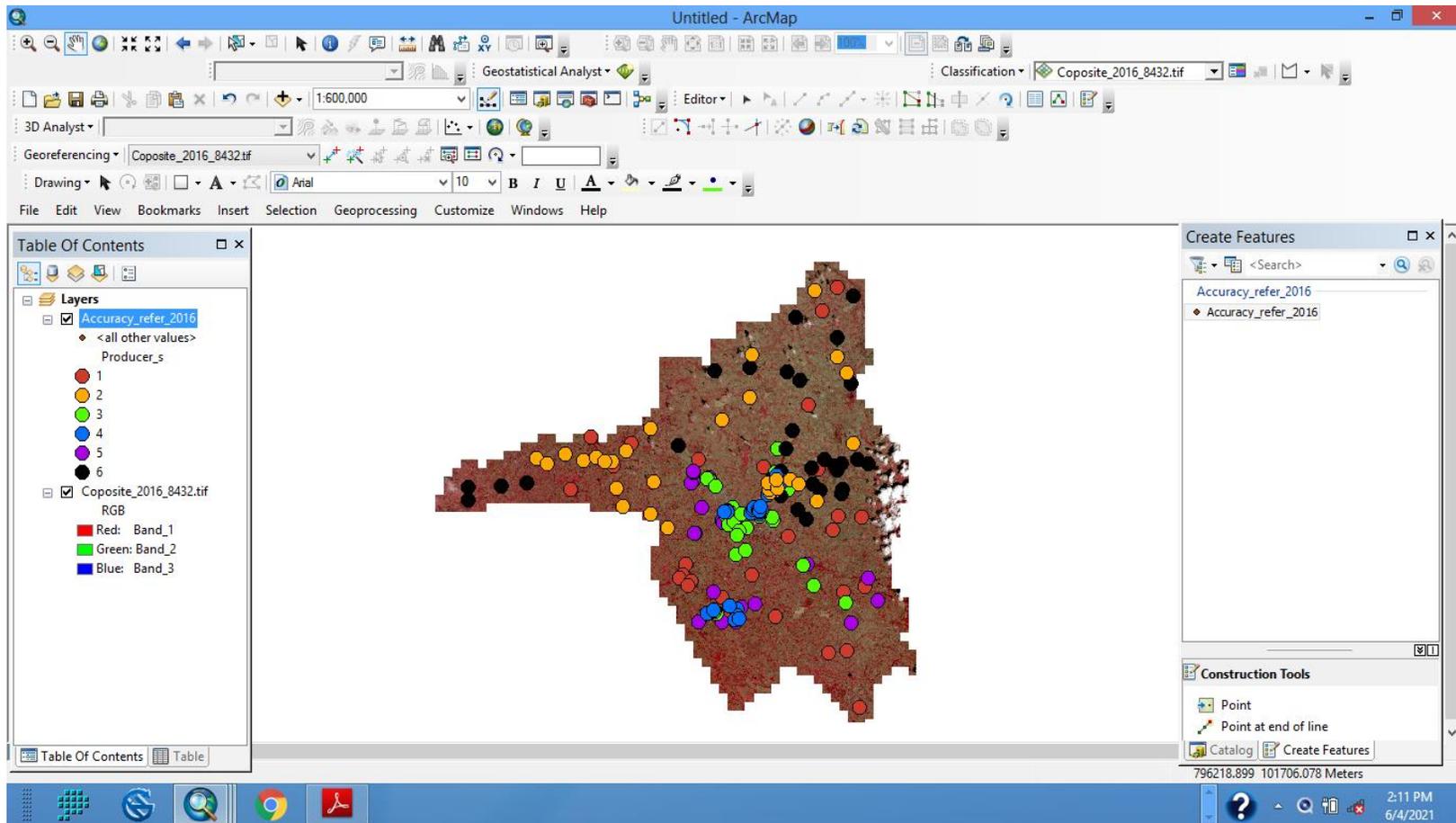
Figure 4.4: Digitized Test pixels for six LULC classes in 2016 Sentinel-2 reference image
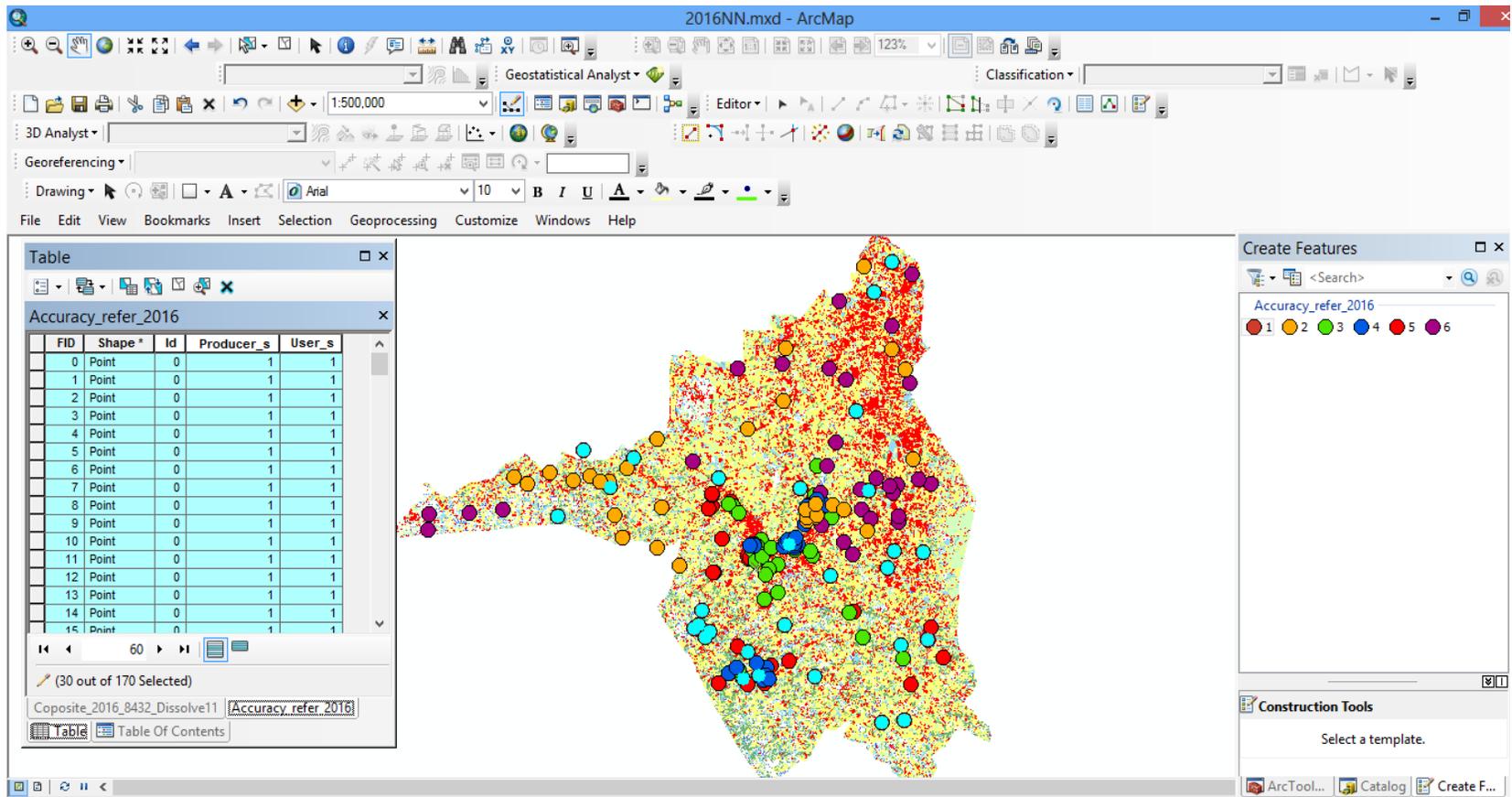
Figure 4.5: Overlaid Test pixels for six LULC classes in 2016 Sentinel-2 classified image

Table 4.2 shows producer's accuracy indicating the percentage of correctly classified ground truth sites and user's accuracy which indicates the proportion of correctly classified sites in the classified image for each of the six LULC for 2000-2020.

Table 4.2: User's and Producer's Accuracy Results (2000, 2016 and 2020) by Rule Based Classification Algorithm

LULC Type	2000		2016		2020	
	Producer's (%)	User's (%)	Producer's (%)	User's (%)	Producer's (%)	User's (%)
Agriculture/Farmland	65.63	70.00	83.87	86.67	87.10	90.00
Built-up Areas	96.67	96.67	93.93	93.33	96.55	93.33
Forest	80.00	93.33	100	90.00	100	90.00
Grassland	76.92	66.67	83.33	83.33	81.25	86.67
Swamp	93.33	93.33	90.32	93.33	90.32	93.33
Water	100	90.00	93.54	96.67	96.67	96.67

Table 4.3: Classification Accuracy Assessment (2000, 2016 and 2020) by Rule Based Classification Algorithm

Image	Overall Accuracy (%)	Kappa Coefficient (%)
2000	85.00	82
2016	90.56	88.67
2020	91.67	90

4.2.3 Land Cover Change Detection and Analysis

LULC change graphs showing to what size each land cover changed into another for the years 2000-2016, 2016-2020 and 2000-2020 is shown in Figures 4.6-4.8 respectively. Table 4.4 shows built-up areas gaining from other land covers by 51.6 km^2 (2000-2016), 14.3 km^2 (2016-2020) and 66.0 km^2 (2000-2020) with agriculture/farmland losing by 67.3-189.0-256.3 km^2 during 2000-2016, 2016-2020 and 2000-2020 respectively. The change graphs for 2000-2016, 2016-2020 and 2000-2020 of the six LULC are shown in figures 4.6-4.8 respectively.

Table 4.4: Magnitude of Change (km^2)

| LULC Type	Change between 2000 and 2016 (km^2)	Change between 2016 and 2020(km^2)	Change between 2000 and 2020(km^2)
Agriculture/Farmland	-67.339198	-188.999791	-256.338989
Built-up Areas	51.647164	14.342217	65.989381
Forest	65.720436	35.248636	104.969072
Grassland/ shrubland	-171.525195	93.895853	-77.629342
Swamp	66.728248	73.149354	139.877602
Water	51.06747	-27.648087	23.419383
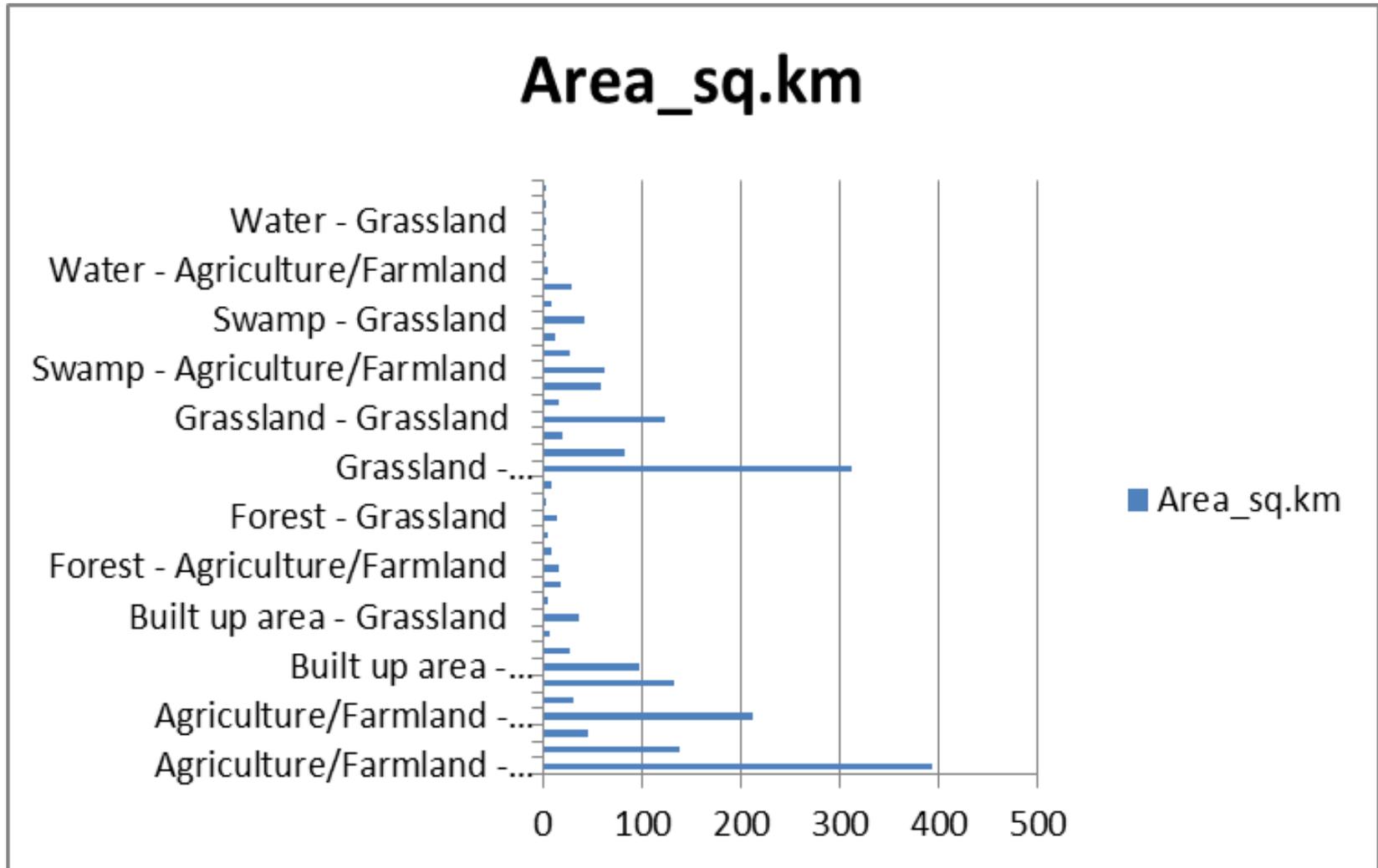
Figure 4.6: LULC Change Graph for 2000 to 2016
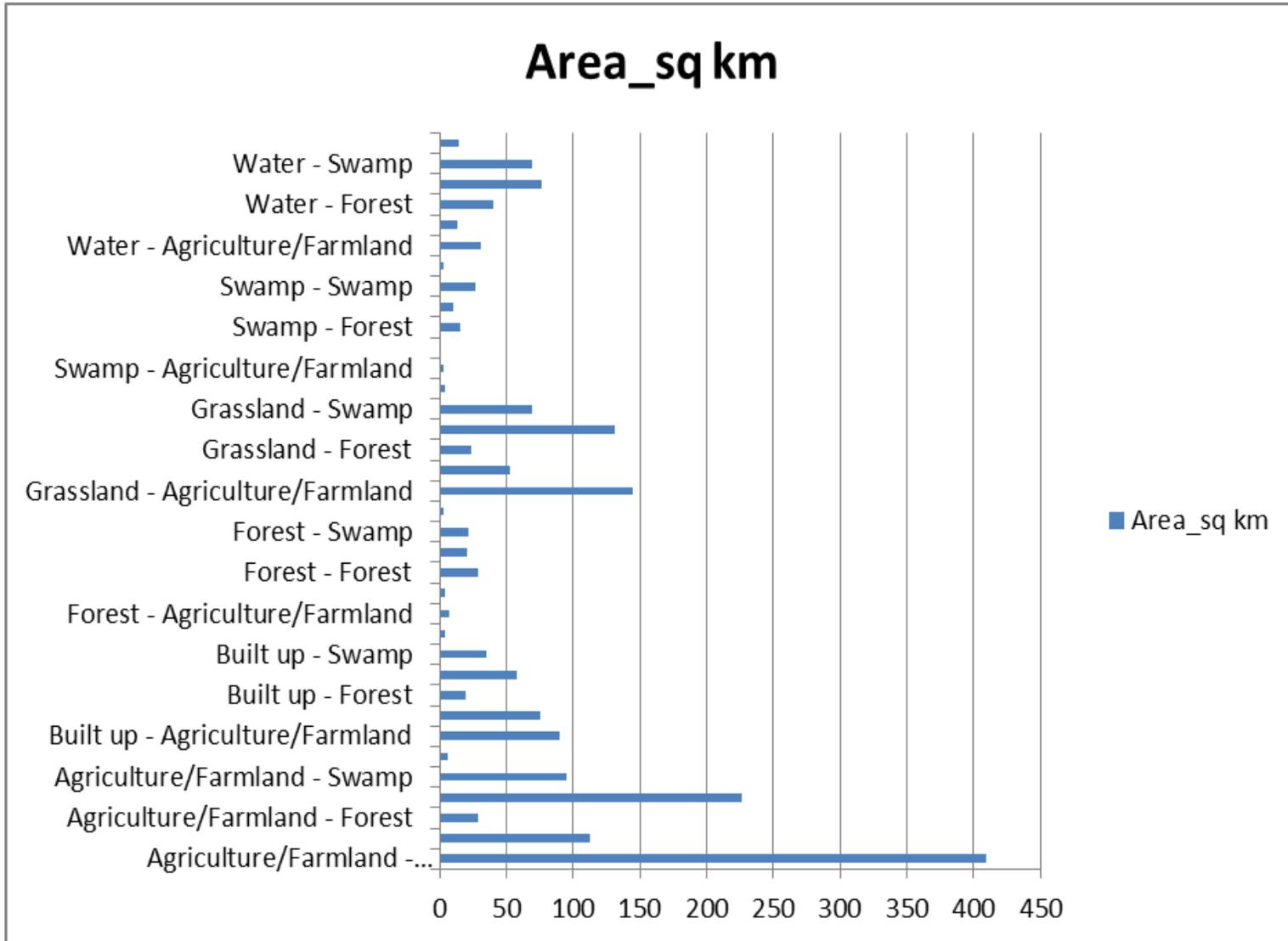
Figure 4.7: LULC Change Graph for 2016 to 2020
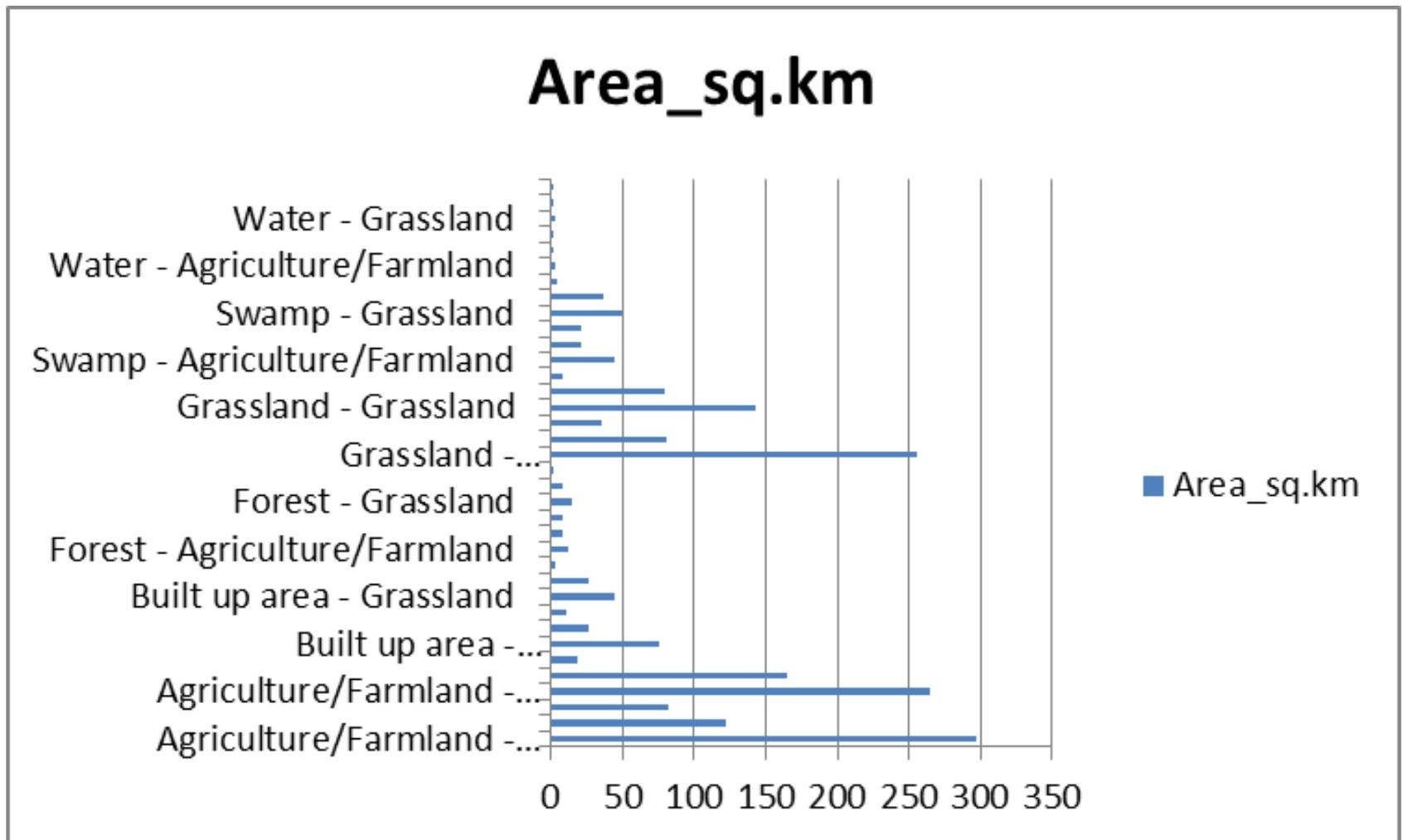
Figure 4.8: LULC Change Graph for 2000 to 2020

Figure 4.9 shows plotted areas of land cover in kilometer square for the three study years (2000-2020).
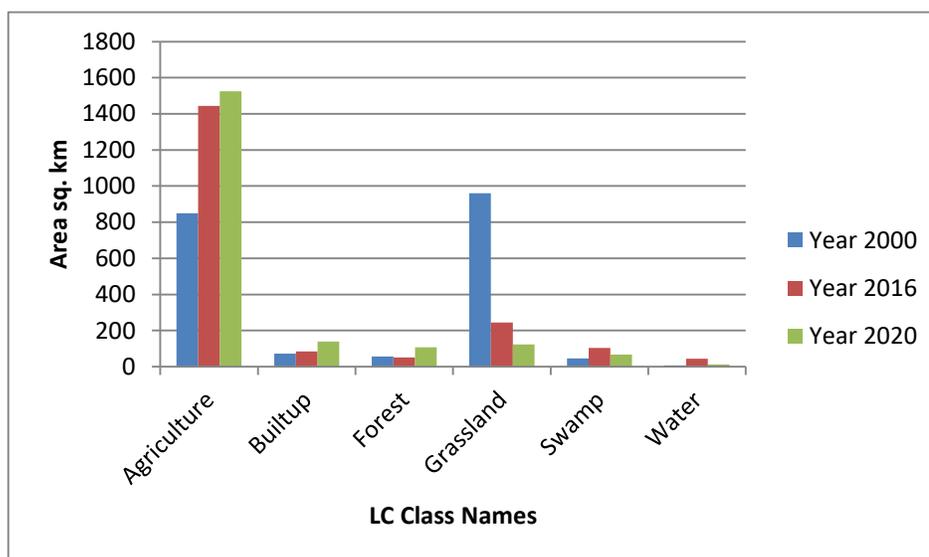
Figure 4.9: Temporal Patterns of LULC Change in km² in 2000 to 2020

4.2.4 Urban sprawl patterns maps for 2000-2016 and 2016-2020

After overlay analysis of the sprawl areas for 2000 and 2016 in ArcMap, twelve urban sprawl areas were detected and mapped. These had different growth patterns as follows; Kipkaren, Jua Kali, Soy, Merewet, Kuinet, Kipkorgot, Turbo and Kapseret trading centers were linear patterns; Koibarak, Tulwet, Leberio and Sarma trading centres were leapfrog patterns covering an area of 71.60 km² to 84.34 km² during 2000 to 2016 respectively as shown in Figure 4.10.

For overlay of sprawl areas for 2016 and 2020, eleven more urban sprawl areas were also identified and mapped. They also had different patterns occurring in Moiben, Sololo trading centres taking leapfrog pattern; Garage, Tugen Estate, Moiben Juction, Chirichir,

Kosachei, Magut, Maili Nne, Kiluka, and Cheptiret trading centres taking linear covering an area of 84.34 km^2 to 138.91 km^2 during 2016 to 2020 respectively as shown in Figure 4.11.
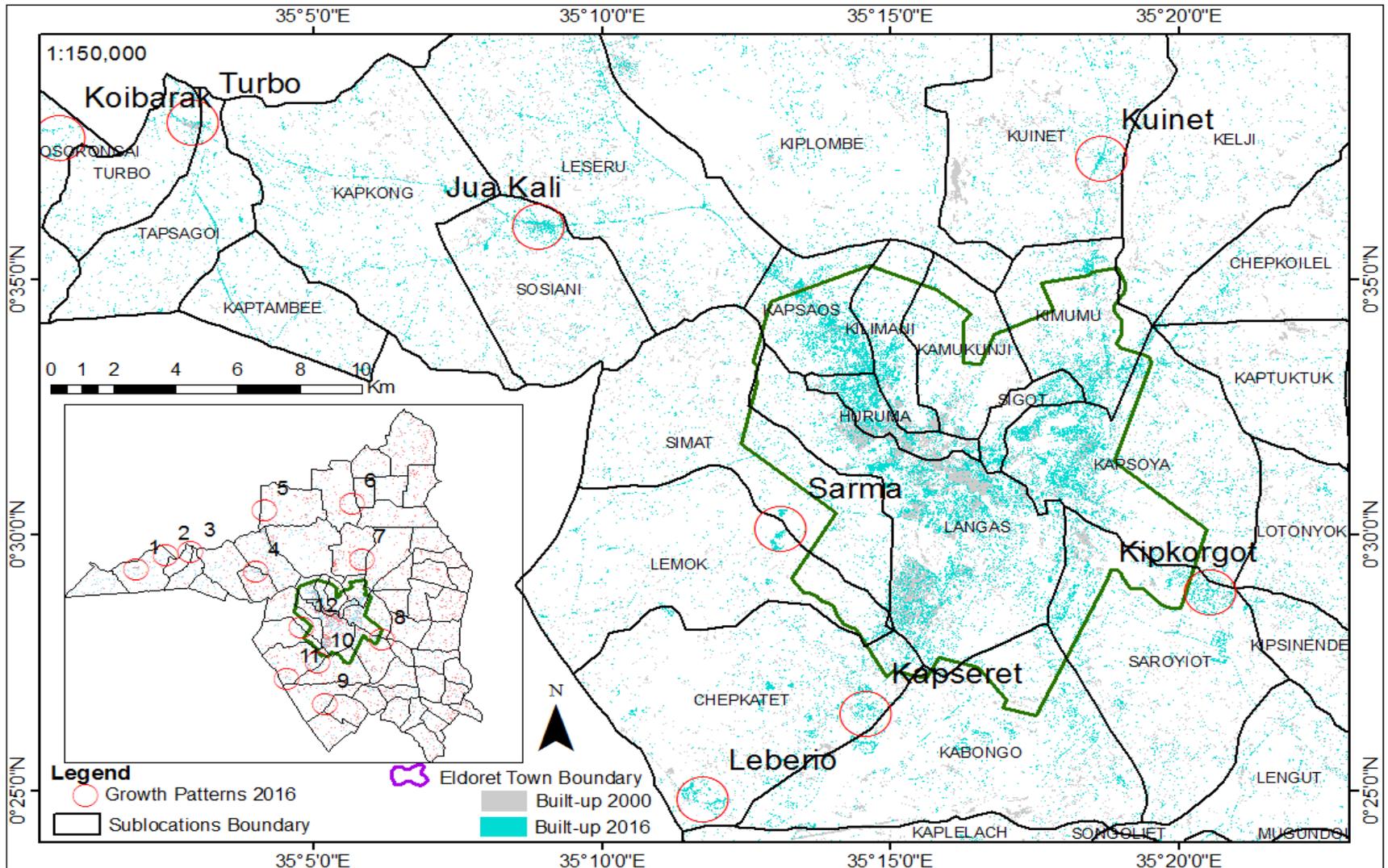
Figure 4.10: Urban Sprawl Patterns 2016 Map of the Study Area
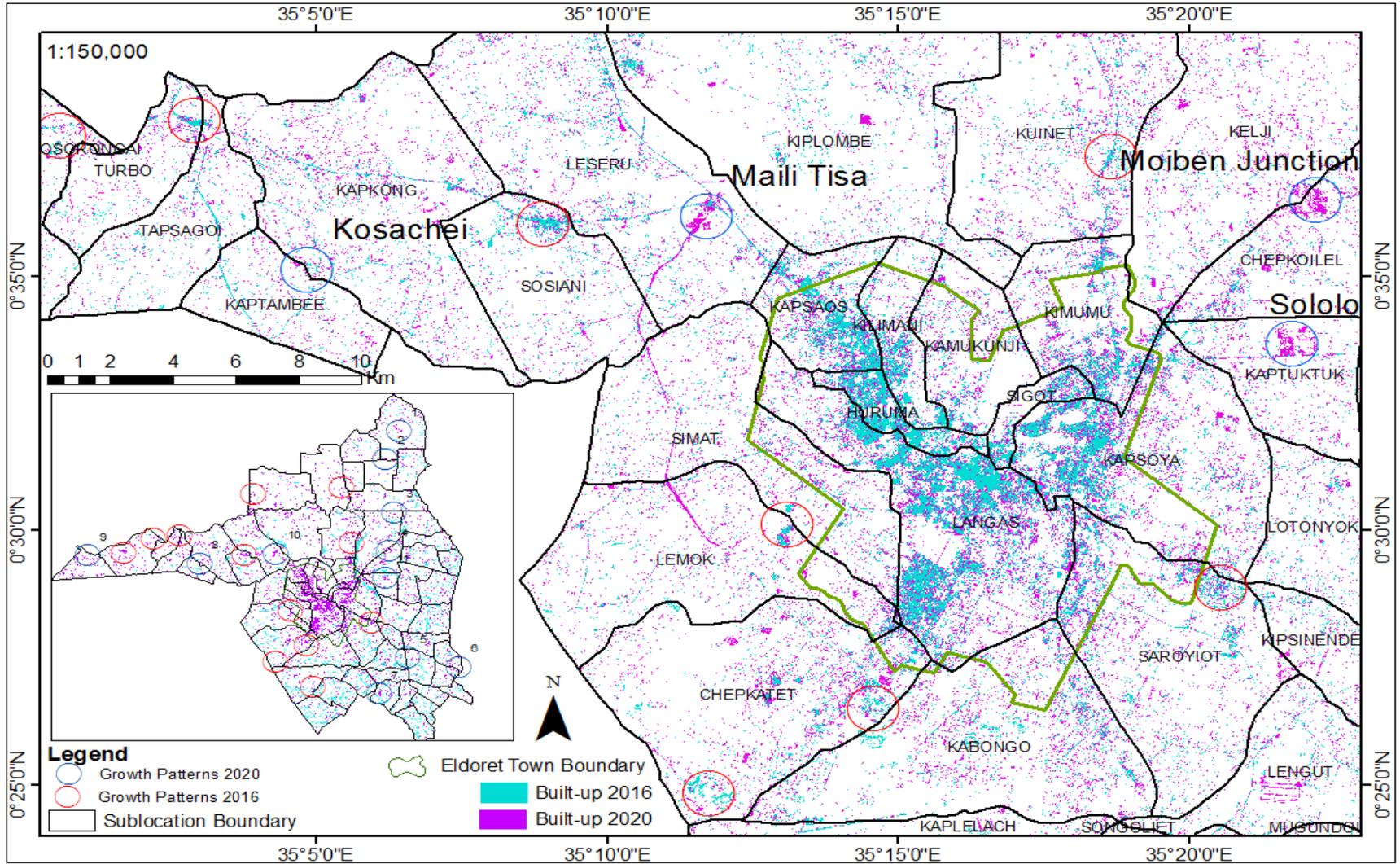
Figure 4.11: Urban Sprawl Patterns 2020 Map of the Study Area

4.3 Contribution of Selected Factors that Supports Urban Sprawl Patterns around Eldoret Town

From urban sprawl patterns maps of 2016-2020, most sprawl areas were occurring near road network. Therefore there was need to show the factors that supports them. This section shows the results of how the eight factors are relating with each other. Their weights obtained after ranking them with AHP is presented in Table 4.6.

Table 4.5: Pairwise Comparison Matrix

	X_1	X_2	X_3	X_4	X_5	X_6	X_7	X_8
X_1	1	4n/n=4	3	2	2	1	7	7
X_2	n/4n=¼	1	½	1	3	1	3	3
X_3	1/3	2	1	1	3	1	3	3
X_4	½	1	2	1	4	5	2	2
X_5	½	1/3	¼	1/3	1	1	1	1
X_6	1	1	1/5	¼	1	1	3	3
X_7	1/7	1/3	½	½	1	1/3	1	1
X_8	1/7	1/3	½	½	1	1/3	1	1

The results in Table 4.6 shows the factors with AHP weightings obtained after inputting values in Table 4.5 into AHP model.

Table 4.6: Weights for AHP for each criterion

Factor	Weight of AHP
Distance to roads (X1)	0.2793 (27.93%)
Distance to powerline (X_4)	0.1737 (17.37%)
Distance to waterline (X_3)	0.1708 (17.08%)
Distance to employment centers (X_2)	0.1138 (11.38%)
Population density (X_6)	0.1036 (10.36%)
Distance to constraints to development (X_5)	0.0602 (6.02%)
Elevation (X_7)	0.0494 (4.94%)
Slope (X_8)	0.0494 (4.94%)

Consistency ratio =   0.10

From the above findings, the following factors are most significant in the order of importance to growth of sprawling patterns; distance to roads (X_1) 27.93% contributes more to urban sprawl growth patterns followed by distance to powerline (X_4) 17.37%, then distance to waterline (X_3) 17.08%, distance to employment centres (X_2) 11.38% is fourth, population density (X_6) 10.36% is fifth, and the weakest are distance to constraints to development (X_5) 6.02% being sixth with elevation (X_7) and slope (X_8) being seventh since they have similar weights of 4.94%.

Table 4.7 shows study area population growth during 1999, 2009, 2019 and interpolated 2000, 2016, 2020 and 2029.

Table 4.7: Observed and Interpolated Population Figures vs Built-up area for the study years

Year	Total Population	Total Area (Sq. Km)	Built-up area (km^2)
1999 Census	419,585	1972.77	-
2000 Interpolated	437,052	1972.77	71.60
2009 Census	630,888	1972.77	-
2016 Interpolated	774,200	1972.77	84.34
2019 Census	845,188	1972.77	-
2020 Interpolated	870,269	1972.77	138.91
2029 Interpolated	1,132,281	1972.77	154

By comparing the relationship between the growth rate of population and built-up area change for the period 2000-2029, also indicates sprawl. This was done by plotting growth rate of population against built-up area for 2000-2016, 2016-2020 and 2020-2029 as shown in Figure 4.12.
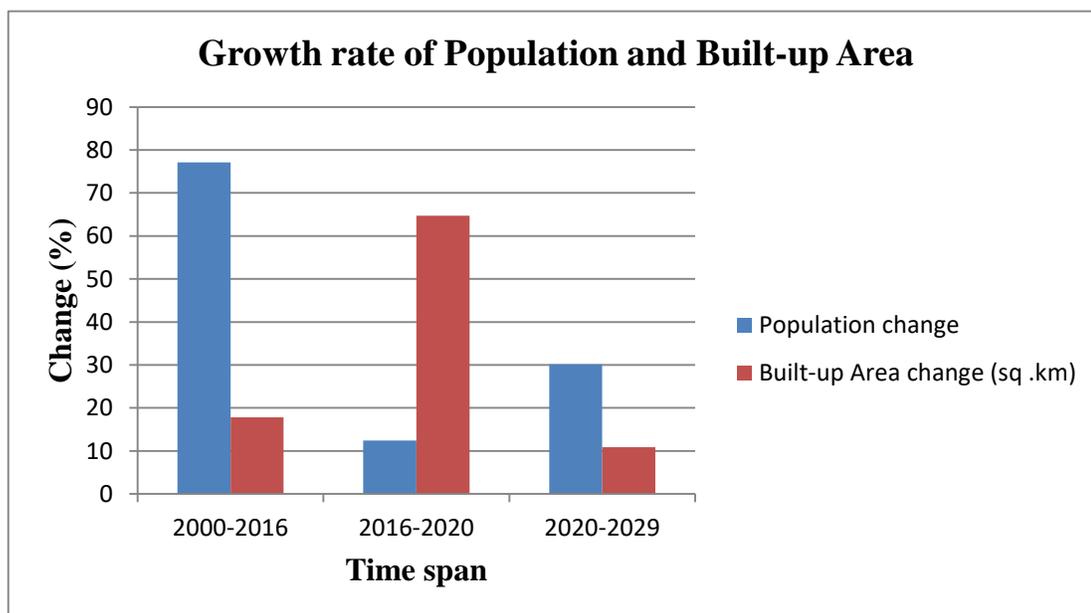
Figure 4.12: Change in Population and Built-up Areas Growth Rate

4.3.1 Surface Maps for Supporting Factors

Distance algorithm was used to create continuous surface maps representing Euclidean distances to roads, employment centers, constraints to development maps, powerline, and water line. Output cell size was set to 10m and processing extent set to shapefile of the study area for all the variables. Maps showing population densities at smallest administrative unit, that is, sub-location for 2000, 2016 and 2020 were created from population data. Elevation and slope maps were created from DEM. Figure 4.13(a)-(h) shows raster layers of supporting factors.

Figure 13(a): Distance to Employment Centers
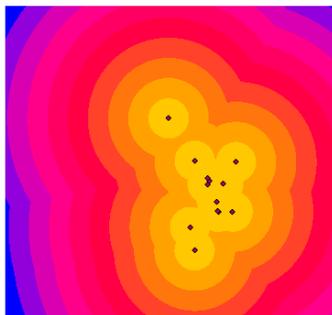
Figure 13(b): Distances to Powerline Transformers

2000	2016	2020
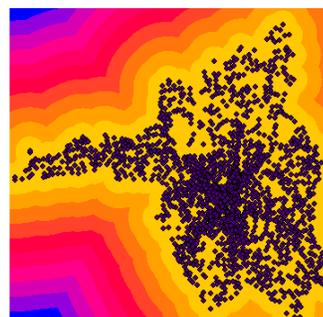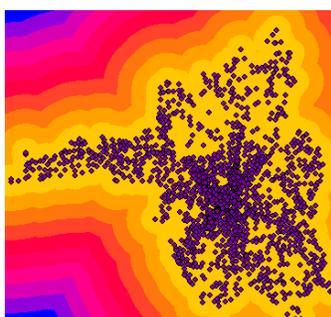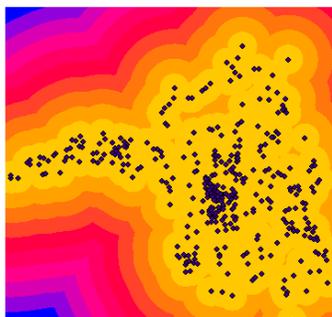
Figure 13(c): Distances to Waterline Network

2000	2016	2020
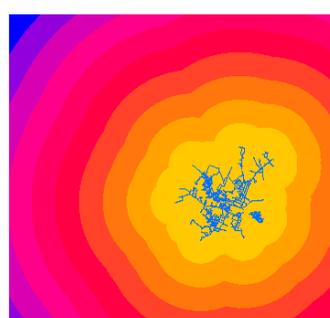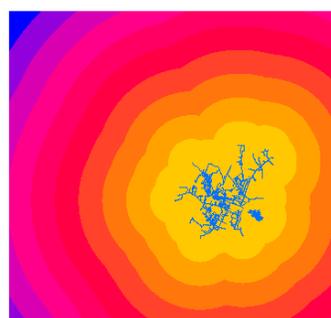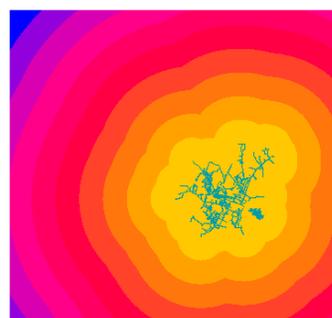
Figure 13(d): Distances to Roads

2000	2016	2020
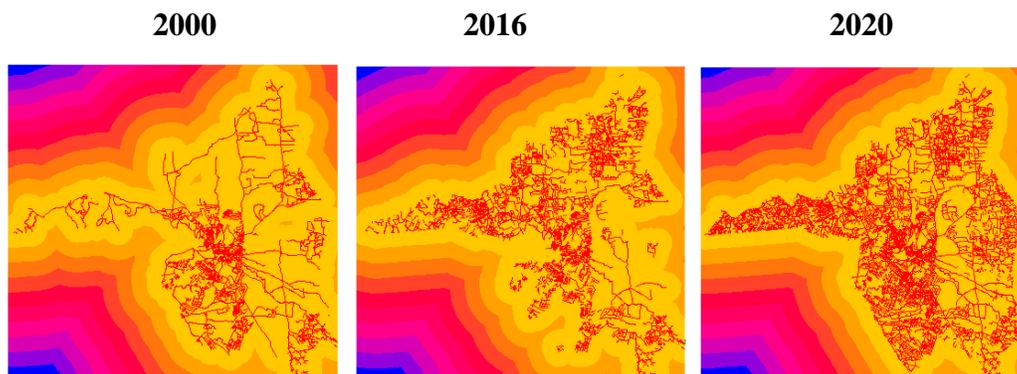
Figure 13(e): Distance to Constraints   Figure 13(f): Elevation   Figure 13(g): Slope

to Development
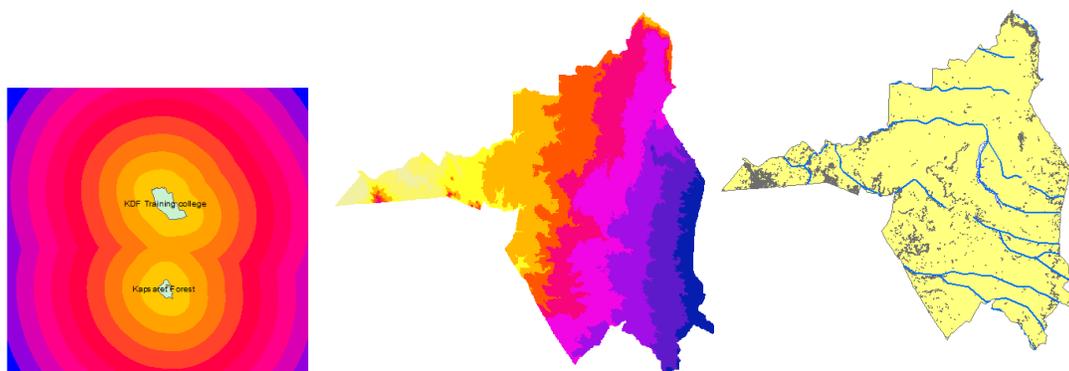
Figure 13(h): Population density

2000	2016	2020
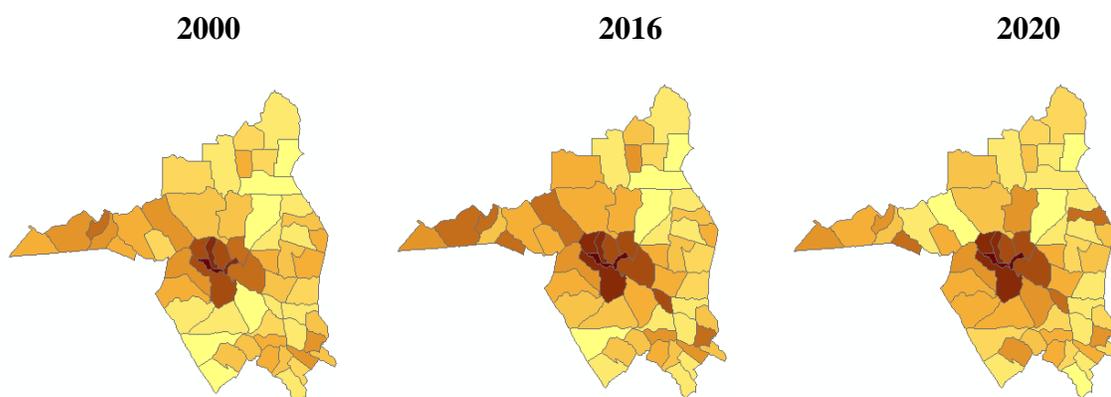
Figure 4.13(a)-(h): Raster Layers of Supporting Factors

4.4 Prediction of Possible Future Urban Sprawl Areas around Eldoret Town in 2029 Using CA-Markov and AHP Model

Using the CA-Markov and AHP models, future sprawl areas for the year 2000-2020 were done and the results are shown in Figure 4.15.

Comparing the simulated and classified LULC map for 2020 (Figure 4.14 a, b), it could be seen that these changes are quite similar and matching. Also the Kappa (overall) value obtained when validating 2020 LULC map was 0.68779 which is substantial according to *Cohen (1960)* with the simulation accuracy being 81.21%.

Now based on these, 2029 sprawl areas were predicted using Markov transition probabilities matrix of 2016-2020 (Table 4.8), simulated 2020 LULC map (Figure 4.14b) and 2020 raster maps (Figure 4.13a-h).
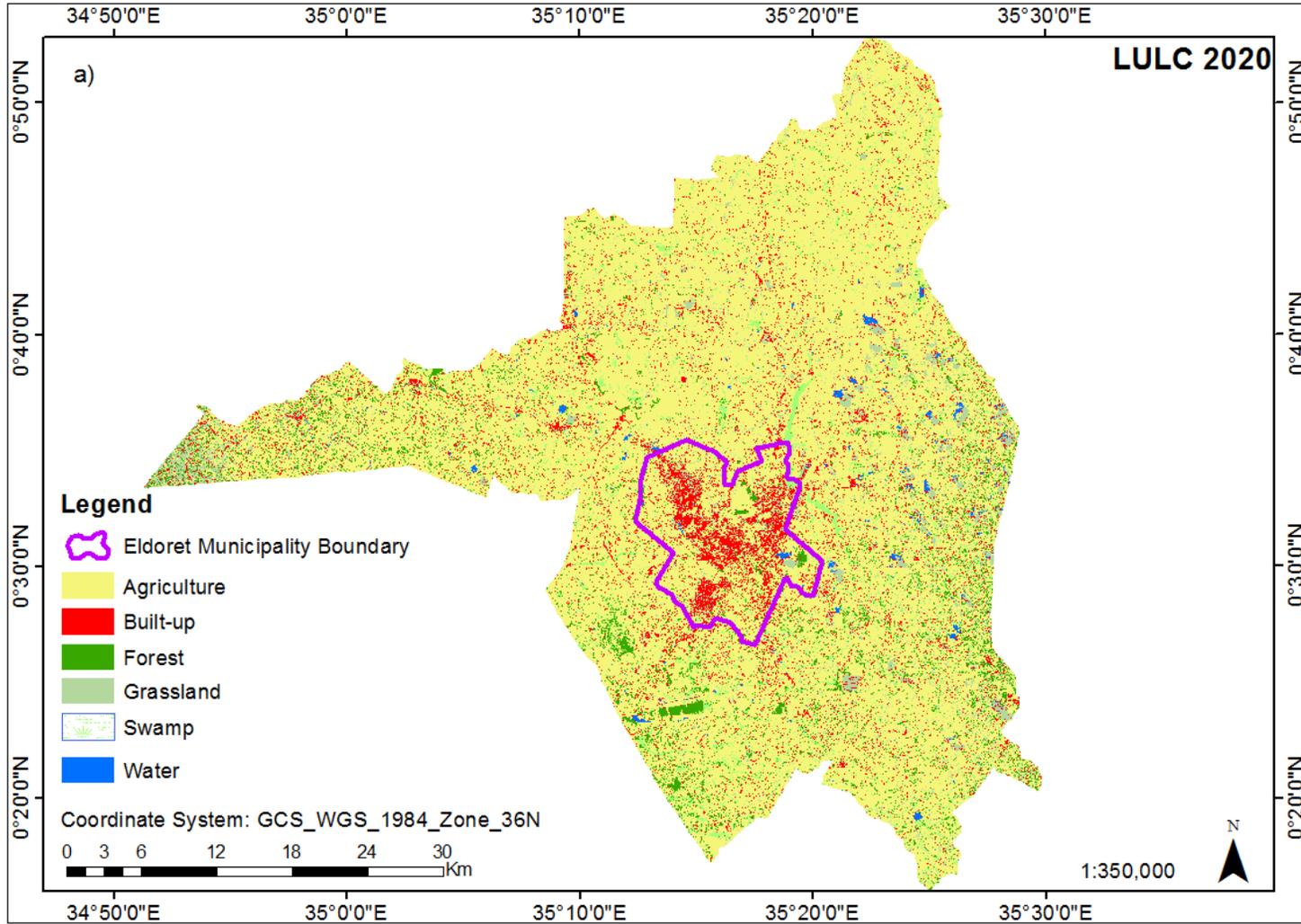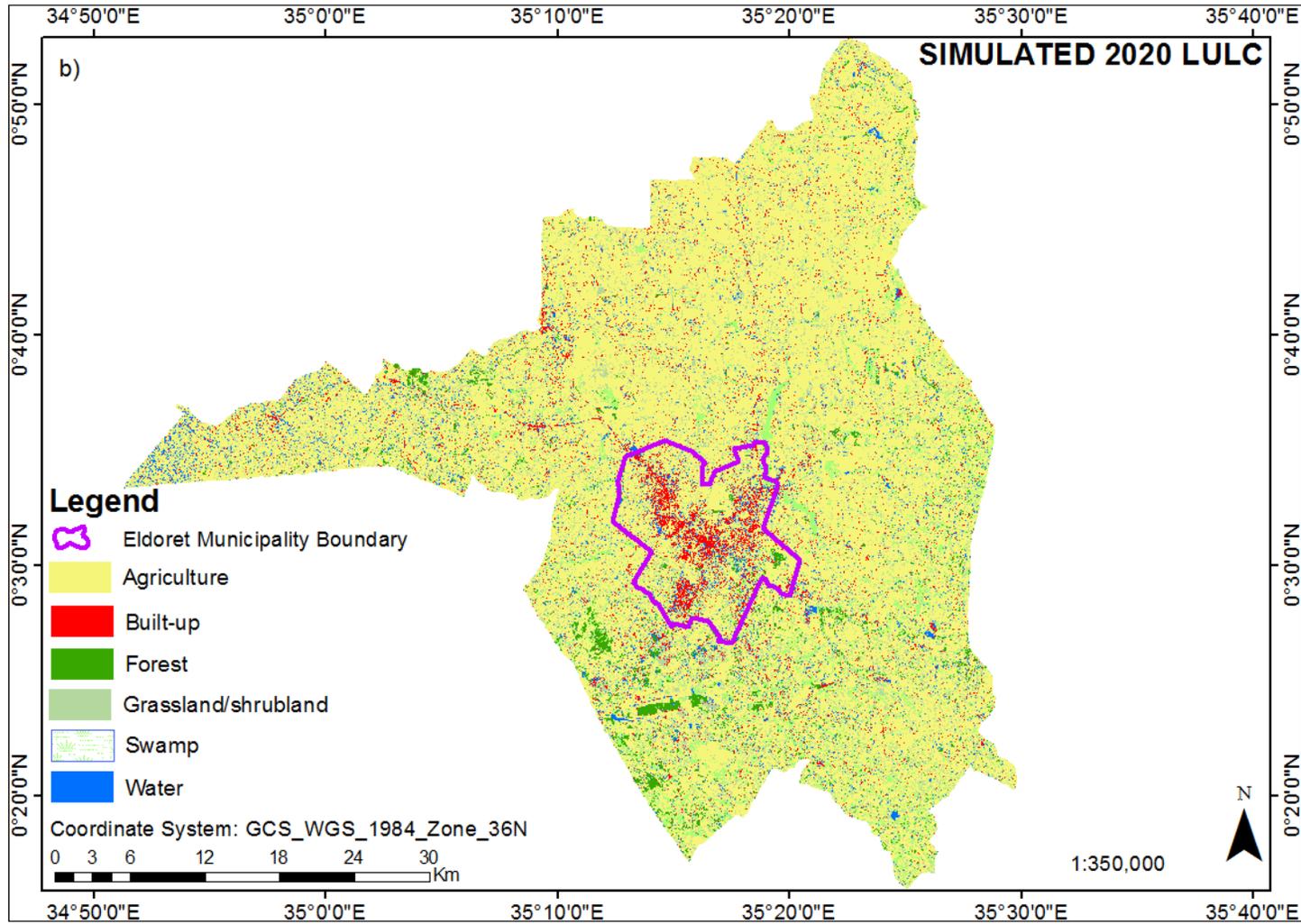
Figure 4.14: a) Classified LULC Map and b) Simulated LULC Map for 2020 based on CA-Markov and AHP Model
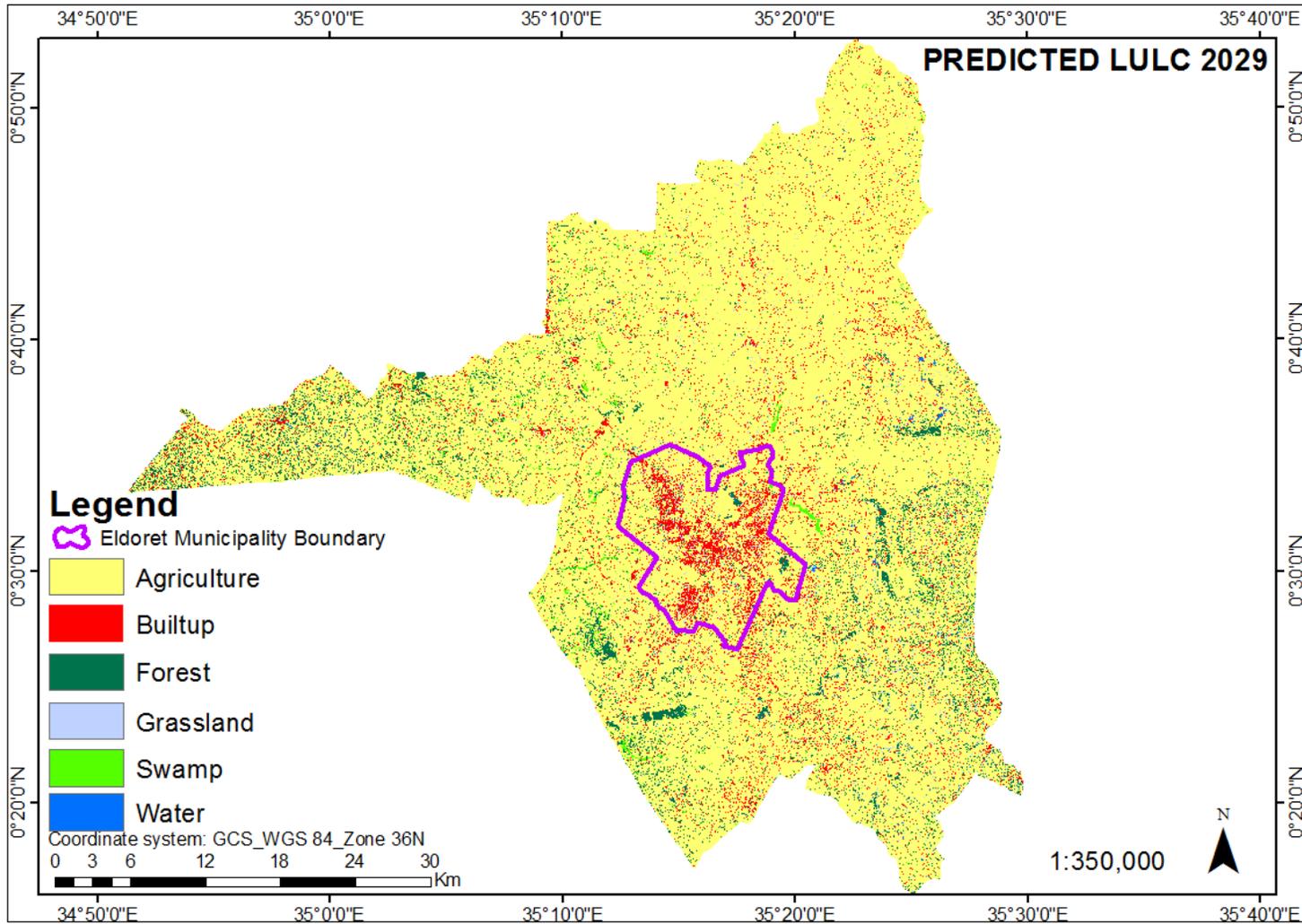
Figure 4.15: Predicted LULC Map for 2029 based on CA-Markov and AHP Model

The sprawl areas for 2020-2029 were then overlaid and eighteen more new sprawl areas that would be built-up by 2029 mapped (Figure 4.16). These sprawl areas also would take different patterns occurring in Kaptuktuk, Kelji, Kapsombee, Torochmoi, two in Kongasis, two in Soy, Kiplombe, Osorongai, two in Lotonyok, Songich, Ndumbeneti sub-locations taking leapfrog pattern; Kuinet, Megun, Lengut and Toloita sub-locations taking linear patterns covering an area of 138.91 km^2 to 154 km^2 during 2020 to 2029 respectively as shown in Figure 4.16.
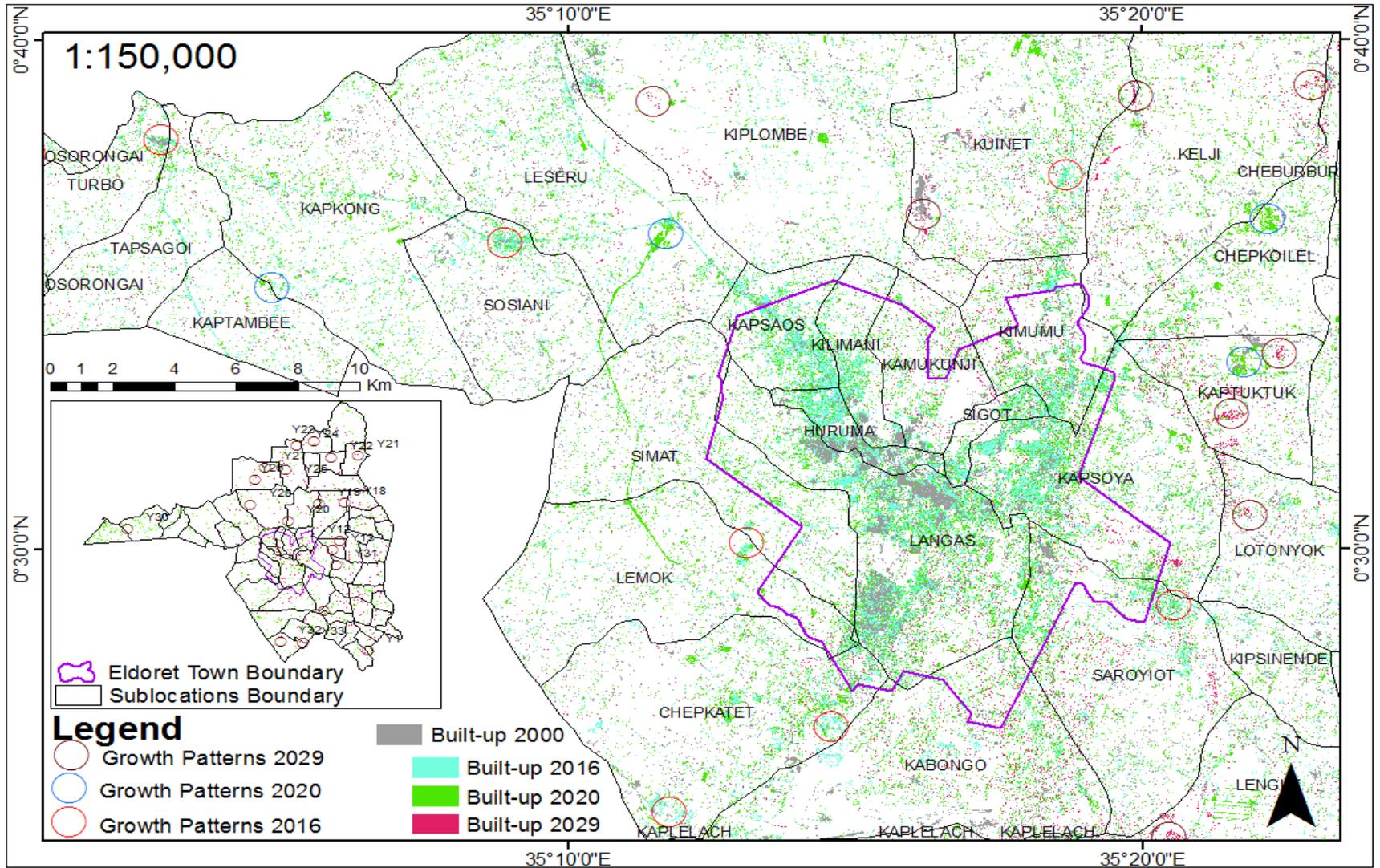
Figure 4.16: Predicted Urban Sprawl Patterns 2029 Map of the Study Area

Figure 4.17 shows a graph of the six LULC for the four years, that is, 2000-2029.
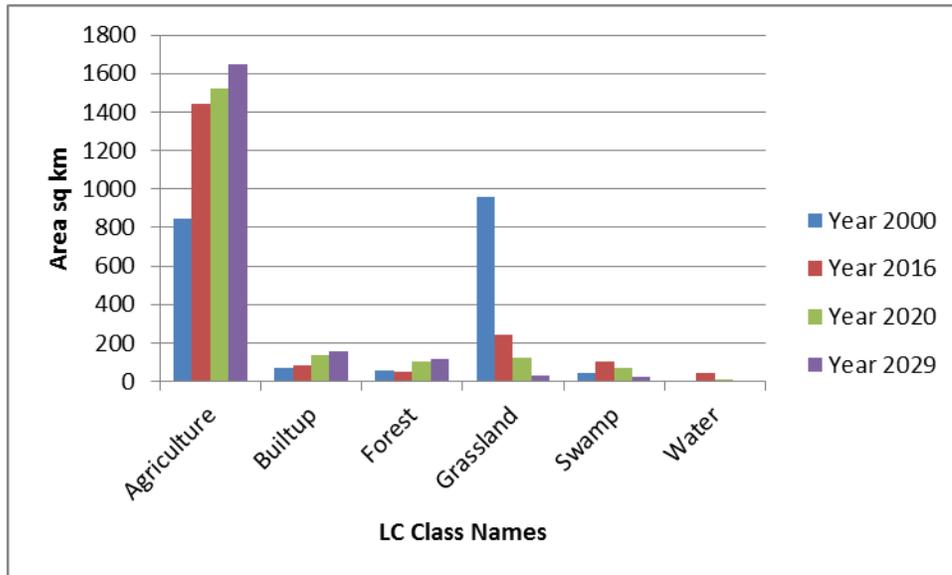
Figure 4.17: Quantity of Previous and Predicted Land Cover Using CA-Markov and AHP Models

The transition probabilities matrix was determined using Markov Chain model as shown in Table 4.8. Also the matrix can be used to ascertain the future potential percentage of change of land cover categories.

Table 4.8: Markov Transition Probabilities Matrix of Periods: 2000-2016 and 2016-2020.

	Class	Agriculture	Swamp	Water	Grassland	Built-up	Forest
2000-2016	Agriculture	0.594752	0.076579	0.033979	0.146961	0.117579	0.030150
	Swamp	0.413714	0.133455	0.231706	0.114661	0.058587	0.047877
	Water	0.545026	0.078542	0.030176	0.141052	0.035284	0.169919
	Grassland	0.785370	0.023611	0.019084	0.117641	0.041026	0.013268
	Built-up	0.442944	0.242964	0.041334	0.140238	0.035000	0.097520
	Forest	0.722307	0.066175	0.021961	0.125090	0.039393	0.025074
2016-2020	Agriculture	0.059664	0.022736	0.003337	0.830809	0.043966	0.039489
	Swamp	0.023657	0.224349	0.005419	0.630614	0.023044	0.092917
	Water	0.042219	0.022039	0.084930	0.576300	0.220139	0.054373
	Grassland	0.092801	0.024009	0.004530	0.720592	0.091197	0.066872
	Built-up	0.108458	0.005415	0.012374	0.386035	0.466402	0.021315
	Forest	0.023065	0.073970	0.002849	0.487615	0.032546	0.0379956

CHAPTER FIVE

DISCUSSIONS

5.1 Introduction

This chapter describes the results obtained as shown in the previous chapter and compares them with other scientific knowledge and literature. This is done according to the objectives of the investigation.

5.2 Urban Sprawl Patterns around Eldoret Town from 2000 to 2020

Findings of this study showed that sprawl areas increased by 67.32 km^2 during 2000-2020 leading to sprawling development manifesting as linear and leapfrog patterns in the suburbs areas.

The 2000-2016 sprawl areas for example, Jua Kali, Turbo, Koibarak and Kipkaren could be as a result of influence of Eldoret-Malaba road since tracks from Mombasa usually parks at these places creating business opportunities to local communities hence their growth. Soy sprawl area along Eldoret-Kitale road could have come up due to employment opportunity at KDF training college at Maili Tisa since it's the nearest trading Centre hence people will prefer to live near work place. Kipkorgot sprawl area along Eldoret-Eldama ravine road could be as a result of topography (elevation and slope) since there is a hill to its North. Also ample land for settlement and also the tarmac road could be factors leading to its growth. Kuinet and Merewet sprawl areas along Eldoret-Ziwa road could be as a result of employment factor since they are near University of Eldoret hence people could prefer to live near work place. Kapseret sprawl

area along Eldoret-Kisumu road could be as a result of employment center since it's near Catholic University, Eldoret National Polytechnic. Also it being near Eldoret town but outside municipality boundary could be a reason since land tenure there is freehold. Tulwet, Leberio and Sarma sprawl areas could be brought by land use since there is ample land for settlements in these places.

For 2016-2020 sprawl areas; Moiben, Tugen estate, Moiben junction sprawl areas along moiben road could be due to availability of fertile land agricultural since the area is well known for farming activities of maize and wheat. Maili nne, Kosachei and Magut sprawl areas along Eldoret-Malaba road could have come up due to the influence of busy A104 highway creating business opportunities to locals. Also Maili nne being near Eldoret town but outside municipality boundary could be a reason since land tenure there is freehold. Cheptiret sprawl area along Eldoret-Nakuru A104 road could have come up due to employment center of Moi University since most students and staff could be residing there. Chirchir, Sololo, Kiluka and Garage sprawl areas could be because of ample land for settlement.

This finding agrees with those of *Wilson et al. (2003)* who found out that sprawl areas can take different spatial patterns including; linear, leapfrog, clustered and scattered patterns. Also a study by *Ashraf M. Dewan and Yusushi Yamaguchi (2014)* shows that land conversion by individuals in Dhaka Metropolitan of Bangladesh region has been increasing due to speculation.

5.2.1 Land Cover Class Discrimination and Change Analysis

Classification techniques by Rule-Based technique discriminated the land cover classes well by use of their spectral values in order to separate features. Land use/cover changes in the study area showed that built-up areas (71.60-138.91 Ha). Forest cover in 2000 was 56.08 (2.82%) km^2 and rose to 51.32 (2.6%) km^2 in 2016 and to 106.76 (5.41%) in 2020. This gradual increase can be attributed to Kenya Forest Service (KFS) in collaboration with the County Government of Uasin Gishu government by continuously planting tree seedlings. In 2019 alone, more than 13 million tree seedlings were planted in Uasin Gishu County, an initiative targeted to increase forest cover to 10% nationally (Kenya News Agency, 2019). This finding resonates with those of *Al-sharif and Bisswajeet Pradhan* in their study of monitoring and forecasting land use change in Tripoli Metropolitan City in 2014 using CA-Markov model revealed that built-up areas increased form 86.4-275.6 km^2 from 1984-2010 respectively. Similar findings were reported by *Ashraf M. Dewan and Yusushi Yamaguchi (2018)* in their study of use of remote technology and GIS to detect and monitor LULC conversion in Dhaka, Bangladesh where built-up areas increased from 4625.4 Ha (11.1%) in 1960 to 20549.7 Ha (49.4%) in 2005.

5.2.2 Accuracy Assessment

Overall classification accuracy results obtained by use of indices (NDVI, NDWI, NDBI, SAVI, and Visible Brightness) in rule-based classification approach in extracting built-up areas were good. However through examination of the accuracies of classified data, all the datasets except Landsat 7 ETM+ met the minimum USGS total accuracy of ≥ 85% set out by Anderson et al. (1976). Low overall accuracy for Landsat 7ETM+ can be because

of the low spatial resolution of 30m of the image. It is worth mentioning that all the images used in this study were taken during the dry spell period in the study area (January, March and December).

Similar findings were given by *Mwakapuja et al. (2013)* who points out the use of indices (NDBI, NDWI, NDBI, SAVI and Visible brightness) in extraction of built-up areas has proved to be an effective method resulting in an accuracy of 82.05% and can be used in other areas with similar characteristics. *Juan et al. (2017)* in a review of built-up indices that are currently in use for urban extraction from remote sensed data, reports that the band ratio for built-up areas (BRBA), normalized built-up area index (NBAI), biophysical composition index (BCI) and combination built-up index (CBI) are robust methods that are available to extract surfaces from complex relief.

5.3 Contribution of Selected Factors that Supports Urban Sprawl Patterns around Eldoret Town

From the results, it is clear that road had great significant impact on the expansion of urban sprawl patterns around Eldoret town during 2000-2020. This can be linked to continuous subdivision of agricultural lands into small plots creates more roads to these plots since every plot should be served with access road (This also agrees with the digitized road maps since there were too many road networks during the study period). It also agrees to a study by *Mohammad et al. (2013)* of urban growth simulation through cellular automata, AHP and GIS in Isfahan. Powerline was second important driving factor and can be because last mile project for electricity connection by government did connections to more rural areas. Employment centers factor had slightly higher AHP

weight since people will tend to live near the work place to save on transportation cost and time thus promoting urban sprawl which depends on other factors.

Population density had less AHP weight than expected since it arises as a result of urban growth. Also Eldoret town is still urbanizing hence there is still more space for settlement. This output collaborates with the research by *Maher et al. (2017)* in a study of upscaling the capability of an integrated CA-Markov model to simulate spatial-time series urban growth trends using an AHP and Frequency Ratio in Malasyia where population density had a lesser AHP weight of 0.42 compared to slope with 0.83.The findings contradicts with that of Muhammad et al. (2019) in his study of analyzing the driving factors causing urban expansion in the peri-urban areas using logistic regression in greater Cairo region, he found out that population density had a weight of 0.933 hence contradicted since it had a greater effect on urban expansion.

Three of the eight factors, that is, constraints to development, elevation and slope had less significant impact on the growth of sprawl patterns in the study area. This can be due to the gentle sloppiness of the study area hence people don't consider them as impediment when they want to settle. For constraints to development, settlements cannot be found in forests and military training camp since they are protected areas. Same outputs were shown by *Sassan Mohammady et al. (2016)* revealing that distance to fault, slope had a least influence in the development of city of Tehran.

Also *Liu et al. (2019)* uses the SLEUTH (Slope, Land Use, Constraints, City, Roads, Hill Shade) model, to simulate the growth of the city in various scenarios of eastern China Hefei from 2015 to 2040. Historical growth scenarios, city planning growth scenarios,

and land suitability growth scenarios were considered and he concluded that by 2040, urban areas will increase to 1434 km^2 in historical growth scenarios, 1190 km^2 in urban planning growth scenarios, and 1217 km^2 in land-adapted growth scenarios, according to forecasts.

5.3.1 Built-up Areas and Urban Sprawl Patterns

Non-porous surfaces such as asphalt and concrete are direct measure of development (*Barnes et al., 2001*, *Sudhira et al., 2004*).

For the study area, the percentage of developed areas and other non-porous surfaces were determined for each year under study such that 3.60% (2000), 4.28% (2016) and 7.04% (2020) respectively. This is an evidence of pattern of urban sprawl and built-up area concentration. The brown-porous surfaces nearly doubled in extent during the two decades covered in this study.

5.3.2 Ratio of Population and Proportion of Developed Areas

Population for each year under study (2000, 2016, 2020 and 2029) was calculated by summing up their interpolated population figures of all the 58 sub-locations.

The population ratio and developed ratio were determined by division of the population and developed area in each year as shown in Table 4.7 by the total population and total extent. If you less the population percentage from the developed percentage, the result will vary from -1 to 1 and if it is 0 or close to 0 it will show an average condition. Higher negative values indicate overcrowding that can cause serious environmental problems.

"Higher positive values indicate higher per capita consumption in urban areas (*Sudhira et al., 2004*)".

The calculated proportion of developed area to proportion of population for each of the 58 sub-locations was near zero (0). For example Turbo sub-location was 0.021, 0.027, 0.057 and 0.061 for the years 2000, 2016, 2020 and 2029 respectively. These near zero (0) values indicates average condition of population in the study area. These zero values can be due to the area being in the peri-urban areas.

Similar findings were reported by *B. Bhatta (2009)* in the study of analysis of urban growth using remote sensing and GIS in Kolkata, India where Eastern and Southern zones had almost zero values indicating average condition of population but contradicts the results in the Northern and Central zones had negative values indicating crowding.

5.3.3 Employment Centers and Built-up Areas

Per capita income is considered as one of economic parameter responsible for urban growth (*Almeida et al., 2017*). Employment center was fourth in rank with 11.38% in order of how it contributes to urban sprawl. This can be argued that people are willing to commute a longer distance to work place from where they live hence these economic centers contributed to urban sprawl. Related outputs were shown by *Subasinghe et al. (2016)* who noted that growth nodes are responsible for urban growth, in their study of spatiotemporal analysis of urban growth using GIS and remote sensing in Colombo metropolitan area, Sri Lanka.

5.4 Prediction of Possible Future Sprawl Patterns around Eldoret Town in 2029 using CA-Markov and AHP Model

The integrated remote sensing and GIS, CA-Markov and AHP models were used to predict future urban sprawl for the year 2029 achieving a prediction accuracy of 83%. According to the findings, built-up areas would increase to 154 km^2 in 2029 from 138.9 km^2 in 2020. A study done by *Meisam et al. (2016)* of dynamic simulation of urban expansion through CA-Markov model a case study of Hyrcanian region, Gilan, Iran found similar results that the extent of built-up areas would increase to 71265 and 78075 Hectares 2025 and 2037 respectively. Also, eighty five percent (85%) simulation accuracy was achieved in a study by *Al-Shariff et al. (2013)* in which they integrated CA model with Markov chain to predict future urban sprawl in Tripoli, Libya. In a similar study by *White et al. (1997)* that used only CA model as a basis of integrated dynamic regional modelling, 65% accuracy was achieved. Nevertheless, in a study done by *Mohammad et al. (2013)*, in 12th municipal district in Isfahan, far better 88% simulation accuracy was achieved when CA model with AHP was used. The prediction results shows future built-up areas will be to mostly agricultural lands thus policy makers should restrict themselves to proper urban planning in order to mitigate challenges of urban growth.

CHAPTER SIX

CONCLUSIONS AND RECOMMENDATIONS

6.1 Introduction

This chapter focuses on key findings, draws conclusions, makes recommendations that are expected to influence policy, contributes to the literature on this subject, and proposes areas of further research.

6.2 Conclusions

The discussions in the previous chapter have focused on the extent and pattern of changes in urban sprawl in the area around Eldoret over the last two decades, which will help guide the city's future planning and policymaking.

The LULC classes of particular interest for this study namely built-up area, forest, water, grassland/shrubland, swamp and agricultural or farmlands and sprawl areas for 2000-2029 were isolated efficiently and accurately from both Landsat 7 ETM+ images of 2000 and Sentinel-2 images of 2016 and 2020 by use of indices and supervised classification.

The analysis shows the dispersion of urban growth in the study area. This is a strong sign of urban sprawl and concludes that towns in growing states are not compact.

Using the classified LULC maps of 2000, 2016 and 2020, the future LULC of the study area was successfully modelled and the prediction of future urban sprawl patterns also mapped using CA-Markov and AHP models. Irrevocable effects of urban sprawl have led

to overuse of natural resources for example land and soil. With the effects of urban sprawl, settlements, business and industrial areas are getting closer to these resources and protected areas hence increasing air pollution and damaging ecosystem (*EEA, 2006*).

This study identified eight driving factors derived from literature by researcher who had carried out similar investigations and related these factors to growth patterns to identify those factors having great influence on urban sprawl in the study area around Eldoret town. Three factors such as distance to roads, distance to powerline, distance to water line were the most significant driving factors in the study area during the last 20 years (2000-2020), accounting for 62.38% of the mapped sprawl.

Using the simulated 2020 LULC and 2016-2020 Markov transition probability matrix, the future 2029 LULC of the study area was modelled, predicted and the future 2029 urban sprawl areas mapped successfully.

Most 2016, 2020 and 2029 sprawl areas were outlying sprawl (linear, clustered and isolated) characterized by non-developed to developed land cover occurring beyond existing developed areas. Isolated sprawl were characterized by one or several non-developed pixels some distance from an existing developed area being developed e.g. Kipkorgot, Sarma, Leberio, Moiben Junction, Sololo market centers. In linear sprawl, the pixels that change to built-up area are linked in a linear fashion e.g. Juakali, Turbo, Kapseret, Maili Tisa, Koibaraka market centers. The clustered sprawl areas are large, compact and dense developed some distance from developed area hence no sprawl area qualified to be categorized here.

6.3 Recommendations

Uasin Gishu county government should give priority to roads, powerline and water connections in areas identified for future development and limit these services in areas that are not. This will control urban sprawl and protect agricultural land from conversion.

The study recommends decision makers to come up with policies that limit urban expansion thus saving agricultural lands from conversions. For example; policies that are aimed at increasing densities like vertical construction of residential apartments, embracing Sectional Properties Act No. 21 of 2020 which provide for the division of buildings into units to be owned by individual proprietors and the common property to be owned by the proprietors of the units as a tenant in common, policies that direct people towards city centre and its vicinity instead of city boundaries, making important promotions on urban regeneration and making investment on public transportation thus protecting agricultural land by restricting urban growth with green belt.

Uasin Gishu County policy makers and planners should encourage infill developments since utilities such as sewer, water, roads already exist and at the same time guide these developments so that they enhance the quality of life for example size, architectural design of new infill development.

Ministry of agriculture should give financial support, cheap farm inputs, post-harvest and marketing among others to farmers so as to discourage them from partitioning their land for built-up areas. This will increase production, promote good agricultural practices and give them stable income from farming.

Policy makers and planners should carry out forward planning of areas and provide requisite infrastructure ahead of development so as to avoid proliferation of slums and economic effects brought about when trying to bring services for example a trunk road which is more expensive where people have already settled.

The 2029 prediction model can be used by decision makers as a guide for allocation of resources and services ahead of developments.

Uasin Gishu county physical planning, standards, guidelines and regulations on minimum plot sizes should to be enforced to protect the limited natural resources from exhaustion.

Decision makers and planners could plan for outreach programs aimed at helping a variety of audiences understand the adverse impacts of sprawl and the way to mitigating it.

6.4 Area for further research

Further environmental impact such as water, air pollutions and land surface temperature (LST) rise can be studied in response to growth of sprawl areas in the study area.

REFERECES

Abdullahi, S., Pradhan, B., & Al-sharif, A. A. (2017). Introduction to Urban Growth and Expansion. In Spatial Modeling and Assessment of Urban Form *(pp. 3-15)*. Springer, *Cham.*

Abdullahi, S., Mahmud, A. R. B., & Pradhan, B. (2014). Spatial modelling of site suitability assessment for hospitals using geographical information system-based multicriteria approach at Qazvin city, Iran. *Geocarto International, 29(2), 164-184.*

Aburas, M. M., Ho, Y. M., Ramli, M. F., & Ash'aari, Z. H. (2016). The simulation and prediction of spatio-temporal urban growth trends using cellular automata models: A review. *International Journal of Applied Earth Observation and Geoinformation, 52, 380-389.*

Aburas, M. M., Ho, Y. M., Ramli, M. F., & Ash'aari, Z. H. (2017). Improving the capability of an integrated CA-Markov model to simulate spatio-temporal urban growth trends using an Analytical Hierarchy Process and Frequency Ratio. International *Journal of Applied Earth Observation and Geoinformation, 59, 65-78.*

Adelaja, A., Sullivan, K., & Lake, M. B. (2005, March). Agricultural Viability at the Urban Fringe. *In selected paper presented at the International Conference on Emerging Issues along*

Addison, C., Zhang, S., & Coomes, B. (2013). Smart growth and housing affordability: *A* review of regulatory mechanisms and planning practices. *Journal of Planning Literature, 28(3), 215-257.*

Afram, A., Janabi-Sharifi, F., Fung, A. S., & Raahemifar, K. (2017). *Artificial neural network (ANN) based model predictive control (MPC) and optimization of HVAC systems: A state of the art review and case study of a residential HVAC system. Energy and Buildings, 141, 96-113.*

Almeida, C. M. D., Monteiro, A. M. V., Câmara, G., Soares-Filho, B. S., Cerqueira, G. C., Pennachin, C. L., & Batty, M. (2005). *GIS* and remote sensing as tools for

the simulation of urban land-use change. *International Journal of Remote Sensing, 26(4), 759-774.*

Al-sharif, A. A., & Pradhan, B. (2014). Monitoring and predicting land use change in Tripoli Metropolitan City using an integrated Markov chain and cellular automata models in GIS. *Arabian journal of geosciences, 7(10), 4291-4301.Saudi Society for Geoscience 2013.*

Al-Sharif, A. A., Pradhan, B., Shafri, H. Z. M., & Mansor, S. (2013). *Spatio-temporal* analysis of urban and population growths in Tripoli using remotely sensed data and GIS. *Indian Journal of Science and technology, 6(8), 5134-5142.*

Anderson, J. R. (1993). Problem solving and learning. *American psychologist, 48(1), 35.*

Appiah, D. O., Bugri, J. T., Forkuo, E. K., & Boateng, P. K. (2014). Determinants of peri-urbanization and land use change patterns in peri-urban Ghana. *Journal of Sustainable Development, 7(6), 95.*

Arsanjani, J. J., Helbich, M., Kainz, W., & Boloorani, A. D. (2013). Integration of logistic regression, Markov chain and cellular automata models to simulate urban expansion. *International Journal of Applied Earth Observation and Geoinformation, 21, 265-275.*

Ashtiani, M., & Abdollahi Azgomi, M. (2016). Trust modeling based on a combination of fuzzy analytic hierarchy process and fuzzy VIKOR. *Soft Computing, 20(1), 399-421.*

Armson, D., Stringer, P., & Ennos, A. R. (2012). The effect of tree shade and grass on surface and globe temperatures in an urban area. Urban Forestry & Urban Greening, *11(3), 245-255.*

Banzhaf, H. S., & Lavery, N. (2010). Can the land tax help curb urban sprawl? Evidence from growth patterns in Pennsylvania. *Journal of Urban Economics, 67(2), 169-179.*

Barnes, K.B., Morgan III, J.M., Roberge, M.C., Lowe, S., 2001. *Sprawl development: its patterns, consequences, and measurement. Towson University, Towson.*

Barnes, K. B., Morgan III, J. M., Roberge, M. C., & Lowe, S. (2001). *Sprawl development: its patterns, consequences, and measurement. Towson University, Towson, 1, 24.*

Barnum, T. R., Weller, D. E., & Williams, M. (2017*). Urbanization reduces and homogenizes trait diversity in stream macroinvertebrate communities. Ecological Applications, 27(8), 2428-2442.*

Batty, M., Xie, Y., & Sun, Z. (1999). *Dynamics of urban sprawl.*

Belal, A. A., & Moghanm, F. S. (2011*). Detecting urban growth using remote sensing and GIS techniques in Al Gharbiya governorate, Egypt. The Egyptian Journal of Remote Sensing and Space Science, 14(2), 73-79.*

Bengston, D. N., Fletcher, J. O., & Nelson, K. C. (2004). *Public policies for managing urban growth and protecting open space: policy instruments and lessons learned in the United States. Landscape and urban planning, 69(2-3), 271-286.*

Bertaud, A., & Brueckner, J. K. (2005). *Analyzing building-height restrictions: predicted impacts and welfare costs. Regional Science and Urban Economics, 35(2), 109-125.*

Bhatta (2009) Analysis of urban growth pattern using remote sensing and GIS: a case study of Kolkata, India, *International Journal of Remote Sensing, 30:18, 4733-4746, DOI: 10.1080/01431160802651967*

Bhatta, B. (2010). Causes and consequences of urban growth and sprawl. In Analysis of urban growth and sprawl from remote sensing data *(pp. 17-36). Springer, Berlin, Heidelberg.*

Bhatta, B. (2010). *Analysis of urban growth and sprawl from remote sensing data. Springer Science & Business Media.*

Bhat, P. A., ul Shafiq, M., Mir, A. A., & Ahmed, P. (2017). Urban sprawl and its impact on landuse/land cover dynamics of Dehradun *City, India. International Journal of Sustainable Built Environment, 6(2), 513-521.*

Bird, R. M., & Slack, N. E. (Eds.). (2004). *International handbook of land and property taxation.* Edward Elgar Publishing.

Blaschke, T. (2010). Object based image analysis for remote sensing. *ISPRS journal of photogrammetry and remote sensing, 65(1), 2-16.*

Boiman, O., Shechtman, E., & Irani, M. (2008, June). In defense of nearest-neighbor based image classification. *In 2008 IEEE conference on computer vision and pattern recognition (pp. 1-8). IEEE.*

Boori, M. S., Netzband, M., Choudhary, K., & Voženílek, V. (2015). *Monitoring and modeling of urban sprawl through remote sensing and GIS in Kuala Lumpur, Malaysia. Ecological Processes, 4(1), 1-10.*

Boroushaki, S., & Malczewski, J. (2008). *Implementing an extension of the analytical hierarchy process using ordered weighted averaging operators with fuzzy quantifiers in ArcGIS. Computers & geosciences, 34(4), 399-410.*

Brandt, N. (2014). *Greening the Property Tax.*

Brueckner, J. K. (2000*). Urban sprawl: Diagnosis and remedies. International regional science review, 23(2), 160-171.*

Brueckner, J. K., & Sridhar, K. S. (2012). Measuring welfare gains from relaxation of land-use restrictions: The case of India's building-height limits. *Regional Science and Urban Economics, 42(6), 1061-1067.*

Buettner, T. (2015). Urban estimates and projections at the United Nations: The strengths, weaknesses, and underpinnings of the world urbanization prospects. Spatial Demography, 3(2), 91-108.*Uwe Soergel (2002): Radar Remote Sensing of Urban Areas from Remote Sensing Data*

Bullock, E. L., Healey, S. P., Yang, Z., Oduor, P., Gorelick, N., Omondi, S., ... & Cohen, W. B. (2021). *Three decades of land cover change in East Africa. Land, 10(2), 150.*

Burchell, R. W., Downs, A., McCann, B., & Mukherji, S. (2005). Sprawl costs: *Economic impacts of unchecked development.*

Candau, J. T. (2002). *Temporal calibration sensitivity of the SLEUTH urban growth model* (Doctoral dissertation, University of California, Santa Barbara).

Chen, J., & Chang, H. (2019). Dynamics of wet-season turbidity in relation to precipitation, discharge, and land cover in three urbanizing watersheds, Oregon. *River Research and Applications, 35(7), 892-904.*

Christiansen, P., & Loftsgarden, T. (2011). Drivers behind urban sprawl in Europe. *TØI report, 1136, 2011.*

Council, M. L. U. L. (2005). *Defining Sprawl and Smart Growth.* Working Paper prepared by Public Sector Consultants Inc), *1-9.*

Couch, C., Karecha, J., Nuissl, H., & Rink, D. (2005). Decline and sprawl: an evolving type of urban development–observed in Liverpool and Leipzig. *European planning studies, 13(1), 117-136.*

Cotula, L. (2009). *Land grab or development opportunity?: agricultural investment and international land deals in Africa. Iied.*

Eastman, J. R., & Fulk, M. (1993). *Long sequence time series evaluation using standardized principal components. Photogrammetric Engineering and remote sensing, 59(6).*

Carruthers, J. I. (2002). The impacts of state growth management programmes: A comparative analysis. *Urban studies, 39(11), 1959-1982.*

Cervero, R., & Murakami, J. (2010). *Effects of built environments on vehicle miles traveled: evidence from 370 US urbanized areas. Environment and planning A, 42(2), 400-418.*

Cohen, J. E. (2003). Human population: the next half century. *Science, 302(5648), 1172-1175.*

Cohen, J. (1960). *A coefficient of agreement for nominal scales. Educational and psychological measurement, 20(1), 37-46.*

Congalton, R. G. (1991). *A review of assessing the accuracy of classifications of remotely sensed data. Remote sensing of environment, 37(1), 35-46.*

Corner, R. J., Dewan, A. M., & Chakma, S. (2014). Monitoring and prediction of land-use and land-cover (LULC) change. In Dhaka megacity (pp. 75-97*). Springer, Dordrecht.*

Creswell, J. W., & Creswell, J. (2003). Research design (pp. 155-179). Thousand Oaks, CA: *Sage publications.*

Christofakis, M., & Papadaskalopoulos, A. (2011). *The Growth Poles Strategy in regional planning: The recent experience of Greece. Theoretical and Empirical Researches in Urban Management, 6(2), 5-20*

Christaller, W. (1933). Die zentralen Orte in Suddeutschland: *Eine okonomisch-geographische Untersuchung uber die Gesetzmassigkeit der Verbreitung und Entwicklung der Siedlungen mit stadtischen Funktionen. Jena.*

Czamanski, D., Benenson, I., Malkinson, D., Marinov, M., Roth, R., & Wittenberg, L. (2008). Urban sprawl and ecosystems—Can nature survive*?. International review of environmental and resource economics, 2(4), 321-366.*

das Neves Almeida, T. A., Cruz, L., Barata, E., & García-Sánchez, I. M. (2017). Economic growth and environmental impacts: An analysis based on a composite index of environmental damage. *Ecological Indicators, 76, 119-130.*

de Almeida, C. M., Batty, M., Monteiro, A. M. V., Câmara, G., Soares-Filho, B. S., Cerqueira, G. C., & Pennachin, C. L. (2003). *Stochastic cellular automata modeling of urban land use dynamics: empirical development and estimation. Computers, environment and urban systems, 27(5), 481-509.*

Dewan, A. M., & Yamaguchi, Y. (2009). *Using remote sensing and GIS to detect and monitor land use and land cover change in Dhaka Metropolitan of Bangladesh during 1960–2005. Environmental monitoring and assessment, 150(1), 237-249.*

Eastman, J. R., & Fulk, M. (1993). *Long sequence time series evaluation using standardized principal components. Photogrammetric Engineering and remote sensing, 59(6).*

eCognition, 2014: *User Guide, Defiens Imaging GmbH, Munich*

EEA - European Environment Agency 2006, "Down to earth: soil degradation and sustainable development in Europe: a challenge for the 21st century", *Environmental issue series no.   16, Copenhagen.*

Ermini, B., & Santolini, R. (2017). Urban sprawl and property tax of a city's core and suburbs: Evidence from Italy. *Regional Studies, 51(9), 1374-1386.*

Ettehadi Osgouei, P., Kaya, S., Sertel, E., & Alganci, U. (2019). Separating built-up areas from bare land in mediterranean cities using Sentinel-2A imagery. *Remote Sensing, 11(3), 345.*

Ewing, R., 1997. Counterpoint: *is* Los Angeles-style sprawl desirable? Journal of the American   *Planning Association 63 (1):107-126*

Forrester, J. W. (1996). *System dynamics and K-12 teachers. Retrieved August, 8, 2008.*

Friedman, B. M. (2017). The moral consequences of economic growth. In Markets, morals & religion (pp. 29-42). Routledge.

Galster, G., Hanson, R., Ratcliffe, M. R., Wolman, H., Coleman, S., & Freihage, J. (2001). *Wrestling sprawl to the ground: defining and measuring an elusive concept. Housing policy debate, 12(4), 681-717.*

Gao, F., De Colstoun, E. B., Ma, R., Weng, Q., Masek, J. G., Chen, J., ... & Song, C. (2012). Mapping impervious surface expansion using medium-resolution satellite image time series: a case study in the Yangtze River Delta, China. *International Journal of Remote Sensing, 33(24), 7609-7628.*

García, A. M., Santé, I., Boullón, M., & Crecente, R. (2012). A comparative analysis of cellular automata models for simulation of small urban areas in Galicia, NW Spain. Computers, *environment and urban systems, 36(4), 291-301.*

Gillham, O. (2002). *The limitless city: a primer on the urban sprawl debate. Island Press.*

Grimm, N. B., Grove, J. G., Pickett, S. T., & Redman, C. L. (2000). Integrated approaches to long-term studies of urban ecological systems: Urban ecological systems present multiple challenges to ecologists—Pervasive human impact and extreme heterogeneity of cities, and the need to integrate social and ecological approaches, concepts, and theory. *BioScience, 50(7), 571-584.*

Guan, D., Li, H., Inohae, T., Su, W., Nagaie, T., & Hokao, K. (2011). Modeling urban land use change by the integration of cellular automaton and Markov model. *Ecological modelling, 222(20-22), 3761-3772.*

Halmy, M. W. A., Gessler, P. E., Hicke, J. A., & Salem, B. B. (2015). Land use/land cover change detection and prediction in the north-western coastal desert of Egypt using Markov-CA. *Applied Geography, 63, 101-112.*

Hands on Exercise using eCognition

Harvey, R. O., & Clark, W. A. (1965). The nature and economics of urban sprawl. *Land Economics, 41(1), 1-9.*

Harvey, D. (2009). *Reshaping economic geography: the world development report 2009. Development and change, 40 (6), 1269-1277*

HABITAT-UNEP, U. N. (2000). *Integrating gender responsive environmental planning and management.*

Hasse, J. E., & Lathrop, R. G. (2003). Land resource impact indicators of urban sprawl. A*pplied geography, 23(2-3), 159-175.*

He, C., Shi, P., Xie, D., & Zhao, Y. (2010). Improving the normalized difference built-up index to map urban built-up areas using a semiautomatic segmentation approach. *Remote Sensing Letters, 1(4), 213-221.*

Houshyar, E., SheikhDavoodi, M. J., Almassi, M., Bahrami, H., Azadi, H., Omidi, M., ... & Witlox, F. (2014). Silage corn production in conventional and conservation tillage systems. Part I: sustainability analysis using combination of GIS/AHP and multi-fuzzy modeling. *Ecological Indicators, 39, 102-114.*

Jabari, S., & Zhang, Y. (2013). *Very high resolution satellite image classification using fuzzy rule-based systems. Algorithms, 6(4), 762-781.*

Jackson, J. A. (2005). *Glossary of geology (p. 5th).*

Jacquin, A., Misakova, L., & Gay, M. (2008). *A hybrid object-based classification approach for mapping urban sprawl in periurban environment. Landscape and urban planning, 84(2), 152-165.*

Janiola, M. D. C., Pelayo, J. L., & Gacad, J. L. J. *distinguishing urban built-up and bare soil features from landsat 8 oli imagery using different developed band indices.*

Jat, M. K., Garg, P. K., & Khare, D. (2008). Modelling of urban growth using spatial analysis techniques: a case study of Ajmer city (India*). International Journal of Remote Sensing, 29(2), 543-567.*

Koko, A. F., Yue, W., Abubakar, G. A., Hamed, R., & Alabsi, A. A. N. (2020). *Monitoring and Predicting Spatio-Temporal Land Use/Land Cover Changes in Zaria City, Nigeria, through an Integrated Cellular Automata and Markov Chain Model (CA-Markov). Sustainability, 12(24), 10452.*

Koomen, E., & Borsboom-van Beurden, J. (2011). Land-use modelling in planning practice (*pp. XVI-214). Springer Nature.*

Li, C., Wang, J., Wang, L., Hu, L., & Gong, P. (2014). Comparison of classification algorithms and training sample sizes in urban land classification with Landsat thematic mapper imagery. *Remote sensing, 6(2), 964-983.*

Liu, Y., Li, L., Chen, L., Cheng, L., Zhou, X., Cui, Y., & Liu, W. (2019). Urban growth simulation in different scenarios using the SLEUTH model: A case study of Hefei, East China. *PLoS One, 14(11), e0224998.*

Loonen, W., Heuberger, P., & Kuijpers-Linde, M. (2007). Spatial optimisation in land-use allocation problems. In Modelling land-use change *(pp. 147-165). Springer, Dordrecht.*

Lopez, J. A. (2001). Evaluating the predictive accuracy of volatility models. *Journal of forecasting, 20(2), 87-109.*

Lord, R. G. (1985). Accuracy in behavioral measurement: An alternative definition based on raters' cognitive schema and signal detection theory. *Journal of Applied Psychology, 70(1), 66.*

Macal, C. M., & North, M. J. (2006, December). *Tutorial on agent-based modeling and simulation part 2: how to model with agents.* In Proceedings of the 2006 Winter simulation conference (pp. 73-83). IEEE.

Mahamud, M.A.; Samat, N.; Mohd Noor, N. Identifying Factors Influencing Urban Spatial Growth for The George Town Conurbation. Plan. *Malays. J. 2016, 14. [CrossRef]*

Maier, G., Franz, G., & Schrock, P. (2006). *Urban Sprawl. How Useful Is This Concept?*

Maktav, D., & Erbek, F. S. (2005). Analysis of urban growth using multi-temporal satellite data in Istanbul, Turkey. *International Journal of Remote Sensing, 26(4), 797-810.*

Malleson, N., Heppenstall, A., & See, L. (2010). *Crime reduction through simulation: An agent-based model of burglary. Computers, environment and urban systems, 34(3), 236-250.*

Meisam Jafari, Hamid Majedi, Seyed Masoud Monavari, Ali Asghar Alesheikh & Mirmasoud Kheirkhah Zarkesh (2016) Dynamic simulation of urban expansion through a CA-Markov model Case study: Hyrcanian region, Gilan, Iran, *European Journal of Remote Sensing, 49:1, 513-529, DOI: 10.5721/EuJRS20164927*

McFeeters, S. K. (1996). The use of the Normalized Difference Water Index (NDWI) in the delineation of open water features. *International journal of remote sensing, 17(7), 1425-1432.*

Mishra, V. N., & Rai, P. K. (2016). A remote sensing aided multi-layer perceptron-Markov chain analysis for land use and land cover change prediction in Patna district (Bihar), India. *Arabian Journal of Geosciences, 9(4), 1-18.*

Mittal, I., & Gupta, R. K. (2015). Natural resources depletion and economic growth in present era. SOCH-Mastnath *Journal of Science & Technology (BMU, Rohtak)(ISSN: 0976-7312), 10(3).*

Mohamed, A., & Worku, H. (2020). Simulating urban land use and cover dynamics using cellular automata and Markov chain approach in Addis Ababa and the surrounding. *Urban Climate, 31, 100545*

Mohammady, S., & Delavar, M. R. (2016). Urban sprawl assessment and modeling using landsat images and GIS. *Modeling Earth Systems and Environment, 2(3), 1-14.*

Mohammad, M., Sahebgharani, A., & Malekipour, E. (2013). *Urban growth simulation through cellular automata (CA), analytic hierarchy process (AHP) and GIS; case study of 8th and 12th municipal districts of Isfahan. Geographia Technica, 8(2), 57-70.*

Mokarram, M., Pourghasemi, H. R., Hu, M., & Zhang, H. (2021). Determining and forecasting drought susceptibility in southwestern Iran using multi-criteria decision-making (MCDM) coupled with CA-Markov model. *Science of The Total Environment, 781, 146703.*

Muhammad Adeel (2010) Methodology for identifying urban growth potential using land use and population data: A case study of Islamabad Zone IV. *International Society for Environmental Information Sciences 2010 Annual Conference (ISEIS).*

Musole, M. (2009). Property rights, transaction costs and institutional change: Conceptual framework and literature review. *Progress in Planning, 71(2), 43-85.*

Mwakapuja, F., Liwa, E., & Kashaigili, J. (2013). *Usage of indices for extraction of built-up areas and vegetation features from landsat TM image: a case of Dar es Salaam and Kisarawe peri-urban areas, Tanzania.*

Mwasi, B. N. (2004). *Landscape Change Dynamics in a Semi-arid Part of Baringo District, Kenya, Based on Landsat-TM Data and GIS Analysis. Amsterdam,* The Netherland: Universiteit van Amsterdam, IBED.

Navamuel, E. L., Morollón, F. R., & Cuartas, B. M. (2018). Energy consumption and urban sprawl: Evidence for the Spanish case. *Journal of cleaner production, 172, 3479-3486.*

Nechyba, T. J., & Walsh, R. P. (2004). Urban sprawl. *Journal of economic perspectives, 18(4), 177-200.*

Osman, T.; Divigalpitiya, P.; Arima, T. Driving Factors of Urban Sprawl in Giza Governorate of the Greater Cairo Metropolitan Region Using a Logistic Regression Model. *Int. J. Urban Sci. 2016, 20, 206–225. [CrossRef]*

Osman, T., Divigalpitiya, P., & Arima, T. (2016). Driving factors of urban sprawl in Giza Governorate of Greater Cairo Metropolitan Region using AHP method. *Land Use Policy, 58, 21-31.*

Padmanaban, R., Bhowmik, A. K., Cabral, P., Zamyatin, A., Almegdadi, O., & Wang, S. (2017). Modelling urban sprawl using remotely sensed data: A case study of Chennai city, Tamilnadu. *Entropy, 19(4), 163.*

Paine, D.P., & Kiser, J.D. (2012). Aerial photography & image interpretation. *John Wiley & Sons.*

Parker, C. P., Baltes, B. B., Young, S. A., Huff, J. W., Altmann, R. A., Lacost, H. A., & Roberts, J. E. (2003). Relationships between psychological climate perceptions and work outcomes: a meta-analytic review. *Journal of Organizational Behavior: The International Journal of Industrial, Occupational and Organizational Psychology and Behavior, 24(4), 389-416.*

Parsa, M., Maghsoudi, A., Yousefi, M., & Sadeghi, M. (2016*). Recognition of significant multi-element geochemical signatures of porphyry Cu deposits in Noghdouz area, NW Iran. Journal of Geochemical Exploration, 165, 111-124*.

Polidoro, M., de Lollo, J. A., & Fernandes Barros, M. V. (2011). Environmental Impacts of urban sprawl in Londrina, Parana, Brazil. *Journal of Urban and Environmental Engineering, (52)*

Pooyandeh, M., Mesgari, S., Alimohammadi, A., & Shad, R. (2007, August). *A* comparison between complexity and temporal GIS models for spatio-temporal urban applications. In International Conference on Computational Science and Its Applications (pp. 308-321). *Springer, Berlin, Heidelberg.*

Roberts, G. (Ed.). (2013). Langmuir-blodgett films. *Springer Science & Business Media.*

Ruben, G. B., Zhang, K., Dong, Z., & Xia, J. (2020). Analysis and projection of land-use/land-cover dynamics through scenario-based simulations using the CA-Markov model: A case study in guanting reservoir basin, China*. Sustainability, 12(9), 3747.*

Salem, M., Tsurusaki, N., & Divigalpitiya, P. (2019). *Analyzing the driving factors causing urban expansion in the peri-urban areas using logistic regression: a case study of the Greater Cairo region. Infrastructures, 4(1), 4.*

Samat, N. (2009). Integrating GIS and CA-MARKOV model in evaluating urban spatial growth. *Malaysian Journal of Environmental Management, 10(1), 83-99*

Samat, N. (2009*). Integrating GIS and CA-MARKOV model in evaluating urban spatial growth. Malaysian Journal of Environmental Management, 10(1), 83-99.*

Sang, L., Miller, J. J., Corbit, K. C., Giles, R. H., Brauer, M. J., Otto, E. A., ... & Jackson, P. K. (2011). *Mapping the NPHP-JBTS-MKS protein network reveals ciliopathy disease genes and pathways. Cell, 145(4), 513-528.*

Sari, F. (2020). Assessment of land-use change effects on future beekeeping suitability via CA-Markov prediction model. *Journal of Apicultural Science, 64(2), 263-276.*

Sassan Mohammady, Mahmoud Reza Delavar (2016). Urban sprawl assessment and modeling using landsat images and GIS. *Springer International Publishing Switzerland 2016.*

Saaty, T. L., & Vargas, L. G. (1980). Hierarchical analysis of behavior in competition: Prediction in chess. *Behavioral science, 25(3), 180-191.*

Schoer, K., & EEA, E. E. A. (2006, June). *Calculation of direct and indirect material inputs by type of raw material and economic activities.* In Paper presented at the London Group Meeting (Vol. 19, p. 21).

Siddiqui, A.; Siddiqui, A.; Maithani, S.; Jha, A.K.; Kumar, P.; Srivastav, S.K. Urban Growth Dynamics of an Indian Metropolitan Using CA Markov and Logistic Regression. Egypt. J. Remote Sens. *Space Sci. 2018, 21, 229–236. [CrossRef]*

Shuster, W. D., Bonta, J., Thurston, H., Warnemuende, E., & Smith, D. R. (2005). Impacts of impervious surface on watershed hydrology: A review. *Urban Water Journal, 2(4), 263-275.*

Slack, E. (2002). *Municipal finance and the pattern of urban growth (Vol. 160).* Toronto: CD Howe Institute.

Subedi, P., Subedi, K., & Thapa, B. (2013). Application of a hybrid cellular automaton–Markov (CA-Markov) model in land-use change prediction: a case study of Saddle Creek Drainage Basin, *Florida. Applied Ecology and Environmental Sciences, 1(6), 126-132.*

Subasinghe, S., Estoque, R. C., & Murayama, Y. (2016). Spatiotemporal analysis of urban growth using GIS and remote sensing: A case study of the Colombo Metropolitan Area, Sri Lanka. *ISPRS international journal of geo-information, 5(11), 197.*

Sudhira, H. S., Ramachandra, T. V., & Jagadish, K. S. (2004). Urban sprawl: metrics, dynamics and modelling using GIS. *International Journal of Applied Earth Observation and Geoinformation, 5(1), 29-39.*

Suresh, M., & Jain, K. (2018). Subpixel level mapping of remotely sensed image using colorimetry. *The Egyptian journal of remote sensing and space science, 21(1), 65-72.*

Sutton, P. C. (2003). An empirical environmental sustainability index derived solely from nighttime satellite imagery and ecosystem service valuation. *Population and Environment, 24(4), 293-311.*

Tashayo, B., Honarbakhsh, A., Azma, A., & Akbari, M. (2020). *Combined fuzzy AHP–GIS for agricultural land suitability modeling for a watershed in southern Iran. Environmental Management, 66(3), 364-376.*

Tewolde, M. G., & Cabral, P. (2011). Urban sprawl analysis and modeling in Asmara, Eritrea. *Remote Sensing, 3(10), 2148-2165.*

Thomas Blaschke, Stefan Lang, Eric Lorup, Josef Strobl & Peter Zeil, (2000). Object-oriented image processing in an intergrated GIS/Remote sensing Environment and Perspectives for Environmental Applications. EnviroInfo 2000: Umweltinformatik '00 Umweltinformation für Planung, Politik und Öffentlichkeit Copyright 2000 Metropolis Verlag, Marburg, *ISBN: 3-89518-307-5.*

Torrens, P. M. (2000). *How cellular models of urban systems work (1. Theory).*

Torrens, P. M., & Alberti, M. (2000). Measuring sprawl.

Travisi, C., & Camagni, R. (2005). *Sustainability of urban sprawl: Environmental-economic indicators for the analysis of mobility impact in Italy.*

Travisi, C. M., Camagni, R., & Nijkamp, P. (2010). Impacts of urban sprawl and commuting: a modelling study for Italy. *Journal of Transport Geography, 18(3), 382-392.*

Uasin Gishu County *Land Use Regulatory Framework 2014-2017*

Udeaja, C., Trillo, C., Awuah, K. G., Makore, B. C., Patel, D. A., Mansuri, L. E., & Jha, K. N. (2020). Urban heritage conservation and rapid urbanization: insights from Surat, India. *Sustainability, 12(6), 2172.*

Von Thünen, J. H. (2022). Der isolierte staat in beziehung auf landwirtschaft und nationalökonomie. *Walter de Gruyter GmbH & Co KG.*

Waqar, M. M., Mirza, J. F., Mumtaz, R., & Hussain, E. (2012). Development of new indices for extraction of built-up area & bare soil from landsat data. *Open Access Sci. Rep, 1(1), 4.*

Wassmer, R. W. (2002). *An economic perspective on urban sprawl.* California: California Senate Office of Research.

Wegner, J. D., Auer, S., & Soergel, U. (2009, June). *Accuracy assessment of building height estimation from a high resolution optical image combined with a simulated SAR image. In Proc.,* ISPRS Hannover Workshop 2009—High Resolution Earth Imaging For Geospatial Information (pp. 1-4).

White, R., & Engelen, G. (1997). Cellular automata as the basis of integrated dynamic regional modelling. *Environment and Planning B: Planning and design, 24(2), 235-246.*

Wilson, E. H., Hurd, J. D., Civco, D. L., Prisloe, M. P., & Arnold, C. (2003). Development of a geospatial model to quantify, describe and map urban growth. *Remote sensing of environment, 86(3), 275-285.*

Williams, H. (2019). The contribution of Sir Alan Wilson to spatial interaction and transport modelling. I*nterdisciplinary Science Reviews, 44(3-4), 232-248.*

Wu, K. Y., & Zhang, H. (2012*). Land use dynamics, built-up land expansion patterns, and driving forces analysis of the fast-growing Hangzhou metropolitan area, eastern China (1978–2008). Applied geography, 34, 137-145.*

Xu, H. (2007). Extraction of urban built-up land features from Landsat imagery using a thematic oriented index combination technique. *Photogrammetric Engineering & Remote Sensing, 73(12), 1381-1391.*

Yan, J., Jianping, W., Hongmei, L., Suliang, Y., & Zongding, H. (2005). *The* biodegradation of phenol at high initial concentration by the yeast Candida tropicalis. *Biochemical Engineering Journal, 24(3), 243-247.*

Yeh, A.G. and X. Li. 2001. Measurement and monitoring of Urban Sprawl in Rapidly Growing Region Using Entropy. Photogrammetric Engineering and Remote Sensing. *Vol. 67 N. 1 pp: 88-90.*

Zhang, X., Zhou, J., & Song, W. (2020). Simulating urban sprawl in china based on the artificial neural network-cellular automata-Markov model. *Sustainability, 12(11), 4341.*

Zhang, J., Li, P., & Wang, J. (2014). Urban built-up area extraction from Landsat TM/ETM+ images using spectral information and multivariate texture. *Remote Sensing, 6(8), 7339-7359.*

Zhang, Y., Liu, T., Meyer, C. A., Eeckhoute, J., Johnson, D. S., Bernstein, B. E., ... & Liu, X. S. (2008). Model-based analysis of ChIP-Seq (MACS*). Genome biology, 9(9), 1-9.*

Zhao, P. (2013). *The impact of urban sprawl on social segregation in beijing and a limited role for spatial planning. Tijdschrift voor economische en sociale geografie, 104(5), 571-587.*

Zha, Y., Gao, J., & Ni, S. (2003). Use of normalized difference built-up index in automatically mapping urban areas from TM imagery. *International journal of remote sensing, 24(3), 583-594.*

Zhai, Z., Martínez, J. F., Beltran, V., & Martínez, N. L. (2020). Decision support systems for agriculture 4.0: Survey and challenges. *Computers and Electronics in Agriculture, 170, 105256.*

Zohoori, M., & Ghani, A. (2017). Municipal solid waste management challenges and problems for cities in low-income and developing countries. *International Journal of Science and Engineering Applications, 6(2), 39-48.*

APPENDICES

Appendix I: Total interpolated population figures and total area (Sq. km) per sub-locations in the study area

Sub-locations	Year							Area
	1999-KNBS	2000-Interpolated	2009-KNBS	2016-Interpolated	2019-KNBS	2020-Interpolated	2029-Interpolated	(Sq. km)
Chepsaita	5796	6037	11058	13570	15137	15586	20,279	36.225
Osorongai	12370	12885	19747	24233	16310	16794	21850	58.723
Turbo	6151	6407	5616	6892	5552	5717	7438	15.036
Tapsagoi	4837	5038	3931	4824	4877	5022	6534	22.519
Kaptembere	2704	2817	8415	10327	9474	9755	12692	17.415
Kapkong	10361	10792	12550	15401	7564	7788	10133	58.571
Leseru	14561	15167	21865	26832	5054	5204	6771	63.641
Sosiani	3176	3308	6425	7884	8019	8257	10743	29.425
Kiplombe	12570	13093	20443	25087	24822	25559	33252	98.872
Soy	8699	9061	15926	19544	18531	19081	24826	79.164
Kuinet	7178	7477	12150	14910	20423	21029	27360	56.585
Kongasis	6281	6542	9142	11219	11195	11527	14998	72.933
Merewet	3462	3606	4949	6073	4696	4835	6291	19.226
Torochmoi	2782	2899	3838	4710	4093	4214	5483	26.808
Toloita	3580	3729	5906	7248	6666	6864	8930	32.018
Moiben	7018	7310	8407	10317	15823	16293	21198	78.848
Kapsumbere	1974	2056	2674	3281	3040	3130	4073	35.969
Sergoit	3323	3461	5276	6474	7951	8187	10652	53.075
Chepkoilel	4107	4278	6113	7502	7995	8232	10711	52.895
Kelji	4254	4431	4831	5928	7307	7524	9789	62.988
Cheburbur	2916	3037	4107	5040	12245	12608	16404	22.617

Kimoing	2636	2746	3396	4167	3652	3760	4893	27.095
Kamaua	2522	2627	3222	3954	3409	3510	4567	15.414
Elgey Border	6126	6381	4862	5966	8004	8242	10723	34.420
Tuiyo Luk	3951	4115	5266	6462	6077	6257	8141	31.246
Kaptuktuk	3177	3309	4850	5952	6549	6743	8774	21.057
Kimumu	11142	11606	15083	18509	23447	24143	31,411	20.135
Sigot	8511	8865	27263	33456	43431	44720	58184	4.1738
Kamukunji	15376	16016	18619	22848	26570	27358	35595	16.709
Kilimani	24777	25808	33216	40761	40682	41889	54501	10.273
Kapsaos	14254	14847	28593	35088	42615	43880	57090	14.597
Huruma	35298	36767	38545	47301	48796	50244	65371	5.5619
Langas	60973	63511	93436	114661	127167	130941	170,364	44.885
Simat	10127	10548	12116	14868	17544	18065	23503	44.944
Lemok	7004	7296	9789	12013	13780	14189	18461	45.902
Kapsoya	21545	22442	33438	41034	54827	56454	73451	43.757
Lotonyok	3994	4160	6472	7942	9733	10022	13039	32.667
Tendwo	3935	4099	4880	5989	5739	5909	7688	34.552
Cheptigit	2590	2698	3115	3823	3623	3731	4854	18.375
Kileges/Chepkero	2216	2308	3146	3861	4219	4344	5652	26.982
Kongasis	1895	1974	3844	4717	5210	5365	6980	23.540
Kipsinende	1149	1197	8353	10250	10512	10824	14083	12.636
Saroiyot	3214	3348	9662	11857	21054	21679	28206	47.331
Kabongo	4577	4768	8737	10722	15007	15452	20105	54.752
Chepkatet	5089	5301	9125	11198	14795	15234	19821	54.447
Kaplelach	3178	3310	4338	5323	10206	10509	13673	51.339
Megun	3502	3648	5166	6340	14710	15147	19707	29.250
Ndubeneti	2339	2436	4162	5107	4609	4746	6175	32.886
Songoliet	2470	2573	3508	4305	4781	4923	6405	20.482

Chepterit	3245	3380	4635	5688	6700	6899	8976	19.506
Mugondoi	2956	3079	4389	5386	5419	5580	7260	16.430
Lengut	3018	3144	3446	4229	4668	4807	6254	26.522
Kaptumo	1978	2060	2518	3090	3074	3165	4118	15.323
Emkwen	2067	2153	3007	3690	2861	2946	3833	24.190
Songich	1510	1573	1785	2190	2195	2260	2941	14.238
Chepkongony	3382	3523	4164	5110	4502	4636	6031	14.683
Chesogor	1469	1530	1853	2274	2026	2086	2714	11.509
Kapsundei	4293	4472	5520	6774	6221	6406	8334	15.711
Total	**41958**	**437049**	**63088**	**774201**	**84518**	**870271**	**1,132,285**	**1971.073**
Population	**5**		**8**		**8**			**7**

Appendix II: LULC change from 2000-2016

LULC change (2000-2016)	Area_sq.km
Agriculture/Farmland - Agriculture/Farmland	392.398789
Agriculture/Farmland - Built up	136.931517
Agriculture/Farmland - Forest	44.944671
Agriculture/Farmland - Grassland	211.771614
Agriculture/Farmland - Swamp	30.725677
Agriculture/Farmland - Water	131.241515
Built up area - Agriculture/Farmland	95.846978
Built up area - Built up	26.283359
Built up area - Forest	5.179746
Built up area - Grassland	36.268716
Built up area - Swamp	4.024248
Built up area - Water	17.019804
Forest - Agriculture/Farmland	16.008244
Forest - Built up	8.167661
Forest - Forest	4.78391
Forest - Grassland	12.772227
Forest - Swamp	1.785608
Forest - Water	7.122358
Grassland - Agriculture/Farmland	310.63114
Grassland - Built up	82.029159
Grassland - Forest	18.07423
Grassland - Grassland	121.588623

Grassland - Swamp	14.327566
Grassland - Water	57.979485
Swamp - Agriculture/Farmland	60.745105
Swamp - Built up	25.951305
Swamp - Forest	11.231378
Swamp - Grassland	40.467089
Swamp - Swamp	6.801035
Swamp - Water	28.770091
Water - Agriculture/Farmland	3.539585
Water - Built up	1.178346
Water - Forest	0.419265
Water - Grassland	1.817785
Water - Swamp	0.398941
Water - Water	1.77323

Appendix III: LULC change from 2016-2020

LULC Change (2016-2020)	Area_sq km
Agriculture/Farmland - Agriculture/Farmland	409.082508
Agriculture/Farmland - Built up areas	112.137783
Agriculture/Farmland - Forest	28.75279
Agriculture/Farmland - Grassland	226.216321
Agriculture/Farmland - Swamp	94.791668
Agriculture/Farmland - Water	6.495516
Built up - Agriculture/Farmland	89.899995
Built up - Built up areas	75.192665
Built up - Forest	19.238581
Built up - Grassland	57.855675
Built up - Swamp	34.864218
Built up - Water	3.87099
Forest - Agriculture/Farmland	7.602022
Forest - Built up areas	4.290125
Forest - Forest	28.341958
Forest - Grassland	20.807575
Forest - Swamp	21.062359
Forest - Water	2.737401
Grassland - Agriculture/Farmland	144.755538
Grassland - Built up areas	53.092772
Grassland - Forest	23.610556
Grassland - Grassland	130.841336

Grassland - Swamp	68.832833
Grassland - Water	4.134623
Swamp - Agriculture/Farmland	2.707673
Swamp - Built up areas	1.130432
Swamp - Forest	15.07185
Swamp - Grassland	10.38492
Swamp - Swamp	26.257953
Swamp - Water	2.595016
Water - Agriculture/Farmland	30.876794
Water - Built up areas	13.281348
Water - Forest	40.582326
Water - Grassland	75.895624
Water - Swamp	69.638884
Water - Water	14.069372

Appendix IV: LULC change from 2000-2020

LULC change (2000-2020)	Area_sq.km
Agriculture/Farmland - Agriculture/Farmland	296.906281
Agriculture/Farmland - Built up areas	122.106678
Agriculture/Farmland - Forest	81.328297
Agriculture/Farmland - Grassland	264.894824
Agriculture/Farmland - Swamp	165.440122
Agriculture/Farmland - Water	18.750667
Built up area - Agriculture/Farmland	75.942822
Built up area - Built up areas	26.139355
Built up area - Forest	10.113166
Built up area - Grassland	44.142692
Built up area - Swamp	26.257645
Built up area - Water	2.24033
Forest - Agriculture/Farmland	11.783352
Forest - Built up areas	7.966075
Forest - Forest	7.40807
Forest - Grassland	14.258497
Forest - Swamp	8.462162
Forest - Water	0.980098
Grassland - Agriculture/Farmland	255.151021
Grassland - Built up areas	80.457411
Grassland - Forest	35.569251
Grassland - Grassland	143.114613

Grassland - Swamp	79.44321
Grassland - Water	7.794479
Swamp - Agriculture/Farmland	44.450424
Swamp - Built up areas	21.319573
Swamp - Forest	20.514624
Swamp - Grassland	49.329078
Swamp - Swamp	35.875328
Swamp - Water	3.724719
Water - Agriculture/Farmland	2.86948
Water - Built up areas	1.081009
Water - Forest	0.835292
Water - Grassland	2.537264
Water - Swamp	1.454054
Water - Water	0.358037

Appendix V: National Commission for Science, Technology and Innovation (NACOSTI) research licence

REPUBLIC OF KENYA

NATIONAL COMMISSION FOR
SCIENCE,TECHNOLOGY & INNOVATION

Ref No: 735955

Date of Issue: 10/March/2021

RESEARCH LICENSE
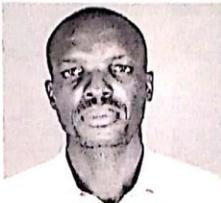
This is to Certify that Mr.. Samson Odhiambo of University of Eldoret, has been licensed to conduct research in Uasin-Gishu on the topic: Analysis of Urban Sprawl Hot Spots around Eldoret Town using Object-Based Image Analysis for the period ending : 10/March/2022.

License No: NACOSTI/P/21/9419

735955

Applicant Identification Number

Director General
NATIONAL COMMISSION FOR
SCIENCE,TECHNOLOGY &
INNOVATION
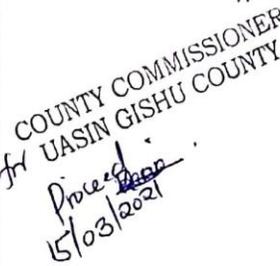
Verification QR Code

NOTE: This is a computer generated License. To verify the authenticity of this document, Scan the QR Code using QR scanner application.

Appendix VI: Eldoret Water and Sanitation (ELDOWAS) data collection approval
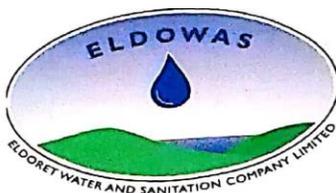
Date _____ 6th May, 2021 _____

Your Ref _____

Our Ref _____ ELDOWAS/ADM/23/IA/VOL. VI/03

University of Eldoret,
P.O Box 1125-30100,
ELDORET

Dear Madam,

RE: COLLECTION OF RESEARCH DATA-SAMSON ODHIAMBO

Reference is made to your letter dated 16th March, 2021

This is to confirm that the above named student has been granted permission to undertake a research on the Topic: "ANALYSIS OF URBAN SPRAWL HOT SPOTS AROUND ELDORET TOWN USING OBJECT –BASED IMAGE ANALYSIS PERFORMANCE".

After successful completion of the research, the student is kindly requested to forward a copy of the findings to this Company for necessary action.

Please note that the student shall not be allowed to undertake any other activity other than the above mentioned.

Yours faithfully
ELDORET WATER AND SANITATION CO. LTD

Dr. Ruth Tuwei
AG: HUMAN RESOURCE & ADMIN. MANAGER

ISO 9001:2015 CERTIFIED

Eldoret Water and Sanitation Company Limited
P.O. Box 8418: Phone 053-2035000/2035202: info@eldowas.or.ke
Mission: Eldowas is committed to providing quality and adequate water services in a cost effective Manner to its stakeholders by qualified and motivated human resource.

Appendix VII: Similarity Index Report